Impact of amyloid-β reduction on secondary pathological changes in transgenic mouse lines modelling Alzheimer-like pathology

Dissertation

zur Erlangung des Grades eines
Doktors der Naturwissenschaften

der Mathematisch-Naturwissenschaftlichen Fakultät
und
der Medizinischen Fakultät
der Eberhard-Karls-Universität Tübingen

vorgelegt
von

Christine Rother
aus Düsseldorf, Deutschland

2023

Tag der mündlichen Prüfung: 13.01.2023

Dekan der Math.-Nat. Fakultät:	Prof. Dr. Thilo Stehle
Dekan der Medizinischen Fakultät:	Prof. Dr. Bernd Pichler
1. Berichterstatter:	Prof. Dr. M. Jucker
2. Berichterstatter:	Prof. Dr. P. Kahle
Prüfungskommission:	Prof. Dr. M. Jucker
	Prof. Dr. P. Kahle
	Prof. Dr. R. Feil
	Prof. Dr. M. Deleidi

Erklärung / Declaration:

Ich erkläre, dass ich die zur Promotion eingereichte Arbeit mit dem Titel:

„Impact of amyloid-β reduction on secondary pathological changes in transgenic mouse lines modelling Alzheimer-like pathology“

selbstständig verfasst, nur die angegebenen Quellen und Hilfsmittel benutzt und wörtlich oder inhaltlich übernommene Stellen als solche gekennzeichnet habe. Ich versichere an Eides statt, dass diese Angaben wahr sind und dass ich nichts verschwiegen habe. Mir ist bekannt, dass die falsche Abgabe einer Versicherung an Eides statt mit Freiheitsstrafe bis zu drei Jahren oder mit Geldstrafe bestraft wird.

I hereby declare that I have produced the work entitled „Impact of amyloid-β reduction on secondary pathological changes in transgenic mouse lines modelling Alzheimer-like pathology“, submitted for the award of a doctorate, on my own (without external help), have used only the sources and aids indicated and have marked passages included from other works, whether verbatim or in content, as such. I swear upon oath that these statements are true and that I have not concealed anything. I am aware that making a false declaration under oath is punishable by a term of imprisonment of up to three years or by a fine.

Tübingen, den ....

Datum / Date Unterschrift /Signature

Acknowledgments

First of all, I would like to thank my supervisor Prof. Dr. Mathias Jucker for allowing me to pursue my doctoral studies in his department of Cellular Neurology at the Hertie Institute for Clinical Brain Research in Tuebingen. Mathias was a demanding and conscientious supervisor, who was always available for scientific exchange and input. His advice helped me to pursue challenging projects and to advance scientifically.

Furthermore, I would like to express my gratitude to the members of my scientific advisory board, Prof. Dr. Philip Kahle and Prof. Dr. Robert Feil, who provided me with scientific guidance and constructive feedback along my research path as a doctoral student.

My sincere thanks go to all my colleagues in the department of Cellular Neurology at the Hertie Institute. Your scientific expertise was highly appreciated and your steady helpfulness and kindness made my time as a doctoral student truly memorable.

I wish to thank our many collaboration partners for your scientific input and discussion, without that would this project not have been successful.

Finally, I would like to thank my family. Your support and encouragement made my doctoral thesis possible.

Abstract

Alzheimer's disease (AD) has grown to a global health crisis which comes with an urgent need for disease-modifying and preventative therapies. To advance current therapeutic approaches, it is crucial to identify the first pathogenic event (presumably amyloid-β misfolding) as well as mechanistically defined biomarkers along AD disease progression.

In the first part of this thesis, we generated biomarker trajectories in an amyloid-β precursor protein (APP) transgenic mouse model that is widely used in the AD research field. We were then able to mimic in this mouse model the discrepancy in clinical settings between a therapeutic reduction of amyloid-β (Aβ) deposition and a lack of cognitive improvement, as assessed by neurofilament levels in the cerebrospinal fluid. Our data indicate an Aβ-dependent disease phase at which Aβ reduction prevented disease-associated neurodegeneration and an Aβ-independent phase characterized by proceeding neurodegeneration despite a reduction of brain Aβ. Interestingly, robust neurodegeneration was mainly associated with a saturated Aβ seeding activity, which in turn was not proportional to the level of brain Aβ deposition. Our data raise the hypothesis that seeding-active Aβ species are an important molecular link between Aβ deposition and neurodegeneration. The evaluation of this concept and its application in humans awaits further investigations.

In the second part of this thesis, we used an APP transgenic mouse model with a prolonged Aβ aggregation lag phase. We then targeted the first Aβ nucleation event *in vivo* and characterized such early Aβ assemblies. Our results revealed that even before Aβ-deposition became histologically detectable, pre-amyloid Aβ species were clearly present. Further, immunotherapeutic targeting of such pre-amyloid seeds led to a substantial reduction in Aβ seeding activity and long-lasting beneficial effect on secondary pathologies. We thereby expand the therapeutic window for a promising Aβ-targeting therapy to a much earlier time point as previously assumed. Moreover, our data indicate that specific binding features of Aβ targeting antibodies determine whether an antibody recognized such early seeds. Since specific amyloid structures are associated with distinct toxicities, this knowledge offers potential implications for future antibody design for immunotherapies.

In conclusion, the results of this thesis demonstrate the presence of pre-amyloid Aβ seeds. Direct targeting of such early Aβ seeds, or an early reduction in brain Aβ, have beneficial effects on secondary pathologies and neurodegeneration. Thus, our results expand the current therapeutic window to a new established disease phase characterized by the presence of pre-amyloid seeds and low Aβ seeding activity with high potential for disease prevention.

Table of contents

1 Introduction

1.1 Alzheimer's disease - from discovery to a global health challenge

In 1906, the psychiatrist and neuropathologist Alois Alzheimer presented the case study of Auguste D. at the Meeting of Psychiatrists in Tuebingen. The first symptoms of the 50-year-old subject, which led to her hospital admission in 1901, were paranoia and sleep disorder, which fast progressed to memory impairment, aggressiveness and confusion (Alzheimer, 1907). The detailed documentation of Auguste D.'s cognitive decline over more than 4 years, with the observed morphologically and histological alterations found in her brain, presented a disease that is now well-known as 'Alzheimer's disease' (Hippius and Neundörfer, 2003). At the time, such unusual cases of illness, not covered by any textbook, became more frequent and Alois Alzheimer acknowledged the need to expand the spectrum of neurological diseases and the requirement of histological examinations for a definite diagnosis (Alzheimer, 1907).

More than 100 years later, the estimated number of patients suffering from dementia exceeds 50 million for 2019 (Nichols *et al.*, 2022) of which approximately 60-80% account for Alzheimer's disease (AD) (*'2020 Alzheimer's disease facts and figures'*, 2020). Studies on dementia prevalence and incidence worldwide noticed regional differences, which may underlie complex factors such as a country's economic development, the life expectancy of a population as well as the quality and quantity of data reporting (Prince *et al.*, 2015; Wu *et al.*, 2017). The prevalence of dementia in Germany in 2018 was 1.91% of the population, which was the third-highest in Europe after Greece (1.99%) and Italy (2.12%) (*'Dementia in Europe Yearbook 2019 - Estimating the prevalence of dementia in Europe'*, 2019). Interestingly, within the past years, a decrease in dementia prevalence and incidence has been noticed (Wu *et al.*, 2017). Although a scientific explanation for this observation remains missing, for western countries an improvement in health among old age and an increase of the educational level have been hypothesized to reduce the risk of developing dementia (Wu *et al.*, 2017). Nevertheless, the total number of people living with dementia is estimated to rise substantially due to a higher proportion of older people in the population and their increasing lifespan (Collaborators GBD 2019 Dementia Forecasting, 2022). An increase in dementia cases is predicted to be accompanied by an increase in the social-economic burden (Wimo *et al.*, 2017; Michalowsky *et al.*, 2019).

The clinical representation of AD was shown to be manifold (Scheltens *et al.*, 2016; Atri, 2019) with memory impairment being one early clinical feature associated with AD (Grober *et al.*, 2008) together with several other signs including changes in personality as well as depression (Bature *et al.*, 2017).

The majority of AD cases are late-onset (LOAD) and sporadic (sAD), which refers to patients experiencing disease onset above 65 years of age and without confirmed genetic disposition in a gene implicated in AD, respectively (Carmona *et al.*, 2018). The proportion of early-onset AD (EOAD) cases, with a clinical onset before the age of 65, is estimated to account for 1-2% (Sassi *et al.*, 2014), although higher portions such as 5.5% (Zhu *et al.*, 2015) have been reported as well. In the case of familial AD (fAD), a mutation causative for AD and the inheritance in an autosomal dominant trait is common (St. George-Hyslop *et al.*, 1987). AD cases involving known causative mutations in *APP*, *PSEN1* and *PSEN2* are estimated to account for approximately 10-15% of all EOAD cases (Ayodele *et al.*, 2021).

1.2 Key pathological events of Alzheimer's disease

The neuropathological profile of AD includes extracellularly aggregated amyloid-β (Aβ) peptides forming senile plaques in a patient's brain as well as intraneuronal misfolded Tau creating tangles (Hardy and Allsop, 1991). Furthermore, AD is a progressive disease featuring chronic inflammation (Kinney *et al.*, 2018), impaired brain homeostasis (De Strooper and Karran, 2016) and neuronal death (Brokaw *et al.*, 2020). A simplified scheme about some key pathological events in AD and some proposed relations between them is provided in Figure 1.

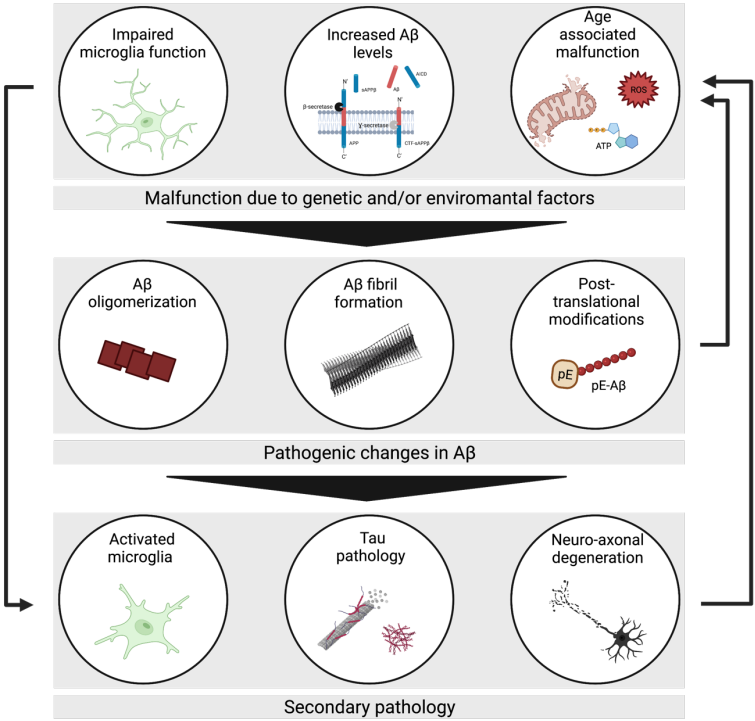

Figure 1 Overview of sequential pathogenic events in Alzheimer's disease. From the top to the bottom: Genetic and/or environmental risk factors potentially lead to malfunction in microglia (Joshi *et al.*, 2013; Parhizkar *et al.*, 2019), disturbed amyloid precursor protein (APP) processing and/or amyloid-β (Aβ) clearance (Selkoe and Hardy, 2016), altered energy supply (Ryu *et al.*, 2021) and/or mitochondrial dysfunction (Takeda *et al.*, 2021). Disturbance of Aβ homeostasis due to one or several of these factors might lead to the formation of neurotoxic Aβ oligomers, mature Aβ fibrils or posttranslational modifications (PTMs) of Aβ. Secondary pathology including activated microglia, tau pathology and neuro-axonal degeneration is followed by pathogenic Aβ changes. However, the link between risk factors, Aβ and secondary pathologies, depicted as a linear course is a current topic of investigation (as reviewed by Hampel *et al.*, 2021). Small arrows on both sites: Scientific evidence suggests a rather circular relationship where disturbed cell homeostasis might enhance/initiate secondary pathologies and vice versa, which again potentially results in more Aβ and associated pathology. Created with Biorender.com

It remains debatable whether Aβ is causative for AD with dementia and cognitive impairment, but it was proposed that Aβ and Tau abnormal protein deposits, together, define AD as a distinctive neurodegenerative disease (Jack *et al.*, 2018).

1.2.1 Amyloid-β peptide and its diverse aggregation entities

Aβ peptides, mainly ending at the amino acid positions $Aβ_{x-40}$ ($Aβ_{40}$) and $Aβ_{x-42}$ ($Aβ_{42}$), are recognized as pathological deposits in an AD patient's brain (Masters *et al.*, 1985; Portelius *et al.*, 2010). Physiological functions for endogenous Aβ based on rodent models, for instance in the regulation of learning and memory, have been formulated (Garcia-Osta and Alberini, 2009; Morley *et al.*, 2010; Puzzo *et al.*, 2011). The pathological accumulation of Aβ has been suggested to occur in response to a disturbed dynamic equilibrium of Aβ production and clearance (Thal, 2015; Thompson *et al.*, 2021). Thus, an increased production and/or a failure of clearance and degradation, for instance, due to genetic disposition, ageing and/or environmental factors, putatively leads to pathological Aβ aggregation and amyloid fibril formation as described by the amyloid hypothesis (Selkoe and Hardy, 2016). In the course of Aβ aggregation, a wide range of assemblies, ranging from small Aβ oligomers to large, insoluble amyloid fibrils have been reported (Chen *et al.*, 2017).

The Aβ oligomer 'pool' associated with AD, encompasses multiple distinct assemblies such as Aβ dimers, (Walsh *et al.*, 2000), trimers, tetramers (Chen and Glabe, 2006) and dodecamers (Lesné *et al.*, 2006). The classification of an Aβ oligomeric assembly and its distinction from a protofibril, a transient stage between Aβ oligomers and amyloid fibrils, lacks a strict nomenclature (Glabe, 2008). Therefore, the general term of an Aβ oligomer, used in the scientific literature, might refer to multiple assemblies with a high level of structural and functional disparity. For instance, some consider soluble Aβ oligomers to be highly diffuse with a tendency to dissociate back to monomers rather than forming larger fibrils (Dear *et al.*, 2020). Further, Aβ oligomers are recognized as neurotoxic assemblies associated with the Aβ aggregation process (Benilova *et al.*, 2012) and there was a myriad of mechanisms proposed how oligomeric Aβ assemblies govern toxicity. For instance, Aβ oligomers might act as ligands for different receptors and compromise cell signalling upon binding (Pagano *et al.*, 2018). Due to integration into lipid membranes, Aβ oligomers putatively disrupt the membrane integrity (Bode *et al.*, 2019). Recently, the first atomic structure of $Aβ_{42}$ oligomers incorporated into a lipid membrane-mimicking environment was published and indicated four $Aβ_{42}$ peptides building a pore (Ciudad *et al.*, 2020). The pore-forming properties of Aβ are considered as another mechanism by which oligomeric Aβ assemblies may exert toxic effects (Arispe *et al.*, 1994; Darling and Shorter, 2020), although the presence of these Aβ pores in patients remains to be shown.

Soluble Aβ from postmortem AD brain material is highly active, reduces dendritic spine density in rodent hippocampus (Shankar *et al.*, 2008) and accommodates neurotoxicity in neuronal cell culture (Hong *et al.*, 2018). Surprisingly, such highly neuroactive, soluble assemblies,

presumably account for only a small proportion of the overall Aβ present in the brain (Hong *et al.*, 2018). Furthermore, soluble Aβ assemblies of an amyloid precursor protein (APP) transgenic mouse model account for less than 1% of total brain Aβ but are potent inducers of Aβ deposition *in vivo* (Langer *et al.*, 2011). A depletion of oligomeric Aβ from Aβ-containing brain homogenate delays Aβ plaque induction when introduced into a transgenic mouse model for cerebral amyloidosis, indicating Aβ oligomers might be important in the early phase of aggregation initiation (Katzmarski *et al.*, 2020). However, several different, soluble oligomeric Aβ conformations were reported, highlighting the great heterogeneity of Aβ oligomers in postmortem brain tissue of AD patients (Bao *et al.*, 2012) and a rodent disease model (Shankar *et al.*, 2009).

Although, Aβ peptides were recognized as the major components of parenchymal Aβ plaques, generally termed 'senile plaques' (Masters *et al.*, 1985; Walker, 2020), other proteins have been identified within plaques as well (Xiong *et al.*, 2019). For instance, the collagenous Alzheimer amyloid plaque component (CLAC), which is believed to have an impact on Aβ plaque morphology (Hashimoto *et al.*, 2020). Although a different terminology for similar plaque types can be used, originally, senile plaques were classified based on different morphologies ranging from diffuse, compact and cored plaques (Walker, 2020). Aβ plaques can be visualized microscopically after immune-histological staining using antibodies directed against Aβ and amyloid specific dyes such as Congo Red (Ikeda *et al.*, 1989). A more recent established class of amyloid dyes, termed luminescent conjugated oligothiophenes (LCOs), displays specific fluorescence emission spectra reflecting structural characteristics of Aβ plaques (Nilsson *et al.*, 2007). Plaque maturation as a function of time visualized by LCO staining in mouse models for cerebral amyloidosis indicates conformational rearrangements within Aβ plaques (Nyström *et al.*, 2013). Diffuse Aβ plaques are proposed to be an early entity in plaque development, mostly containing oligomeric Aβ species, whereby, compact plaques are considered to contain more densely packed Aβ assemblies with a great heterogeneity of aggregation intermediates (Röhr *et al.*, 2020). Further, an enrichment of β-sheet Aβ assemblies within the core, surrounded by rather diffuses Aβ assemblies, was recognized in dense-cored plaques (Röhr *et al.*, 2020). Data indicate that all three plaque morphologies can be detected in AD patients' brains, although the proportion of dense-cored plaques increases with age (Dickson and Vickers, 2001). In addition to these morphotypes, recently, another plaque morphology associated with EOAD has been identified and termed 'coarse-grained' plaque (Boon *et al.*, 2020). In comparison to cored plaques, this morphotype is predominately composed of $A\beta_{40}$ the main aggregate in cerebral amyloid angiopathy (CAA) (Boon *et al.*, 2020). CAA describes the observed aggregation of Aβ around the cerebral vasculature (Suzuki *et al.*, 1994b; Alonzo *et al.*, 1998). In more than 60% of AD patients, CAA was detected (Serrano-Pozo *et al.*, 2013)

and is considered as a major contributor to cerebrovascular pathologies such as altered cerebral blood flow (Thal *et al.*, 2009) and brain haemorrhages in AD (Yates *et al.*, 2011; Greenberg *et al.*, 2020). Coarse-grained plaques were observed exclusively in symptomatic AD patients and therefore, the authors concluded this plaque morphotype to be clinically relevant (Boon *et al.*, 2020). Recent data indicate a protective role for dense-cored plaques due to the sequestration of toxic, diffuse Aβ (Huang *et al.*, 2021). The contribution of senile plaques to secondary pathologies in AD remains controversial since only a minimal correlation between Aβ deposition and degree of cognitive decline has been described (Nelson *et al.*, 2012). Also, a great heterogeneity in conformational variants of aggregated Aβ within plaque cores was observed in sAD and fAD patients (Rasmussen *et al.*, 2017) as well as in patients with slow and fast disease progression (Qiang *et al.*, 2017; Liu *et al.*, 2021). Despite the effort to allocate distinct Aβ assemblies to certain pathological events in AD, the individual contribution remains uncertain.

1.2.2 Tau pathology in the context of amyloid-β

The protein Tau is a member of the microtubule-associated protein-family, involved in maintaining microtubule stability and dynamic (Weingarten *et al.*, 1975). Tau pathophysiology has been recognized in AD (Grundke-Iqbal *et al.*, 1986) as well as in many other neurodegenerative diseases (Spillantini and Goedert, 2013). Recently, cryo-electron microscopy of Tau fibrils derived from patients with various tauopathies offered a detailed classification based on structural folds (Shi *et al.*, 2021b). In the human central nervous system (CNS), six Tau isoforms are expressed, based on alternative splicing, containing 0, 1, or 2 N-terminal inserts and 3 or 4 repeats in the microtubule-binding domain (Goedert *et al.*, 1988, 1989a; b). In the course of AD, Tau can form higher-order fibrils within neurons forming neurofibrillary tangles (NFT) (Wood *et al.*, 1986) neuropil threads (NT) and as well as neuritic plaques (NP) (Braak *et al.*, 1986) which refer to Tau-positive dystrophic neural processes surrounding Aβ plaques (Dickson, 1997).

Protein phosphorylation is one of the most common post-translation modifications regulating essential cellular processes (Manning *et al.*, 2002). The longest human Tau isoform contains 85 potential phosphorylation sites of which approximately 50% have been reported to be phosphorylated in AD brains (Noble *et al.*, 2013). Based on *in vitro* experiments using Tau isolated from human AD brain extracts, the phosphorylation state of Tau, hence referred generally as p-Tau, is suggested to impact Tau's ability to maintain microtubule assembly and dynamics (Alonso *et al.*, 1994). It has been proposed that in the course of AD, Tau becomes hyperphosphorylated and thereby loses its ability to bind and stabilize microtubule (Alonso *et*

al., 1996; Wang *et al.*, 1996) but gains increased aggregation properties (Despres *et al.*, 2017) which potentially leads to the formation of paired helical filaments (PHFs) resulting in NFT (Alonso *et al.*, 2001). Many kinases are implicated in Tau phosphorylation from which three are strongly linked to diseases, namely glycogen synthase kinase 3 (GSK3) (Amaral *et al.*, 2021), cyclin-dependent kinase 5 (Wilkaniec *et al.*, 2018) and extracellular signal-regulated kinase 2 (Qi *et al.*, 2016). Tau pathology correlates, more closely with the severity of dementia in AD compared to Aβ pathology (Arriagada *et al.*, 1992; Ingelsson *et al.*, 2004). How Tau contributes to AD pathogenesis is currently not clearly defined, although experimental data provide evidence for the interrelationship between Aβ and Tau pathology (Busche and Hyman, 2020).

An inhibition of GSK3β reduces Tau phosphorylation without significant alterations of total tau and Aβ levels (Choi *et al.*, 2014). Furthermore, an Aβ-dependent enhancement of GSK3β activity via α_{2A}-adrenergic receptor signalling leads to increased Tau phosphorylation (Zhang *et al.*, 2020). Aβ-mediated dysfunction in a mouse model expressing human APP is rescued upon endogenous Tau reduction (Roberson *et al.*, 2007). Furthermore, Aβ plaque formation in a three-dimensional human neuronal cell culture leads to high levels of aggregated phosphorylated Tau. Convincingly, a reduction of Aβ production in these cultures results in decreased Aβ pathology and attenuated Tau pathology (Choi *et al.*, 2014). Furthermore, the inhibition of Aβ generation in a mouse model for amyloidosis reduces cerebral Aβ pathology and attenuates an increase of Tau in cerebrospinal fluid (CSF) (Schelle *et al.*, 2017). Aggregated Tau species isolated from patients with Aβ plaque pathology reveal higher bioactivity in a cell biosensor assay compared to human cases with solely Tau pathology (Bennett *et al.*, 2017). In line with this observation, *in vivo* Tau seeding is enhanced in mouse models with Aβ pathology (He *et al.*, 2017; Vergara *et al.*, 2019) and injection of $A\beta_{42}$ fibrils leads to increased numbers of NFT in Tau transgenic mice (Götz *et al.*, 2001). Interestingly, in a mouse model with human and murine Tau, Aβ plaques appear to be larger, indicating Tau may also influence Aβ plaque pathology (Jackson *et al.*, 2016), whereas, in the absence of murine Tau in the same model, Aβ plaques appear smaller (Pickett *et al.*, 2019).

In humans, Aβ and Tau are considered to be both associated with cognitive decline in preclinical AD patients and necessary for memory decline (Hanseeuw *et al.*, 2019; Sperling *et al.*, 2019). However, the underlying molecular relationship between Aβ and Tau, due to their co-occurrence and the involvement of several regulators in both pathologies, including microglial activation, endocytic system and lipid metabolism, awaits further investigation (Busche and Hyman, 2020).

1.2.3 The ambivalent role of microglia in Alzheimer's disease

The inflammatory response in the CNS generally termed neuroinflammation, can be triggered by various pathological events such as infections, exposure to neurotoxins and head trauma (Leng and Edison, 2020). Furthermore, complex pathways including the complement system (Lian *et al.*, 2016; Liddelow *et al.*, 2017; Litvinchuk *et al.*, 2018) and cytokine signalling (Fillit *et al.*, 1991; Patel *et al.*, 2005; Heneka *et al.*, 2012) can modulate the neuroinflammatory response.

Microglia are recognized as phagocytosis-competent immune cells resident in the brain (Ransohoff and Cardona, 2010), with implications in brain development (Paolicelli *et al.*, 2011), maintenance of synaptic plasticity (Nguyen *et al.*, 2020) and immune surveillance (Nimmerjahn *et al.*, 2005). In recent years, human genome-wide association studies identified more than 25 AD-associated genetic variants in or in close proximity of genes uniquely expressed in microglia (Yang *et al.*, 2021), positioning neuroinflammation as a putative target for treatment intervention (Leng and Edison, 2020).

Whether microglia function in neurodegeneration is beneficial or deleterious remains debatable. One currently recognized assumption proposes an initial beneficial role of the immune response in AD, which may become detrimental when it develops into a chronic state (Webers *et al.*, 2020). The level of microglial activation correlates well with Aβ deposition in MCI and AD patients (Fan *et al.*, 2017; Dani *et al.*, 2018). Furthermore, microglial activation, Aβ and Tau together are a reliable and precise predictor for cognitive worsening with microglia forecasting the spreading of Tau (Pascoal *et al.*, 2021). Transcriptional profiling and single microglia sequencing in APP and Tau transgenic mouse models indicate Aβ but not Tau pathology provokes microglial response that is associated with an upregulation of known AD-related risk genes (Sierksma *et al.*, 2020). So-called disease-associated microglia (DAM) is an AD-specific microglia population with a distinct transcriptional profile (Keren-Shaul *et al.*, 2017). Interestingly, distinct transcriptional DAM profiles in response to solely Aβ pathology (AD1) or Aβ plus Tau pathology (AD2) have been reported (Gerrits *et al.*, 2021). While AD1-microglia are associated with a direct response to Aβ and share high similarity to the phagocytic/activated profile reported for amyloid mouse models (Keren-Shaul *et al.*, 2017; Sierksma *et al.*, 2020), the AD2-microglia profile has not been reported before and its functional role remains to be assigned (Gerrits *et al.*, 2021).

Trem2 (triggering receptor expressed on myeloid cells 2) is a cell surface receptor expressed in microglia (Klesney-Tait *et al.*, 2006) which positively regulates phagocytosis and downregulates the inflammatory response in AD (Hickman and Khoury, 2014). Conversion from homeostatic microglia to DAM follows a two-step mechanism with an initial Trem2-

independent and a second Trem2-dependent step (Keren-Shaul *et al.*, 2017). A genetic variant in Trem2 resulting in an amino acid substitution at position 47 (of histidine for arginine), was detected in AD patients and hypothesized to govern an increased risk for AD through impaired inflammatory responses (Guerreiro *et al.*, 2013; Jonsson *et al.*, 2013). Microglia clustering around Aβ plaques is Trem2-dependent and in patients carrying a Trem2 risk variant, fewer plaque-associated microglia have been observed (Prokop *et al.*, 2019). Similar has been observed in disease models (Meilandt *et al.*, 2020; Lee *et al.*, 2021). A lost plaque association of microglia results in more diffuse Aβ-plaques, mitigated microglial activation and increased Tau pathology (Wang *et al.*, 2016; Yuan *et al.*, 2016; Meilandt *et al.*, 2020; Lee *et al.*, 2021). These observations are in line with the proposed 'barrier' function of microglia, protecting neurons from the diffuse Aβ halo around plaques which may contain toxic oligomeric species (Condello *et al.*, 2015). Interestingly, the effects of Trem2 on Aβ seems to be disease stage-dependent as at later disease stage a decrease in plaque accumulation was noted (Meilandt *et al.*, 2020).

The protective barrier function was shown to decline in ageing microglia, resulting in more severe Tau pathology and axonal dystrophy around Aβ plaques (Condello *et al.*, 2015; Yuan *et al.*, 2016). 'Inflammaging' describes a chronic activation of the immune system which, in course of ageing, potentially becomes damaging (Franceschi *et al.*, 2000, 2018). Data indicate chronic activation of microglia can compromise the homeostatic function and thereby eventually lead to neuronal cell loss (Sobue *et al.*, 2021).

Microglia have been assigned an ambivalent role in AD: on one hand they were implicated in Aβ clearance (Liu *et al.*, 2010; Rivera-Escalera *et al.*, 2019) and on the other hand microglial activation might provoke neurotoxicity (Liddelow *et al.*, 2017). Data interpretation aiming to enlighten microglia function and signalling in health and disease remains challenging due to recognized differences of microglial responses and transcriptional profiles in distinct experimental models (Das *et al.*, 2016; Melief *et al.*, 2016).

1.3 Amyloid precursor protein cleavage

Aβ is a cleavage product of the subsequent processing of APP by β- and γ-secretase, termed amyloidogenic pathway (Fig. 2b, Vassar et al. 1999; De Strooper et al. 1998). The alternative pathway involves an initial α-secretase processing step instead of β-secretase cleavage (Fig. 2a, Sisodia 1992; Kuhn et al. 2010).

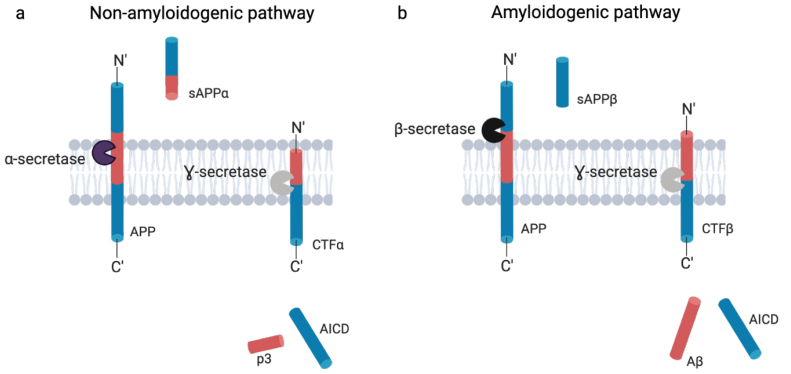

Figure 2 Schematic presentation of amyloid precursor protein processing (APP). (**a**) In the non-amyloidogenic pathway, the first cleavage of APP is conducted by α-secretase, followed by proteolytic processing by γ-secretase resulting in p3 and intracellular domain of APP (AIDC). (**b**) The amyloidogenic pathway is initiated by β-secretase and subsequently γ-secretase cleavage, liberating amyloid-β (Aβ) isoforms with variable carboxy-terminus and AIDC. Additionally, after the initial secretase cleavage by α- and β-secretase, soluble APP α (sAPPα) and β (sAPPβ), respectively, are released. Created with Biorender.com

APP is a type I transmembrane protein, harbouring the Aβ sequence within the membrane-spanning domain (Goldgaber *et al.*, 1987; Kang *et al.*, 1987; Tanzi *et al.*, 1987). Due to alternative splicing, three major isoforms of APP with 695, 751 or 770 amino acids, termed APP_{695}, APP_{751} and APP_{770}, respectively, are expressed (Müller *et al.*, 2017). Different intracellular trafficking routes for APP have been described. In cell culture, APP can be cleaved on the plasma membrane (Sisodia, 1992), however, the majority of synthesized APP was shown to traffic from the trans-Golgi network (TGN) directly to early endosomes with only a minority of APP reaching the plasma membrane (Toh *et al.*, 2017a). Clathrin-depending endocytosis of APP from the plasma membrane subjects APP into the endocytic compartment for cleavage (Cirrito *et al.*, 2008). From the endosomal pathway, retrograde transport might localize APP back to the TGN (Vieira *et al.*, 2010), where the majority of APP is processed in cell culture experiments (Choy *et al.*, 2012). APP trafficking can have a great impact on health and disease, as APP sorting determines cleavage and therefore, missorting can result in an increased Aβ production (Tan and Gleeson, 2019).

1.3.1 The α - and β-secretase cleavage of the amyloid precursor protein

The β-secretase, also known as beta-site amyloid precursor protein cleaving enzyme 1 (BACE1), is an aspartyl protease with two aspartic acids in its catalytic centre (Vassar *et al.*, 1999). The enzymatic optimum of BACE1 is at low pH (Sinha *et al.*, 1999). Consistently, the enzyme colocalizes with Golgi and endosomes (Vassar *et al.*, 1999), organelles providing an acidic environment. APP cleavage by BACE1 is considered to be the rate-limiting step in the generation of Aβ peptides (Capell *et al.*, 2002; Toh *et al.*, 2017b). BACE1 cleavage of APP results in soluble APP β (sAPPβ) and a membrane-bound carboxyl-terminal fragment β (CTFβ) (Vassar *et al.*, 2014). The CTFβ fragment serves as a substrate for γ-secretase cleavage, resulting in the intracellular domain of APP (AIDC) and the release of Aβ peptides (De Strooper *et al.*, 1998; Wolfe *et al.*, 1999). Additional to its role in the initialization of the amyloidogenic pathway, BACE1 has been suggested to be involved in proteolytic degradation of Aβ resulting in $Aβ_{x-34}$ ($Aβ_{34}$) due to a correlation of $Aβ_{34}$ and the overall clearance rates of $Aβ_{x-38}$ ($Aβ_{38}$), $Aβ_{40}$ and $Aβ_{42}$ in CSF of amyloid positive patients (Liebsch *et al.*, 2019). Nevertheless, the underlying cleavage mechanism of Aβ peptides by BACE1 awaits further investigation.

The alternative processing of APP, the non-amyloidogenic pathway, is carried out by α-secretase and results in soluble APP α (sAPPα) and carboxyl-terminal fragment α (CTFα) (Sisodia, 1992; Kuhn *et al.*, 2010). In humans, so far 20 members of the ADAM (a disintegrin and metalloprotease) protein family have been identified (*'ADAM metallopeptidase domain containing'*, no date; Souza *et al.*, 2020) from which ADAM10 was shown to be mainly responsible for α-secretase activity in neurons (Kuhn *et al.*, 2010). ADAM10 is a membrane-bound proteinase which cleaves APP within the Aβ domain, releasing sAPPα to the extracellular space (Sisodia, 1992; Kuhn *et al.*, 2010) and membrane-bound CTFα, where it is further cleaved by γ-secretase liberating AICD and p3 (Haass and Selkoe, 1993; Nhan *et al.*, 2015).

1.3.2 Liberation of amyloid-β isoforms by γ-secretase cleavage

The γ-secretase is a protease complex consisting of four subunits, namely presenilin enhancer 2 (PEN2), anterior pharynx-defective 1 (APH-1), nicastrin and presenilin-1 or 2 (PS1 or 2) (Kimberly *et al.*, 2003; Sato *et al.*, 2007; Lu *et al.*, 2014). Presenilin is the catalytic subunit of this complex and is located within the membrane domain, making γ-secretase an intramembrane aspartyl protease (De Strooper *et al.*, 1998; Wolfe *et al.*, 1999). PEN2 and APH-1 are believed to have functions in stabilizing the protease complex (Prokop *et al.*, 2004;

Niimura *et al.*, 2005) and nicastrin in the substrate recognition (Shah *et al.*, 2005). The γ-secretase catalyses the regulated intramembranous proteolysis of different type I transmembrane proteins such as APP and is important for proper Notch signalling (De Strooper *et al.*, 1998, 1999).

The first proteolysis of CTFβ by γ-secretase occurs at the epsilon site on position 48 or 49 producing either $A\beta_{x-45}$ or $A\beta_{x-46}$, respectively (Weidemann *et al.*, 2002; Sato *et al.*, 2003). This initial proteolysis is followed by a tripeptide cleavage of $A\beta_{x-48}$ to $A\beta_{x-45}$ or $A\beta_{x-49}$ to $A\beta_{x-46}$ to $A\beta_{x-43}$, resulting in $A\beta_{42}$ and $A\beta_{40}$, respectively (Takami *et al.*, 2009). This tripeptide cleavage is facilitated by three substrate-binding pockets in γ-secretase (Bolduc *et al.*, 2016b).

The previous substrate shedding of APP, resulting in CTFα or CTFβ, is required prior to γ-secretase cleavage and is considered to be generally true for γ-secretase substrates (Struhl and Adachi, 2000). However, γ-secretase substrate recognition is an ongoing topic of research and experimental evidence indicates γ-secretase can cleave APLP1 (amyloid precursor-like protein 1), a member of the APP protein family (Schauenburg *et al.*, 2018) and the membrane-bound receptor B-cell maturation antigen (BCMA) (Laurent *et al.*, 2015) without previous shedding. The underlying substrate recognition mechanism is currently undefined but data suggest a rather passive recognition based on size, where nicastrin act as gate-keeper by sterically blocking substrates retaining longer ectodomains (Bolduc *et al.*, 2016a). Furthermore, the flexibility of the substrate's transmembrane domain (Götz *et al.*, 2019), as well as the formation of a hybrid β-strand of cleavage substrate and catalytic subunit PS1 (Yang *et al.*, 2018; Zhou *et al.*, 2019) are hypothesized to be crucial elements for substrate recognition. Recently, data indicate that γ-secretase together with BACE1 and APP form a large, enzymatic active complex *in vitro*, resulting in an $A\beta_{42}$ to $A\beta_{40}$ ratio similar to the one observed in cell culture (Liu *et al.*, 2019).

1.3.3 Genetic variants affecting amyloid precursor processing in health and disease

Disease causative mutations in the genes *APP*, *PSEN1* and *PSEN2* encoding for APP and the catalytic subunits of γ-secretase, PS1 and PS2, respectively, are hypothesized to govern AD by altering APP processing (Selkoe and Hardy, 2016). For instance, the AD causative double mutation in *APP*, resulting in an amino acid substitution at position 670 from lysine to asparagine and at position 671 from methionine to leucine (Mullan *et al.*, 1992). This mutation was found in two families from Sweden experiencing EOAD and therefore was termed APP_{Swe} (Mullan *et al.*, 1992). The APP_{Swe} genetic variant leads to an increase in total Aβ (Citron *et al.*, 1992), without significantly changing the $A\beta_{42}$ to $A\beta_{40}$ ratio (Ancolio *et al.*, 1999). A different

APP mutation, first described in a Londoner cohort (termed APP_{Lon}) leads to an amino acid substitution at position 717 from valine to isoleucine (Goate *et al.*, 1991). APP_{Lon} carriers display increased levels of $A\beta_{42}$ peptides compared to $A\beta_{40}$ and thus harbour an increased $A\beta_{42}$ to $A\beta_{40}$ ratio (Suzuki *et al.*, 1994a; Scheuner *et al.*, 1996). A convenient explanation for the different outcomes observed in these two mutant *APP* might be provided by the location of the amino acid substitutions. In the APP_{Swe} variant the amino acid sequence alteration is located at the cleavage site for BACE1 (Tomasselli *et al.*, 2003; Deng *et al.*, 2013), whereas the APP_{Lon} affects the γ -secretase cleavage site (De Jonghe *et al.*, 2001).

A great proportion of mutations associated with fAD are detected in the catalytic subunit PS1 of γ-secretase (*'PSEN-1 - ALZFORUM'*, no date). *PSEN1* mutations associated with AD lead to an increase in $A\beta_{42}$ when genetically introduced into mice (Borchelt *et al.*, 1996; Duff *et al.*, 1996). Interestingly, a comprehensive *in vitro* analysis of 138 AD-associated *PSEN1* mutations indicates that the vast majority of tested genetic variants indeed increase the $A\beta_{42}$ to $A\beta_{40}$ ratio, although, lower the total production of Aβ compared to wildtype *PSEN1* (Sun *et al.*, 2017). The use of such an artificial *in vitro* setting might limit the applicability of these data to the complex environment in a patient's brain, as stated by the authors (Sun *et al.*, 2017). Despite its function as a catalytic active subunit in γ-secretase, PS1 is implicated in many cellular events such as macroautophagy (Lee *et al.*, 2010), neuronal apoptosis (Zhang *et al.*, 1998) and insulin signalling (Maesako *et al.*, 2011). AD causative mutations in *PSEN1* can elevate the cellular cholesterol levels in cell culture (Grimm *et al.*, 2005). A cholesterol-rich membrane composition is hypothesized to favour the colocalization of APP with the active BACE1 and γ-secretase complex within lipid rafts and thereby enhancing the amyloidogenic pathway (Cho et al. 2019).

Additional to malign mutations associated with AD, a protective mutation in *APP* has been reported as well (Jonsson *et al.*, 2012). This *APP* variant harbours a missense mutation and results in an amino acid substitution at position 673 from alanine to threonine (A673T), close to the BACE1 cleavage site (Jonsson *et al.*, 2012). It was first discovered in the Icelandic and Scandinavian populations and is suggested to be protective against AD by lowering the overall production of Aβ (Jonsson *et al.*, 2012). Interestingly, an alteration at the same position to valine (A673V) leads to an increased risk to develop AD by an enhanced Aβ production (Di Fede *et al.*, 2009). Although, an association with AD is only given at a homozygous state of this variant (Di Fede *et al.*, 2009).

Alterations of the amyloidogenic pathway due to genetic variants in *APP* as well as in the involved secretases are highly complex and demand a further scientific investigation to fully understand the underlying mechanisms. Together, malign as well as protective alterations point toward the great significance of this pathway for health and disease.

1.4 Translational animal models of Alzheimer's disease pathology

In order to perform experimental research which aims to elucidate pathological sequences in AD, choosing an appropriate disease model is decisive for the transferability of results from the model to humans. The most common disease models in biomedical research are rodent models with rats and mice accounting for approximately 95% of all laboratory animals (Hickman *et al.*, 2017). Rodents as well as non-human primates, the closest biological relatives to humans, do not develop the full AD phenotype in their lifespan (Walker and Jucker, 2017).

Genetically modified marmosets harbouring a deletion of exon 9 of *PSEN1* show enhanced production of $A\beta_{42}$ in fibroblast cells and might present the first primate model of fAD (Sato *et al.*, 2020). Whether this model develops Aβ and Tau pathology in the brain, reassembling the human AD phenotype, remains to be seen. The authors expect the onset of Aβ pathology in these animals from 2-3 years of age (Sato *et al.*, 2020). Great fields of applications are considered for such an AD model including biomarker studies as well as testing of clinical therapeutics (Sato *et al.*, 2020). However, the close proximity of non-human primates to humans evokes ethical debates about their use in biomedical research (Olsson and Sandøe, 2010; Prescott, 2020).

Genetically modified mouse lines overexpressing human genes involved in the generation of Aβ, such as *APP* and *PSEN1*, with or without AD-associated mutations, are reassembling the Aβ plaque pathology of AD and lack NFT (Drummond and Wisniewski, 2017). To overcome this limitation, AD-derived Tau intracranially introduced into amyloid-laden mouse brains can result in NFT and NP formation (He *et al.*, 2017). Another approach for the establishment of Tau pathology in an amyloidosis mouse model is an additional genetic modification of the gene encoding for Tau, *MAPT* (Oddo *et al.*, 2003). *MAPT* harbouring a mutation which leads to an amino acid substitution of proline for leucine at position 301 in human Tau results in frontotemporal dementia with parkinsonism linked to chromosome 17 in humans (Hutton *et al.*, 1998; Spillantini *et al.*, 1998) and tangle formation in mice (Oddo *et al.*, 2003). In a small proportion of sAD patients screened, genetic variants in *MAPT* have been identified and although putatively not causative for the disease, were hypothesized to co-operate with pathological changes in Aβ (Sala Frigerio *et al.*, 2015). Recent work on Tau fibril structures via electron microscopy expands the current classification of Tau pathology, since disease-specific differences in Tau folding have been detected which were unrecognized beforehand (Shi *et al.*, 2021b). This analysis might help to evaluate how accurate Tau pathology in animal models may model the pathology observed in humans.

Mouse models are far from perfect in remodelling the full spectrum of AD pathology but an isolated investigation of a specific pathological feature, often considered as a disadvantage, provides the opportunity to study mechanistic relationships in a simplified model (Radde *et al.*, 2008). Furthermore, the in-depth characterization of the homogenous disease model and tissue collection along the full disease course allows treatment intervention at precise disease stage. These aspects make a disease model for biomedical research superior to patients, potentially possessing great variability in terms of pathology and disease stage which escape current detection methods using biomarkers.

1.5 Biomarkers along Alzheimer's disease continuum

In 2016, a system was introduced which suggests dividing the major biomarkers used in AD diagnostic into three categories (A/T/N) and thereby becoming a useful tool for an unbiased, descriptive classification of AD based on biomarkers (Jack *et al.*, 2016). In this scheme, 'A' refers to pathophysiological changes in Aβ, 'T' gives a measure for Tau pathology and 'N' reflects neurodegeneration (Jack *et al.*, 2016). The A/T/N framework has been edited and refined in the past years with the aim to improve its predictive value and accuracy (Ebenau *et al.*, 2020; Bucci *et al.*, 2021; Cullen *et al.*, 2021; Delmotte *et al.*, 2021; Song *et al.*, 2022). Some biomarker changes according to the A/T/N system are presented as a scheme in Figure 3.

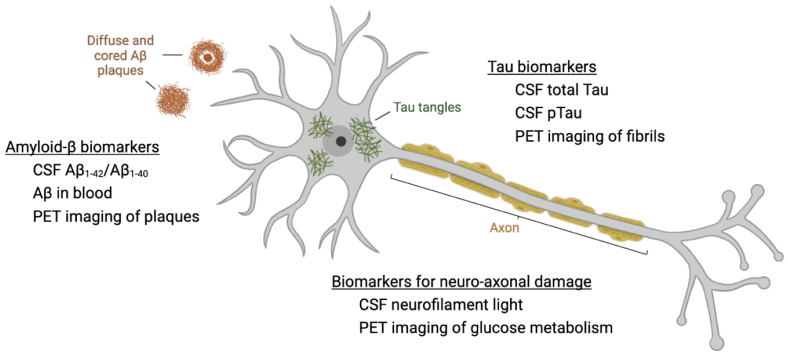

Figure 3 Schematic representation of a neuron with amyloid-β (Aβ) and Tau pathology and the respective biomarkers for Alzheimer's disease (AD) in line with the A/T/N scheme. The A/T/N system is intended to provide an unbiased descriptive classification of AD based on biomarkers, which can be measured using positron emission tomography (PET) and in body fluids including blood and cerebrospinal fluid (CSF) (Jack *et al.*, 2016). 'A' presents biomarker changes in Aβ most likely due to aggregation. 'T' describes pathological changes in tau, which can reflect tau pathology and to some

degree, Aβ pathology induced release of phosphorylated Tau into the CSF. 'N' provides a biomarker measure for neuro-axonal damage. Adapted from (Hansson, 2021), created with BioRender.com.

1.5.1 Biomarkers for cerebral amyloid-β pathology

The pathological event of Aβ deposition in the brain can be detected by biomarker changes specific for Aβ such as *in vivo* imaging of plaques using positron emission tomography (PET) as well as estimating Aβ in the body fluids CSF and blood (Jack *et al.*, 2016).

High ligand retention on amyloid PET using PET-ligands such as Pittsburgh compound B (PiB), an ^{11}C-labeled thioflavin-T derivate which binds to the amyloid structure of Aβ, is specific for β-amyloidosis (Klunk *et al.*, 2004). More recently, ^{18}F-labeled Aβ tracers targeting specifically insoluble Aβ fibrils in plaques have been approved for AD diagnostic measures (Hansson, 2021). PET scans in AD provide information about the topography (Pascoal *et al.*, 2020) and severity of pathological changes, such as the overall amyloid load (Clark *et al.*, 2011; Fleisher *et al.*, 2011; Bullich *et al.*, 2021). Therefore, PET imaging is a powerful tool for diagnosing as well as monitoring the disease progression. However, with increasing age of patients, the accuracy of an Aβ-PET scan for AD diagnosis decreases as the prevalence of amyloid pathology was shown to increase with age in cognitively normal and impaired individuals (Jansen *et al.*, 2015).

Fluid biomarkers for the detection of pathological changes in Aβ are currently based on blood and CSF (Zetterberg and Blennow, 2021). In CSF, significant differences in $Aβ_{38}$ $Aβ_{40}$ and $Aβ_{42}$ levels were found in AD patients compared to healthy controls, but interestingly, solely the $Aβ_{42}$ to $Aβ_{40}$ ratio was able to discriminate AD from non-AD dementias such as frontotemporal dementia (Janelidze *et al.*, 2016). A decrease in CSF $Aβ_{42}$ is also proposed to be one of the earliest biomarker changes in AD, detectable with current methods (Milà-Alomà *et al.*, 2020). The ratio between $Aβ_{42}$ and $Aβ_{40}$ shows high accuracy in detecting cortical Aβ aggregation, although these fluid biomarkers detected more Aβ-positive individuals compared to the Aβ-PET scan (Milà-Alomà *et al.*, 2021). The reason for this discordance might underly the applied Aβ-PET threshold (Milà-Alomà *et al.*, 2021). However, further validation is needed. Using the ratio of $Aβ_{42}$ to $Aβ_{40}$ offers the advantageous option to normalize inter-individual differences in the overall production and clearance of Aβ (Janelidze *et al.*, 2016; Deltombe *et al.*, 2022). Blood-based biomarkers for Aβ are less invasive compared to lumbar biopsy and becoming increasingly sensitive (Teunissen *et al.*, 2022). Evaluation of Aβ plasma biomarkers such as $Aβ_{42}$ to $Aβ_{40}$ ratios using mass spectrometry reveals high levels of concordance with Aβ-PET results (Nakamura *et al.*, 2018). However, due to the comparable low change in $Aβ_{42}$ to $Aβ_{40}$

ratios in blood, so far blood-based biomarkers for Aβ reach not the sensitivity and specificity of CSF Aβ measures (Zetterberg and Blennow, 2021).

1.5.2 Tau phosphorylation state as a biomarker in Alzheimer's disease

Similar to Aβ plaques, Tau pathology can be visualized by increased ligand retention on PET using either Tau specific PET-ligands such as [^{11}C]PBB3 (Maruyama *et al.*, 2013) or ligands binding Aβ and Tau aggregates like [^{18}F]FDDNP (Shoghi-Jadid *et al.*, 2002; Wang and Edison, 2019). Nevertheless, Tau PET imaging is limited to the visualization of Tau deposits (Leuzy *et al.*, 2019), whereas the detection of early disease-related changes in Tau, for instance, the phosphorylation-state, requires fluid-biomarker analysis (Barthélemy *et al.*, 2020a).

Several p-Tau species have been identified in the blood (Barthélemy *et al.*, 2020b) and CSF (Ishiguro *et al.*, 1999) in patients associated with AD. In CSF, three broadly recognized biomarkers are Tau phosphorylated at threonine-181 (p-Tau-181), at threonine-217 (p-Tau-217) and threonine-231 (p-Tau-231) (Suárez-Calvet *et al.*, 2020). In particular, the CSF and blood p-Tau-181 variant is an established biomarker for AD, a good indicator for Aβ pathology (Clark *et al.*, 2021) and predictive for memory decline (Therriault *et al.*, 2021). The p-Tau-217 variant measured in CSF is highly indicative for Aβ plaque load and exceeds p-Tau-181 in specificity and sensitivity (Barthélemy *et al.*, 2020c; Janelidze *et al.*, 2020a). Interestingly, in fAD the levels of specific p-Tau species detected in CSF change over the time course of AD progression, indicating a dynamic process in Tau phosphorylation depending on the pathological state and disease stage (Barthélemy *et al.*, 2020a). An increase in CSF p-Tau-181 and p-Tau-217 was detected when Aβ plaque onset becomes apparent by PiB-PET, however, a decrease is recognized at the onset of Tau pathology, detectable by PET (Barthélemy *et al.*, 2020a). Some p-Tau species in the blood are reliable biomarkers for Tau and Aβ pathology (Barthélemy *et al.*, 2020b; Janelidze *et al.*, 2020b; O'Connor *et al.*, 2020; Ashton *et al.*, 2021). Recently, combinations of several blood-biomarkers such as $A\beta_{42}$ to $A\beta_{40}$ ratio, p-Tau-217 or p-Tau-181 with other accessible measures, for instance, plasma neurofilament light (NfL) reveal promising results with increased accuracy for the prediction of cognitive decline and the risk for AD (Cullen *et al.*, 2021; Palmqvist *et al.*, 2021).

1.5.3 Neurofilament light reflects disease-unspecific neurodegeneration

A hypothetical biomarker model along the AD continuum (preclinical, prodromal and dementia stage), predicts Aβ and Tau pathology are followed by progressive neuronal and synaptic loss resulting in tissue atrophy (Hampel *et al.*, 2021).

Fluid biomarkers for neurodegeneration have the potential to detect early pathological changes decades before severe brain atrophy becomes apparent (Pereira *et al.*, 2017; Preische *et al.*, 2019). Neurofilament proteins, encompass NfL, NfM (neurofilament middle), NfH (neurofilament heavy), peripherin and α-internexin, which are the structural building blocks of intermediate filaments found in the cytoplasm of neurons (Yuan *et al.*, 2017). The release of neurofilaments into CSF and blood is considered as a result of neuronal death or axonal damage although, the mechanism underlying NfL liberation is currently unknown (Thebault *et al.*, 2020). In neurological healthy infants between zero and four years of age, high NfL levels have been detected in blood serum (Nitz *et al.*, 2021), which is hypothesized to reflect programmed cell death in the developing CNS (Buss *et al.*, 2006). NfL is one of the most recognized biomarkers for neuronal loss in AD and other neurodegenerative diseases, including Creutzfeldt-Jakob disease (CJD) (Kanata *et al.*, 2019), amyotrophic lateral sclerosis and frontotemporal dementia (Olsson *et al.*, 2019). Increased levels of NfL are also detectable in patients who experienced traumatic brain injury (Graham *et al.*, 2021), classifying NfL as a general marker for neuronal damage. Since the majority of AD patients are experiencing late disease onset (Carmona *et al.*, 2018), it is important to acknowledge that NfL increases due to normal ageing, which is hypothesized to reflect age-dependent neurodegeneration (Idland *et al.*, 2017) and/or remodelling of neural circuits (Kaeser *et al.*, 2021).

In AD patients, elevated CSF NfL concentrations provide a measure that can dissect AD and control groups (Zetterberg *et al.*, 2016; Olsson *et al.*, 2019; Dhiman *et al.*, 2020). Further, CSF NfL concentrations correlate with an increase in brain atrophy in patients with MCI (Zetterberg *et al.*, 2016) and are an indicator for the severity of cognitive impairments in patients with AD and frontotemporal dementia (Olsson *et al.*, 2019). Similar has been observed in blood plasma, where NfL levels predict a decline in cognitive performance (Sugarman *et al.*, 2020; He *et al.*, 2021). In rodent disease models as well as AD patients, NfL levels in blood and CSF correlate with each other (Bacioglu *et al.*, 2016; Jin *et al.*, 2019). These data indicate blood NfL is a non-invasive, accessible biomarker with biological relevance for neurodegeneration. Interestingly, plasma NfL is not predictive for the conversion of MCI to AD (Sugarman *et al.*, 2020) whereas the serum NfL rate of change anticipates disease progression at early, pre-symptomatic stages of fAD (Preische *et al.*, 2019). Furthermore, high baseline levels in plasma NfL are associated with an increased risk to develop AD (De Wolf *et al.*, 2020).

NfL is a many-sided biomarker reflecting on one hand neurodegeneration in disease and on the other age-dependent neurological processes, which together point towards the importance of the combination of several disease-specific biomarkers for a reliable diagnosis of AD.

1.6 Mechanisms of amyloid formation in Alzheimer's disease

Many neurodegenerative diseases share general commonalities such as their chronic and progressive nature, an increased prevalence with ageing, neuronal loss in specific areas and selective brain volume loss (Gan *et al.*, 2018; Soto and Pritzkow, 2018). A molecular hallmark of these diseases, is the initial misfolding of a protein, inducing further aggregation of more proteins in a template-dependent manner, resulting in disease-specific amyloid deposition (Prusiner, 2012; Walker and Jucker, 2015).

Such templated protein aggregation was initially used to describe the infectious agent of scrapie, a prion disease affecting sheep (Griffith, 1967). The term 'prion' was established in 1982 and describes a 'proteinaceous infectious particle' (Prusiner, 1982). The cellular prion protein (PrP^{C}) is a host-encoded cell-surface glycoprotein (Stahl *et al.*, 1987; Haraguchi *et al.*, 1989). The disease-associated prion protein (PrP^{Sc}) forms pathological deposits (Prusiner, 1998a) as observed in bovine spongiform encephalopathies (BSE) in cattle (Hope *et al.*, 1988) and CJD in humans (Merz *et al.*, 1983). Although PrP^{Sc} and PrP^{C} do not differ in amino acid sequence, they possess different biochemical features and tertiary protein fold (Prusiner, 1998b). PrP^{Sc} was shown to have a higher degree of β-strand structural fold compared to PrP^{C} (Pan *et al.*, 1993).

1.6.1 Amyloid-β templated aggregation

Templated protein aggregation can lead to amyloid fibrils with a characteristic cross-β fold due to the alignment of β-strands of the incorporated proteins perpendicular to the fibrils' long axis (Tycko, 2015). The initial step of the aggregation process is termed 'nucleation' and describes the formation of an aggregation nucleus or seed, which refers to the smallest unit, presumably an oligomer, facilitating amyloid fibril formation (Chatani and Yamamoto, 2018). One of the first assays to follow amyloid formation *in vitro* established ThT fluorescence spectroscopy to visualize the aggregation process of Aβ (LeVine, 1993). The time-dependent aggregation follows a sigmoidal curve which was divided into three distinct sections; the lag, elongation and plateau phase (Jarrett and Lansbury, 1993). Interestingly, the longitudinal amyloid-PET load in MCI and AD patients follows a sigmoid formation as well when plotted as a function of time (Clifford *et al.*, 2013). A schematic overview of the distinct primary and secondary nucleation pathways, which will be described in the following sections, as well as the elongation phase of Aβ aggregation, is provided in Figure 4.

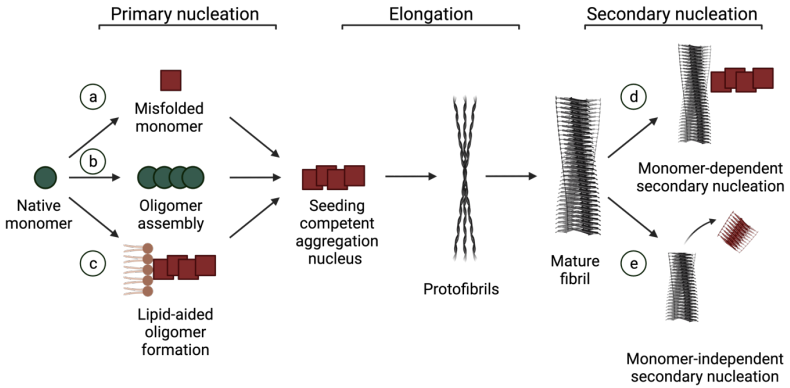

Figure 4 Nucleation pathways of amyloid-β aggregation. Primary nucleation of amyloid-β (Aβ) monomers results in a seeding competent aggregation nucleus which facilitates elongation into protofibrils and mature fibrils formation. Aβ fibrils can facilitate secondary nucleation events. The molecular mechanism of Aβ primary nucleation is currently undefined. Three potential pathways are depicted in a, b and c. **a)** The nucleation according to the nucleation-dependent model describes the initial misfolding of an Aβ monomer with subsequential recruitment of additional monomers which are forced into an aggregation-prone fold. **b)** The nucleation-conversion model describes the assembly of Aβ monomers into oligomers while preserving their native fold. The close proximity of monomers is considered to favour the change of a structural conversion into an aggregation-prone nucleus. **c)** Heterogenous primary nucleation describes the association of Aβ monomers with heterogeneous molecules such as lipid membranes which potentially facilitate an initial misfolding of Aβ, resulting in accelerated aggregation. In d and e, secondary nucleation events are shown. **d)** In the monomer-dependent nucleation process, the surface of a mature fibril is considered to aid nucleation of associated Aβ monomers. **e)** The monomer-independent nucleation pathway describes the fragmentation of a fibril into smaller seeding competent units. Created with BioRender.com.

The molecular mechanism of Aβ nucleation is a current topic of investigation and several models have been proposed among two, the classical 'nucleation-dependent model' (Jarrett and Lansbury, 1993) and the 'nucleation conformational conversion model', will be described.

1.6.2 Aggregation models to describe the primary nucleation of amyloid-β

Amyloid aggregation, according to the nucleation-dependent model, is believed to occur above a critical Aβ concentration of initially naïve folded proteins, leading to the formation of an aggregation nucleus (Jarrett and Lansbury, 1993) (Fig. 4a). This nucleation event is considered to involve the transition from a largely α-helical or intrinsically disordered Aβ peptide to an amyloid fold by partial exposure of disordered protein segments and/or a rearrangement of the secondary protein structure, both being energetically unfavourable

(Zheng *et al.*, 2016; Grasso and Danani, 2020). Therefore, the formation of such a nucleation seed is considered to be a rare and rate-limiting event in the Aβ aggregation cascade (Eisenberg and Jucker, 2012; Ghosh *et al.*, 2016).

The nucleated conformational conversion model might present a variation of the classic nucleation-dependent model (Serio *et al.*, 2000). In the nucleation-dependent model, structural rearrangement is a precondition for aggregation, while in the conversion model, the formation of Aβ assemblies precedes structural conversion (Serio *et al.*, 2000; Chatani and Yamamoto, 2018). The nucleation conformational conversion model proposes a leading role of early aggregates in the nucleation process (Lee *et al.*, 2011). Small oligomers or prefibrillar intermediates are hypothesized to form, thereby increasing the chance of intermolecular interactions and facilitating the conversion into a β-sheet rich structure which subsequently functions as a seeding competent nucleus (Garcia *et al.*, 2014) (Fig. 4b). The differences between both models might appear minor, however, a precise understanding of the molecular mechanism of Aβ nucleation, generally termed 'seed formation', is essential as it potentially presents the earliest target opportunity to prevent amyloid aggregation.

1.6.3 Driving forces for homogenous and heterogenous primary nucleation events

Due to the transient nature of early aggregation assemblies, direct experimental examination of their formation is challenging and thus many data modelling amyloid formation were obtained by theoretical computer studies (Grasso and Danani, 2020) or by adaption of general mechanisms from other research areas, such as crystallography (So *et al.*, 2016).

The critical concentration of a protein, which refers to the monomer concentration required for polymerization to occur (Jarrett and Lansbury, 1993), together with its aggregation propensity was shown to be decisive for aggregation (Ciryam *et al.*, 2013). Furthermore, supersaturation, defined as the ratio between the cellular protein concentration and the critical concentration of a protein, was proposed to be a major driver of protein aggregation in neurodegenerative diseases (Ciryam *et al.*, 2015). In line with this, $A\beta_{42}$ peptides aggregated and formed oligomers *in vitro* above a critical monomer concentration (Novo *et al.*, 2018). In cell culture, synthetic $A\beta_{42}$ but not $A\beta_{40}$ was shown to aggregate within lysosomal/endosomal compartments after internalization by murine cortical neurons and neuroblastoma cells (Hu *et al.*, 2009). An uptake into lysosomal/endosomal compartments increased the concentration of Aβ by two orders of magnitude compared to that in the extracellular fluid, which was hypothesized as a driving factor in the aggregation process (Hu *et al.*, 2009).

In vitro performed aggregation studies based on homogenous monomeric Aβ solutions examine the 'homogenous primary nucleation' (Srivastava *et al.*, 2019). Additionally, environmental factors like the presence of surfaces have the potential to either accelerate or inhibit nucleation (Grigolato and Arosio, 2021). The initial amyloid nucleation as a result of cooperative interactions of distinct molecules is referred to as 'heterogenous primary nucleation' (Srivastava *et al.*, 2019) (Fig. 4c). $A\beta_{42}$ nucleation was greatly enhanced by cholesterol-rich lipid membranes via a heterogeneous nucleation pathway (Habchi *et al.*, 2018). Furthermore, in cell culture, $A\beta_{42}$ aggregation was observed on cell surfaces, which was accelerated by actin-driven cell membrane protrusion (Kuragano *et al.*, 2020). It is hypothesized, heterogeneous Aβ nucleation requires lower concentrations of Aβ peptides and is, due to the great complexity within a cell, more likely to occur in natural systems compared to homogeneous nucleation (Srivastava *et al.*, 2019). However, current scientific models lack the ability to incorporate all putative biologically relevant nucleators in their study designs and therefore can model the nucleation process only incomplete.

1.6.4 Secondary nucleation pathways

The presence of mature amyloid fibrils creates the possibility of a 'secondary nucleation' pathway (see Törnquist *et al.*, 2018 for review). This type of nucleation can be further divided into 'monomer-dependent secondary nucleation', describing the formation of a new aggregation nucleus by monomers, catalysed by the surface of an amyloid fibril (Zimmermann *et al.*, 2021) (Fig. 4d) and 'monomer-independent secondary nucleation', for instance, fragmentation referring to an amyloid fibril breakage that results in smaller fragments which serve as new nucleation seeds (Marrero-Winkens *et al.*, 2020) (Fig. 4e). Above a critical concentration of $A\beta_{42}$ fibrils, secondary nucleation is hypothesized to overtake primary nucleation (Cohen *et al.*, 2013). Similar to secondary nucleation via fragmentation, an exogenous formed seed can act as a template and induce/accelerate aggregation *in vitro* (Jarrett and Lansbury, 1993; Harper and Lansbury, 1997) and *in vivo* (Kane *et al.*, 2000; Meyer-Luehmann *et al.*, 2006) when introduced into a system with available respective monomer entities.

2 Material and Methods

2.1 Experimental animals and conducted treatments and interventions

To study biomarker trajectories and their dependency on Aβ, female and male heterozygous C57BL/6J-TgN(Thy1-APPSw,Thy1-PSEN1*L166P)21 (APPPS1) mice (Radde *et al.*, 2006) as well as transgene-negative (WT) mice were used. Male heterozygous C57BL/6J-TgN(Thy1.2-hAPP751-KM670/671NL)23 (APP23) mice were (Sturchler-Pierrat *et al.*, 1997) used for passive immunization studies. Heterozygous male and female C57BL/6 JNpa-Tg(Thy1App)23/1Sdz (APP23N) mice were used as hosts for *in vivo* seeding assays as well as for titer experiments following passive immunization. No differences were noted in phenotype between APP23 and APP23N. All mice were bred at the Hertie Institute for Clinical Brain Research (Tübingen, Germany) and experiments were performed according to the veterinary office regulations of Baden-Wuerttemberg (Germany), after approval by the local Animal Care and Use Committee. An estimation of the required group size was done using the statistical power analysis program G*Power or based on experience from previous experiments.

2.1.1 BACE1 inhibitor treatment

The BACE1 inhibitor NB-360 provided by Novartis was milled and mixed into food pellets for rodents at a concentration of 0.5 g NB-360 kg^{-1} food pellets. APPPS1 and WT mice were fed *ad libitum* either BACE1 inhibitor containing pellets or control pellets without NB-360 but with identical formula (Neumann *et al.*, 2015; Schelle *et al.*, 2017). APPPS1 mice were either treated for 3 months, referred to as 'short-term' or for 9.5 and 20 months, both referred to as 'chronic' treatment. The chronic treatment was also conducted with WT mice. Short-term treatments were initiated at the age of 1.5, 12 and 18.5 months, referred to as 'young', 'adult' and 'aged' groups, respectively. The chronic treatment for 20 months was initiated at the age of 1.5 months and is further referred to as 'young-chronic' whereas the 9.5-month treatment was started at 12 months of age and accordingly is referred to as 'adult-chronic'.

2.1.2 Passive immunization

Male APP23 mice received passive immunization intraperitoneally for 5 consecutive days. For this, antibodies were thawed on ice and applied at a concentration of 0.5 mg per mouse and day. Mice used for biochemical and histological analyses of Aβ as well as secondary

pathologies within the brain were either sacrificed 1.5 or 6 months post-injection. Mice used for the antibody titer study were sacrificed 1, 7, or 21 days post-injection.

The chimeric murinized (cm) versions of the human antibody Gantenerumab (cmGantenerumab, (Bohrmann *et al.*, 2012)), Aducanumab (cmAducanumab, (Sevigny *et al.*, 2016; Arndt *et al.*, 2018)), Solanezumab (m266 (DeMattos *et al.*, 2001)), Crenezumab (mC2 (Adolfsson *et al.*, 2012)) and Donanemab (mE8 (DeMattos *et al.*, 2012)) were used. Furthermore, the monoclonal murine anti-wheat auxin immunoglobulin G (IgG) 2a (Amsbio, Abingdon, UK) and murine IgG2a antibody P1.17 (unknown antigen (Sevigny *et al.*, 2016)) as control 1 (Ctrl 1) and control 2 (Ctrl 2), respectively, were used as control antibodies. *cm*Gantenerumab, m266, and mC2 were provided by Lundbeck (Copenhagen, Denmark), cmAducanumab (cmAdu) and P1.17 were provided by Biogen (Cambridge, MA), and mE8 was provided by the Fraunhofer Institute for Cell Therapy (Dresden, Germany). The antibodies were recombinantly generated and purified. The antibody variable light chain-murine kappa constant domain and variable heavy chain-mIgG constant domain were cloned into a mammalian cell expression vector. After cell transfection, the culture media was collected and ultracentrifuged. Antibodies were isolated applying either protein-A or protein-G Sepharose affinity chromatography with a subsequent buffer exchange to PBS (Invitrogen, Carlsbad, CA) according to standard protocols for monoclonal antibody purification. Sterile filtration of antibodies was performed using 0.2 μm filters. Antibodies were stored at -80°C. The antibody Beta1 has been described previously (Paganetti *et al.*, 1996; Meyer-Luehmann *et al.*, 2006).

2.1.3 Intracerebral injections into APP23 host mice

Bilateral stereotaxic injection of 2.5 μl of a sample was done into the hippocampi of 2- to 3-month-old APP23 mice (n=5-7 mice per group). For this, mice were deeply anaesthetized via intraperitoneal injections of either the 3-component anastatic (fentanyl 0.05 mg kg^{-1} body weight, midazolam 5 mg kg^{-1} body weight, medetomidine 0.50 mg kg^{-1} body weight) or a mixture of ketamine (110 mg kg^{-1} body weight) and xylazine (20 mg kg^{-1} body weight) in saline. A Hamilton syringe was used to deliver the sample into the hippocampus (anteroposterior, –2.5 mm; left/right, ±2.0 mm; dorsoventral, –1.8 mm) at a rate of 1.25 µl min^{-1} and further held in the injection site for 2 min before being withdrawn. The incision has been cleaned and closed. In case the 3-component anastatic was used, an antidote (flumazenil 0.5 mg kg^{-1} body weight and atipamezole 2.5 mg kg^{-1} body weight) was applied subcutaneously. Mice were monitored closely after surgery until full recovery.

For the preparation of brain homogenates (see below), of APPPS1 mice treated with BACE1 inhibitor or corresponding control pellets, homogenisation buffer (150 mM NaCl, 5 mM EDTA, 50 mM Tris, and Pierce protease and phosphatase inhibitor) (Thermo Fisher Scientific, Waltham, MA) was used, except for brains from the group 'young-chronic', which were homogenised in PBS (Gibco, Thermo Fisher Scientific). Brain homogenates from one treatment group were pooled and centrifuged at 3000 *g* for 5 min. The supernatant was collected (referred to as 'seeding extract'), aliquoted and frozen at -80°C. For each injection, a fresh aliquot was thawed shortly before usage. For the estimation of the seeding dose 50 (SD_{50}), seeding extracts were serially diluted up to 10^{-4} in PBS and also injected.

PBS-homogenates from mice receiving passive immunization with control antibody or cmAdu were used for bilateral stereotaxic injections. Brain homogenates of one treatment group were pooled aliquoted and frozen at -80°C. For each injection, a fresh aliquot was thawed shortly before usage.

Enzymatic liquified ARPA ('Antibody Recognition Profiling of amyloid β assemblies', see below) fractions (F1 to F2) of PBS-homogenates from the frontal cortex of three pooled AD patients (see below) were used for bilateral stereotaxic injections. After separation by size and enzymatic digestion, the fractions were aliquoted, frozen at -80°C and shortly before usage thawed. Fractions were serially diluted up to 10^{-2} in PBS to estimate the SD_{50}.

Mice receiving seeding extract of APPPS1 mice were sacrificed 6 months post-injection, whereas mice inoculated with brain homogenate of mice receiving passive immunization or ARPA fractions containing human brain material, were sacrificed after 8 months.

2.1.4 Collection of cerebrospinal fluid and brain

Mice were deeply anaesthetized using a mixture of ketamine (115 mg kg^{-1} body weight) and xylazine (10 mg kg^{-1} body weight) in saline via an intraperitoneal application. As soon as the mouse showed a negative pedal reflex response, as an indicator of deep pain recognition, CSF collection was initiated. CSF was collected as described previously (Eninger *et al.*, 2022). Briefly, the dura mater was punctured with a syringe (30 G, 0.3 x 8 mm needle size) to access the cisterna magna. Using a 20 µl GELoader tip (Eppendorf Vertrieb), CSF was collected. After centrifugation at 2000 *g* for 10 min, CSF was checked for any kind of cell debris or blood contamination. CSF was aliquoted and frozen at -80°C.

Following CSF collection, each mouse was perfused transcardially with ice-cold PBS (Gibco, Thermo Fisher Scientific). The brain was accessed. Mouse brains used for histological as well as biochemical analyses were bisected by a mid-line sagittal cut and the lower brainstem and

the cerebellum were removed. One hemisphere was snap-frozen on dry ice, while the other was fixed in 4% paraformaldehyde (PFA) in PBS for 2 days at 4°C. After fixation, the brain was incubated in 30% sucrose in PBS for 2 days at 4°C and subsequently frozen in 2-methyl-butane on dry ice. All frozen brain samples were stored at -80°C until further analyses. For solely histological analyses, mouse brains were not bisected and fixed as a whole in PFA as described.

2.2 Human brain tissue

Human tissue samples were obtained from 6 clinically and pathologically diagnosed AD cases (54 to 81 years of age; all Braak stage VI) as well as two healthy subjects (80 and 86 years). The samples were obtained from the Emory University Goizueta Alzheimer's Disease Research Center (ADRC) and acquired under proper Institutional Review Board (IRB) protocols with consent from families. Human brain tissue was homogenized in PBS (Gibco, Thermo Fisher Scientific) at a final concentration of 10% (w/v), aliquoted and frozen at -80°C until further analyses.

2.3 Biochemical analyses of brain samples

2.3.1 Brain tissue homogenisation

Frozen brain tissue was homogenised at 10% (w/v) in sterile PBS (Gibco, Thermo Fisher Scientific) or homogenisation buffer (150 mM NaCl, 5 mM EDTA, 50 mM Tris, and Pierce protease and phosphatase inhibitor) (Thermo Fisher Scientific, Waltham, MA) with the Precellys®24 high-throughput tissue homogeniser (Bertin Technologies; 7-ml lysing tubes with 2.8-mm ceramic beads). Homogenisation was carried out at 5500 r.p.m twice for 10 s with a 10-s break in between. To prepare seeding extract, 10% brain homogenate was centrifuged for 5 min at 3000 *g*. The supernatant was collected, henceforth referred to as 'seeding extract', aliquoted and frozen at -80°C until further use.

2.3.2 Brain amyloid-β estimation by electrochemiluminescence-linked immunoassay

Aliquots of 10% brain homogenates or seeding extracts were thawed on ice. For direct formic acid extraction, thawed brain homogenates were mixed with cold formic acid (FA; Sigma-Aldrich; minimum purity of 96%) at a ratio of 1:3.2. Samples were sonicated on ice for 35 s and centrifuged at 25,000 *g* for 1 h at 4°C. The supernatants were collected and neutralized (1:20) with neutralisation buffer (1 M Tris base, 0.5 M Na_2HPO_4, 0.05% NaN_3 (w/v)).

For the serial extraction of Aβ, 130 µl brain homogenate was mixed with an equal amount of 2% Triton X-100 and incubated on ice for 15 min. During this incubation time, every 5 min samples were shortly vortexed. Samples were centrifuged at 100,000 *g* for 15 min at 4°C, the supernatant was collected (termed 'Triton-soluble fraction'), aliquoted and frozen at -80°C. The pellets were further used for FA extraction. According to the volume of the aspirated supernatant, the pellet was mixed with cold 70% (v/v) FA (diluted in H_2O). Sonication, centrifugation and supernatant neutralisation was done as described before. This fraction was termed the 'FA-soluble fraction'.

An estimation of $Aβ_{x-38,}$ $Aβ_{x-40}$ and $Aβ_{x-42}$ in brain homogenates/ seeding extracts was done by an electrochemiluminescence (ECL)-linked immunoassay (Meso Scale Discovery), based on the commercially available V-PLEX Aβ Peptide Panel 1 Kit using either 6E10 or 4G8 as detection antibodies. The assays were performed according to the manufacturer's instructions. In brief, the pre-coated 96-well plates were blocked for 1 h with buffer (Diluent 35, Meso Scale Discovery) and washed three times with 0.05% Tween 20 (Carl Roth) in PBS (v/v). In order to stay within the linear range of the assay, formic acid extracts were diluted up to 1:300, depending on the Aβ load of the sample. Diluted extracts were incubated with either SULFO-TAG™-labeled 6E10 or 4G8 detection antibody for 2 h at room temperature. Unbound detection antibodies were removed by washing three times with 0.05% Tween 20 (Carl Roth) in PBS (v/v). MSD Read Buffer T was added and the plate was immediately read on the Sector Imager 6000. Internal reference samples were included as controls on every plate. Data analysis was performed using either the MSD DISCOVERY WORKBENCH software 2.0 or 3.0. Samples measurements with a coefficient of variation (CV) >20% of the calculated sample concentration were excluded. For individual Aβ values below the respective assay detection limit, a fixed value, the lower limit of detection of the plate divided by $\sqrt{2}$, was imputed (Maia *et al.*, 2013).

Brain Aβ in formic acid extracts from the 2- to 8-month-old untreated APP23 mice were measured on the Simoa™ platform (Quanterix, Billerica, MA) using the Simoa Human $Aβ_{40}$ 1.0 and Simoa Human $Aβ_{42}$ 1.0 immunoassay kits (Quanterix, Billerica, MA), according to manufacturer's protocol. Formic acid extracts were diluted at 1:16 and 1:4 for $Aβ_{40}$ and $Aβ_{42}$, respectively.

2.3.3 Antibody Recognition Profiling of amyloid-β assemblies (ARPA)

Agarose electrophoresis was used to semi-natively separate Aβ assemblies by size (Bagriantsev *et al.*, 2006). A 2% low-melting agarose gel (w/v) (Thermo Fisher Scientific) in

semi-denaturing buffer (200 mM glycine and 25 mM Tris base) and 0.1% sodium dodecyl sulfate (SDS) was prepared in a gel cassette (Thermo Fisher Scientific). For electrophoretic separation, the gel was placed into a Bolt Mini Gel Tank (Thermo Fisher Scientific), filled with semi-denaturing buffer containing 0.1% SDS (v/v). Brain homogenate (65 μg total protein) was mixed with sample buffer (20 mM Tris-acetate (w/v), 0.5 mM EDTA (v/v), 2% SDS (v/v), 0.025% bromophenol blue (v/v), 5% glycerol (v/v)), incubated for 7 minutes at room temperature and instantly loaded into the agarose gel. Note that for intracerebral injections of ARPA fractions, seeding extract was loaded instead of 10% brain homogenate. The SeeBlue Plus2 pre-stained protein standard (Thermo Fisher Scientific) was used as a reference and gel electrophoresis proceeded until the phosphorylase marker band migrated 4 cm within the gel. The agarose gel was fractionated into pieces of 0.7 cm x 0.5 cm for the comb fraction (F1), and 0.7 cm x 1 cm for all other fractions (F2 to F7). Each fraction was placed into a 1.5 ml tube (Protein LoBind, Eppendorf AG) and either used for enzymatic liquefaction or melting with denaturing sample buffer.

The gel fragment for enzymatic digestion was diluted to 0.5% agarose (w/v) in elution buffer (50 mM Bis-Tris, 1 mM EDTA, pH 6.8), melted at 65°C for 10 min at an agitation rate of 1,200 r.p.m and cooled down to 43°C for 15 min. Agarase from *Pseudomonas atlantica* (Sigma-Aldrich) at a concentration of 0.5 U 100 μl^{-1} agarose (0.5%) incubated for 1 h at 43°C with a constant shaking of 1,200 r.p.m. Samples were frozen and stored at -80°C until further use.

For quantitative analyses by western blotting, an agarose piece was melted using denaturing sample buffer (62.5 mM Tris-HCl pH 6.8; 8.3% glycerol (v/v), 2% SDS (v/v), 100 mM dithiothreitol (DTT), 0.025% bromophenol blue (w/v)) at 90°C for 10 min. Melted fractions were stored at -20°C until further processing.

Protein G Dynabeads™ (Thermo Fisher Scientific) and Aβ-targeting antibodies (as described above) were used for immunoprecipitation (IP) of size-separated Aβ assemblies from liquified agarose pieces. The conjugation of the capture antibody to the beads was performed according to the manufacturer's instructions. Antibody conjugated beads were mixed with enzymatically digested agarose pieces and incubated overnight at 4°C while mixing. The sample to bead ratio for amyloid-laden brain material was 1:1 and for brain material derived from pre-depositing mice, a sample to bead ratio of 5.25:1 was used. Also, 75-time more sample as input was used when derived from pre-depositing mice compared to amyloid-laden brain material. Unbound sample was removed from the coupled beads by washing twice with PBS-T (0.05% Tween20 (v/v)). Beads were transferred into new tubes and bound proteins were eluted using 1x NuPAGE LDS Sample Buffer (Thermo Fisher Scientific) containing

150 mM DTT at 70°C for 10 min. The eluate was transferred to a new 1.5 ml tube (Protein LoBind, Eppendorf AG), frozen and stored at -80°C until denaturing immunoblot analysis.

Western blot analyses were carried out using NuPAGE 4-12% Bis-Tris Protein Gels (Thermo Fisher Scientific) with 1x MES SDS Running Buffer (Thermo Fisher Scientific). After gel electrophoresis, proteins were blotted onto a nitrocellulose membrane (semi-dry; Bio-Rad Laboratories, Hercules, CA), equilibrated in glycine transfer buffer (192 mM glycine, 25 mM Tris base, 20% methanol (v/v)). The membrane was placed in PBS (Gibco, Thermo Fisher Scientific) and boiled for 5 min at 90°C. Blocking of unspecific binding sites was done with 5% milk in PBS-T (w/v) for 1 h at room temperature. Primary antibody decoration using anti-Aβ 6E10 antibody (1:2500; BioLegend, San Diego, CA) was done overnight at 4°C followed by decoration with secondary HRP-coupled goat anti-mouse antibody (1:30000; Jackson ImmunoResearch, Cambridgeshire, UK) for 1 h at room temperature. After primary and secondary incubation steps, the membrane was washed 5-times for 5 min with PBS-T. Using SuperSignal West Dura Extended Duration Substrate (Thermo Fisher Scientific) and either highly sensitive X-ray films (Amersham Hyperfilm ECL, GE Healthcare, Chicago, IL) or a chemiluminescence imager (XSTELLA1.00; Raytest Isotopenmessgeräte GmbH, Straubenhardt, Germany), densitometric values were obtained. Images from XSTELLA1.00 were further quantitatively processed with the AIDA image analyzer v.4.27 (Raytest Isotopenmessgeräte GmbH). Adjustments to the contrast of immunoblots were for illustration purposes only and did not influence quantitative analyses.

2.4 Pharmacokinetics of antibodies in blood plasma

The antibody concentration in mouse plasma was determined by ELISA. Lyophilized synthetic $A\beta_{1-40}$ and $A\beta_{1-42}$ peptides in trifluoroacetate salt (Bachem, Bubendorf, Switzerland) were dissolved in dimethyl sulfoxide (DMSO) at a concentration of 4.33 and 4.51 µg μL^{-1}, respectively. The peptides were aliquoted and stored at -80°C until usage. To test for m266 and Beta1 in blood plasma, $A\beta_{1-40}$ and $A\beta_{1-42}$ were used, respectively. For an estimation of cmAdu in blood plasma, pre-aggregated $A\beta_{1-42}$ was used. For this, 100 µM $A\beta_{1-42}$ was incubated with 10 mM HCl (Merck, Darmstadt, Germany) and 150 mM NaCl (VWR Chemicals, Radnor, PA) in a final volume of 100 µL for 3 days at 37°C, leading to Aβ aggregation. Pre-aggregated $A\beta_{1-42}$ was stored at 4°C until further use. For coating, 96-well plates (Thermo Fisher Scientific) were washed with PBS (Gibco, Thermo Fisher Scientific) and coated with 10 ng of synthetic Aβ species in coating buffer (50 mM Sodium Carbonate; pH 9.6 with NaHCO3) overnight at 4°C on a shaker at 40 r.p.m. Unbound Aβ species were removed by

washing the plates four times with 0.05% PBS-T (0.05% v/v Tween-20). Unspecific binding sites were blocked with 1% BSA (Sigma-Aldrich) in PBS-T for 2 h at room temperature on a shaker. After washing the plates with PBS-T, samples or standards diluted in PBS-T containing 0.1% BSA were added to the plates in triplicates and incubated overnight at 4°C on a shaker at 40 r.p.m. Plasma samples were measured in dilution 1:200 and 1:2000. After a washing step with PBST-T, secondary antibody incubation was performed at room temperatures for 2 h on the shaker. The alkaline phosphatase-conjugated AffiniPure rabbit anti-mouse IgG (H+L) antibody (1:5000; Jackson ImmunoResearch, Cambridgeshire, UK) was used as a secondary antibody for m266 and Beta1 titer estimation, while for cmAdu, the peroxidase-conjugated AffiniPure goat anti-mouse IgG (H+L) antibody (1:2500; Jackson ImmunoResearch, Cambridgeshire, UK) was used. Unbound secondary antibody was removed by washing with PBS-T. For m266 and Beta1, detection buffer (10 mM DEA (Sigma-Aldrich), 0.5 mM MgCl2 (Merck, Darmstadt, Germany; pH 9.6) was added and incubated with colour reaction solution (16.89 mM 4-nitrophenyl phosphate [pNPP] (Sigma-Aldrich) in detection buffer) in the dark at room temperature for 15 min. The absorption was measured in a Mithras LB940 system (Berthold Technologies, Bad Wildbad, Germany) at 405 nm. For cmAdu, the plates were incubated with TMB Substrate Solution (Thermo Fisher Scientific) for 2 min at room temperature followed by the addition of stop solution (1 M H2SO4; Merck). The absorbance was measured in a Mithras LB940 system as well but at 450 nm. Data analyses were done with PRISM software (GraphPad; version 6). The absorbance values obtained for the standard curves were plotted against the logarithmic concentration of the antibodies and curve fitting to a 4PL symmetric model (Beta1) or a 5PL asymmetric model (m266 and cmAdu) was applied. The standard curve was interpolated for the sample absorbance. These values were transformed from the logarithmic concentration with a 10x function and corrected for the applied dilution. The corrected concentrations were plotted versus time.

2.5 Histology

The PFA fixed forebrains were coronally into 25-μm-thick sections with a freezing-sliding microtome (SM2000R; Leica Biosystems) and collected in a 12-well plate. Sections were stored in cryoprotectant solution (35% ethylene glycol and 25% glycerol in PBS (Gibco, Thermo Fisher Scientific)) until further use.

2.5.1 Immunohistochemistry staining for amyloid-β, microglia, Tau and bleedings

Tissue sections were stained free-floating. To stain for Aβ, the polyclonal antibody CN6 (a follow-up antibody of CN3) directed against Aβ was used (Eisele *et al.*, 2010). Microglial staining was performed with one of the following polyclonal antibodies: anti-Iba1 antibody (1:500; Wako Chemicals) or with anti-Pu.1 antibody (1:1000, Cell Signaling, Danvers, MA), both raised in rabbits. The mouse monoclonal antibody AT8 (Thermo Fisher Scientific, Waltham, MA), recognizing Tau phosphorylated at serine-202 and threonine-205, was used to stain p-Tau-positive neuritic changes (Sturchler-Pierrat *et al.*, 1997).

As a detection reagent, the Vectastain Elite ABC kit (Vector Laboratories, Burlingame, CA) was used as previously described (Eisele *et al.*, 2010). Following detection, sections were mounted on slides and co-stained with Congo Red according to standard protocols.

The Perls Prussian Blue method was used as previously described (Winkler *et al.*, 2001) to visualize ferric iron in hemosiderin, and hematoxylin and eosin (H&E) which would be an indication for bleedings.

2.5.2 Staining amyloid with luminescent conjugated oligothiophenes

Sections were mounted on slides and dried overnight at room temperature. Sections were dehydrated in PBS (Gibco, Thermo Fisher Scientific) for 10 min and subsequently double-stained with the LCOs qFTAA and hFTAA (2.4 µM qFTAA and 0.77 µM hFTAA in PBS) for 30 min at room temperature in the dark (Rasmussen *et al.*, 2017). Unbound LCOs were removed by three PBS washing steps for 10 min each. Sections were mounted using fluorescent mounting media (BIOZOL Diagnostica Vertrieb GmbH) and were kept in the dark at 4°C until microscope analyses.

2.5.3 Quantitative analyses of amyloid-β load

The Aβ load was quantified on every 12th or 36th serial and systematically sampled section, double-stained with CN6 and Congo Red. The stereological analysis was performed using a microscope with a motorized *x-y-z* stage coupled to a video-microscopy system (Stereo Investigator; MBF Bioscience, Williston, VT) as previously described (Meyer-Luehmann *et al.*, 2006). The area (%) covered by Aβ-positive staining was calculated in two-dimensional sectors at a single focal plane (20x/0.45 Zeiss Achroplan).

The quantification of plaque number and size of individual Aβ plaques in CN6/Congo Red double-stained sections was done at a digital resolution of 0.442 μm pixel^{-1} using the Zeiss

AxioScan.Z1 slide scanner (10x/0.45 Plan-Apochromat, Carl Zeiss Microscopy GmbH, Göttingen, Germany). For each image, z-stacks were acquired and flattened to a single plane using a wavelet-based extended depth-of-field algorithm. Images were scaled down to a resolution of 1.326 μm pixel^{-1} for Aβ plaque visualization and segmentation, fully automatically by a custom-written plugin for Fiji (version 2.0.0-rc-69/1.52p).

The quantification of CAA frequency, as well as severity, was done manually by blinded observers on every 12th CN6/Congo Red-stained brain section. To calculate the CAA score, the CAA frequency was multiplied by its severity as previously described (Winkler *et al.*, 2001; Schelle *et al.*, 2019).

2.5.4 Quantitative analyses of microglia

The microglial activation state was quantified on Iba1/Congo Red double-stained coronal sections. Every 12th section was imaged using the Zeiss AxioScan.Z1 slide scanner as described above. Image processing of two sections per mouse, manually outlined, was done using a custom-written Fiji plugin (version 2.0.0-rc-69/1.52p). Microglia were automatically identified in the selected area whereas the Congo Red signal was excluded by using only the red channel of the RGB image. The obtained image histogram was normalized to the full grayscale range. For background removal, a rolling ball background subtraction filter of 100px size was used. Microglia were automatically categorized into four groups based on cell size: resting (colourized red; area <50 μm^2), resting-intermediate (colourized yellow; 50 μm^2 ≤ area < 80 μm^2), activated (colourized green; 80 μm^2 ≤ area < 120 μm^2) and activated, plaque-associated (colourized blue; area ≥ 120 μm^2). Objects smaller than 10 μm^2 were excluded from the analysis.

Aβ plaque-associated microglia were quantified in Pu.1-antibody decorated and Congo Red stained brain sections. Ten plaques (or all plaques in case less than 10 plaques were present) per section were randomly selected and the microglia (nuclei) in the immediate vicinity (i.e. two times the plaque diameter) of each plaque were counted. To estimate the diameter and area of Congo Red-positive plaques, the Stereo Investigator software was used and the number of microglia per μm^2 plaque was assessed. The average number of microglia associated with plaques multiplied by the total plaque number, as described above, was used to calculate the number of total plaque-associated microglia.

2.5.5 Quantitative analysis of neuronal dystrophy

Neuronal dystrophy, visual as punctate plaque-associated neuritic structures, was quantified in AT8/Congo Red double-stained brain sections. Imaging was done using the Zeiss AxioScan.Z1 slide scanner as described above and image processing proceeded with a custom-written Fiji plugin (version 2.0.0-rc-69/1.52p). The obtained RGB image was transformed to the CIELAB Color Space to detect Aβ plaques within the sections. The plugin resulted in a mask image of Congo Red-stained structures that solely included the plaques. The area around the detected plaques was expanded and the pTau-positive signal at 10 μm, 20 μm and 50 μm from the outer edge of the plaque core was quantified.

2.5.6 Quantitative and spectral amyloid plaque analyses

Using qFTAA/hFTAA double-stained coronal sections, the number of Aβ plaques positive for qFTAA and/or hFTAA was quantified. Since the quantification was done on every third section of this set, every 36th section was used for analysis. Spectral analysis of 20 plaques per mouse was performed on a Zeiss LSM 510 META confocal microscope. For excitation, an argon 458-nm laser was used. A spectral detector (Carl Zeiss MicroImaging GmbH) acquired continuous emission spectra from 470 to 695 nm. Aβ-amyloid cores were identified by a 40x oil-immersion objective (1.3 N.A.; Zeiss) and qFTAA/hFTAA-positive plaques for analysis were randomly chosen. Within each plaque core, three regions of interest were selected and emission spectra measured (Rasmussen *et al.*, 2017), while CAA was excluded from the analysis. The obtained emission spectra were normalized to their respective maxima and the mean spectral signature for each plaque was calculated and all values obtained for one mouse were averaged. The ratio of emission intensity at the qFTAA blue-shifted peak (502 nm) and hFTAA red-shifted peak (588 nm) was calculated (Rasmussen *et al.*, 2017).

2.6 Estimation of the seeding dose

The SD_{50} was assessed similar to a previously described protocol (Ye *et al.*, 2017). Brain sections double-stained with CN6 and Congo Red were used to count mice with induced Aβ deposition within the hippocampus (the injection site) versus the total number of mice per tested dilution. Induced Aβ deposition was rated by 3 independent raters, blinded to experimental groups. The calculation of SD_{50} was done according to Reed and Muench as well as Spearman-Kerber methods. A logarithmic curve-fitting using Equation Log versus response with three parameters (GraphPad Prism™ version 5) was based on numbers obtained by the Reed and Muench calculation. The specific seeding activity per Aβ monomeric equivalent was

calculated by dividing SD_{50} by the concentration of Aβ within the sample injected into host mice.

2.7 Neurofilament light measurement

NfL in murine CSF was determined by a highly sensitive Simoa™ NF-Light Advantage assay Kit (Quanterix). For this, CSF samples were prediluted up to 1:1000 in NF-Light sample diluent and measured in duplicate on a Simoa HD-1 or HD-X Analyzer (Quanterix) according to the manufacturer's protocol, and as previously published (Kaeser *et al.*, 2021).

2.8 Statistical Analyses

Statistics were performed using the PRISM software (GraphPad) or Microsoft Excel v.16. Data were tested for normality using the Shapiro-Wilk test. If the majority of data passed the normality test, analysis of variance (ANOVA) was performed, otherwise, the non-parametric Kruskal-Wallis test was used for comparison. Significant effects revealed by ANOVA were followed by either *post hoc* Dunnett's or Tukey's multiple comparisons tests. In case only two data sets were analyzed, an unpaired two-sided *t*-test was done to compare population means. The mean and standard error of the mean (s.e.m.) are reported for each experimental group.

3 Results and Discussion

3.1 Biomarker trajectories and their amyloid-β-dependency in a mouse model of cerebral amyloidosis

Two commonly used mouse models for amyloidosis are 'APP23', a mouse model expressing human APP harbouring the Swedish double mutation under the control of neuron-specific Thy1 promotor (Sturchler-Pierrat *et al.*, 1997) and 'APPPS1', which additionally carries an AD-associated mutation in *PSEN1* at position 166 (substitution of leucine for proline) (Radde *et al.*, 2006). APPPS1 mice express an increased level of $A\beta_{42}$ compared to $A\beta_{40}$ and show Aβ plaque pathology in the cortex and hippocampus at around 2 months and 4-6 months of age, respectively (Radde *et al.*, 2006).

To investigate the trajectories of parenchymal Aβ deposition and secondary pathologies, including brain Aβ plaque pathology, Aβ seeding activity and neurodegeneration, we plotted the normalized biomarker changes in APPPS1 mice from 1.5 to 22 months of age (Fig. 5).

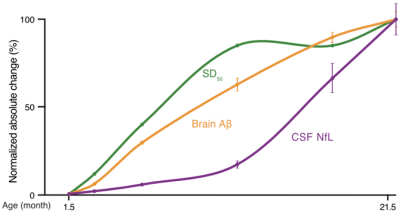

Figure 5 Biomarker trajectories of in APPPS1 mice. The normalized absolute changes (%) in brain Aβ levels (yellow), brain Aβ seeding activity (SD_{50}) (green), and CSF NfL (purple) are shown as a function of age in APPPS1 mice from 1.5 to 21.5 months. The data were mainly taken from previous publications (for brain Aβ estimated by immunoassays and for *in vivo* Aβ seeding activity: (Ye *et al.*, 2017); for CSF NfL: (Bacioglu *et al.*, 2016) and from in-house mouse biobank). From each of the NfL values of APPPS1 mice, the mean of the NfL values of transgene-negative (WT) mice of the same age was subtracted since WT mice also reveal an age-related increase (Kaeser *et al.*, 2021). Curves were generated in Numbers (Apple Inc., Cupertino, CA) using the "curved connection line" option. The yellow curve indicates an almost linear increase for brain Aβ until it reaches a plateau. The Aβ seeding activity visualized as green curve, increases more rapidly and reaches a plateau as early as ~12-mo of age. CSF NfL shown as purple curve indicates a long phase with only a slight increase until ~10-11-mo of age, after which a more rapid increase takes place. Mean and ± s.e.m. are shown. Created with Affinity Designer version 1.10.4.

The biological activity of Aβ to induce amyloid pathology, so-called the 'Aβ seeding activity', was determined by a well-established *in vivo* titration assay in APP23 host mice (Ye *et al.*,

2017). The SD_{50} is defined as the log 10 of the brain extract dilution at which 50% of the host mice showed induced Aβ deposition (Ye *et al.*, 2017). In 'young' APPPS1 mice, the SD_{50} increased sharply and reached shortly after a plateau (Fig. 5). The brain Aβ load followed an almost linear increase terminating in a plateau at a later age of APPPS1 mice (Fig. 5). The curve of brain Aβ load was similar to the curve predicted for human AD patients (Jack *et al.*, 2013). Neuronal loss in APPPS1, which was not shown to be a prominent feature in the APPPS1 mouse line, occurred mainly in close proximity to Congo Red positive amyloid (Radde *et al.*, 2006). In an inducible mouse model for neurodegeneration, the increase of NfL in CSF and blood serum correlated with neuronal damage (Brureau *et al.*, 2017). APPPS1 mice revealed a prolonged lag phase in CSF NfL with almost no increase up to 10-12 months of age, followed by a sharp increase (Fig. 5). At the time when CSF NfL increased, the brain Aβ pathology as well as the Aβ seeding activity already plateaued (Fig. 5).

To elucidate the Aβ-dependencies of the above-mentioned pathological events along with disease progression in APPPS1 mice, biomarker changes in response to an inhibition of the proteolytic production of Aβ at different disease stages were investigated.

3.1.1 Efficient reduction of amyloid-β at different stages of cerebral amyloidosis

The BACE1 inhibitor NB-360, developed by Novartis Pharma AG (Basel, Switzerland) is a small molecule compound that efficiently crossed the blood-brain barrier and blocked APP cleavage in various animal models, including rats, dogs and APP transgenic mice (Neumann *et al.*, 2015). In the present study, the inhibitor was milled into chow at a concentration of 0.5 g inhibitor kg^{-1} food pellets and available *ad libitum*. Previous experiments in APPPS1 mice, a model with an enhanced rate of plaque deposition, confirmed NB-360 as a suitable BACE1 inhibitor. For instance, treatment initiation in APPPS1 mice at 1.5 months of age for 6 months efficiently reduced brain and CSF Aβ compared to the control groups (Bacioglu *et al.*, 2016; Schelle *et al.*, 2017). Additionally to APPPS1, several other APP-transgenic mouse lines such as APP23 (Schelle *et al.*, 2017), APP51/16 (Neumann *et al.*, 2015), tg-ArcSwe and $App^{NI\text{-}GF}$ (Meier *et al.*, 2021), showed statistically relevant reduction of brain Aβ upon NB-360 treatment. These data indicate an efficient BACE1 inhibition by NB-360 in a wide range of mouse models for cerebral amyloidosis (Neumann *et al.*, 2019).

In line with these data, upon BACE1 inhibition in APPPS1 mice, we observed brain Aβ reduction at every disease stage compared to control vehicle groups (Fig.6).

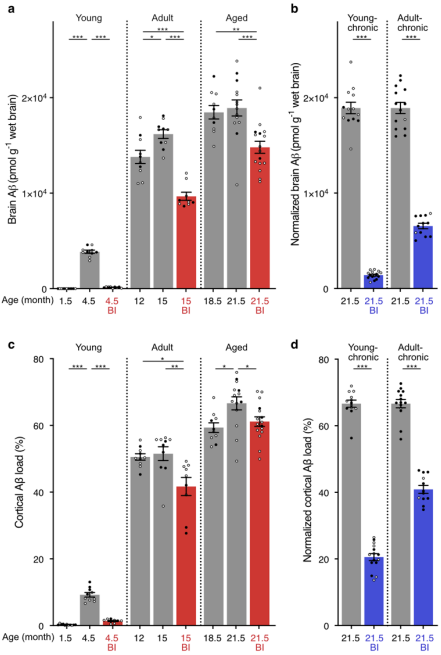

Figure 6 Brain Aβ in APPPS1 mice after short-term or chronic BACE1 inhibition. The brain Aβ (human $Aβ_{x–40}$ and $Aβ_{x–42}$) in APPPS1 mice was measured by immunoassays. **(a)** Brain Aβ at baseline and after short-term BACE1 inhibitor (BI) treatment in 'young', 'adult', and 'aged' mice. A short-term BACE1 inhibition caused a significant decrease in brain Aβ compared to the respective age-matched control groups and was below baseline in the 'adult' and 'aged' groups (one-way ANOVA: 'young', $F_{(2, 27)}$= 547.1; 'adult', $F_{(2, 26)}$= 35.31, 'aged': $F_{(2, 37)}$= 10.33, all P<0.001; post hoc Tukey's multiple comparisons, *P< 0.05, **P<0.01, ***P<0.001). **(b)** Brain Aβ levels in the 'young-chronic' and 'adult-chronic' groups were normalized to the 21.5-month-old control mice in the 3-month treatment group shown in (a). Two-tailed unpaired t-tests revealed significantly lower brain Aβ levels in the BI-treated mice ('young-chronic': $t_{(26)}$=30.69; 'adult-chronic': $t_{(24)}$=17.99, both ***P<0.001). (**c**) Total Aβ immunostaining in the neocortex was determined by stereological analysis, and the results mirrored brain Aβ load assessed by the immunoassays shown in (a). BI treatment caused a significant decrease in Aβ immunostaining compared to the respective age-matched control group (one-way ANOVA: 'young', $F_{(2, 27)}$= 155.8, P<0.001; 'adult', $F_{(2, 26)}$= 7.25, P=0.003; 'aged': $F_{(2, 37)}$= 4.95, P=0.013; all P<0.05; post hoc Tukey's multiple comparisons, *P<0.05, **P<0.01, ***P<0.001). (**d**) Cortical Aβ immunostaining in the 'young-chronic' and 'adult-chronic' groups was normalized to the 21.5-month-old control mice of the 3-month treatment group shown in (c). Two-tailed unpaired t-tests show significantly lowered Aβ-immunostaining in both groups ('young chronic': $t_{(26)}$=30.99; 'adult-chronic': $t_{(24)}$=14.77; both ***P<0.001). All data are represented as group means ± s.e.m. Open circles are data obtained from male and filled circles from female mice. Created with Affinity Designer version 1.10.4.

At advanced disease stages with high Aβ plaque burden, NB-360 treatment reduced brain Aβ load measured by immunoassays below baseline (Fig. 6a, b). Short-term BACE1 inhibitor treatment of 'young' APPPS1 mice, where the 3-month inhibitor treatment was initiated at 1.5

months of age, largely prevented brain Aβ deposition compared to age-matched controls (Fig. 6a). BACE1 inhibitor treated 'young' group reached only 3.8% of the Aβ load of the age-matched control group. Interestingly, when the treatment was initiated at a later disease stage in the 'adult' and 'aged' group at 12 and 18.5 months of age, respectively, short-term treatment not only prevented further increases but reduced brain Aβ load below baseline, which refers to the time point when the treatment was initiated (Fig. 6a). The same was true for the 'adult-chronic' group, where inhibition was initiated at 12 months and terminated at 21.5 months of age (Fig. 6b). Mice chronically treated with the BACE1 inhibitor from 1.5 to 21.5 months of age, referred to as 'young-chronic', showed only 7.4% of total brain Aβ compared to 21.5 months old untreated APPPS1 mice (Fig. 6b).

In the same mice, similar results were obtained when the Aβ load was determined by immune-histological measures, however, less pronounced or partially lost (Fig. 6c, d). The immune-histological analyses of Aβ in 'young' and 'young-chronic' mice after BACE1 inhibition revealed 15.1% and 30.8% of the immunostaining of age-matched, untreated APPPS1 mice (Fig. 6a, b), which is roughly four times higher compared to the results obtained by immunoassays (Fig. 6c, d). Longitudinal *in vivo* imaging of Aβ plaque formation and growth in APPPS1 mice treated with a BACE1 inhibitor, detected a reduction in Aβ plaque density by 18.9% (Peters *et al.*, 2017). Since immune-histological quantification is an estimate of the area covered by stained Aβ plaques it might fail to adequately reflect differences in plaque density, which could explain the observed discrepancy between biochemical and immune-histological measures. The fluid biomarker signatures and PET scan analyses of AD patients, who received BACE1 inhibitor treatment, displayed a similar discrepancy (Querol-Vilaseca *et al.*, 2022). While Aβ CSF was reduced up to 80%, brain amyloid load quantified by PET scan indicated a reduction of solely 20% (Querol-Vilaseca *et al.*, 2022). Further, a postmortem investigation of the neuropathology of a patient receiving BACE1 inhibitor revealed that Aβ reduction occurred specifically in pre-synaptic areas (Querol-Vilaseca *et al.*, 2022). Thus, Aβ in certain cellular regions might escape detection and quantification by common histological staining and imaging methods.

3.1.2 Resistance of amyloid-β seeding activity upon reduction of cerebral amyloid-β

To investigate the sensitivity of Aβ seeding-active species to BACE1 inhibition in APPPS1 mice, the SD_{50} was determined for BACE1 inhibitor treated APPPS1 mice at different disease stages. For this, the *in vivo* titration assay in APP23 host mice according to Ye *et al.*, 2017 was conducted using brain material from BACE1 treated APPPS1. For this, brain homogenates within one treatment group were pooled, processed to seeding extract and intracerebrally injected at serial dilutions into APP23 host mice (Fig. 7a, b). Although brain Aβ was reduced

as a response to BACE1 inhibitor treatment at all disease stages (Fig. 6), no equivalent reduction in the SD_{50} has been observed (Fig. 7c).

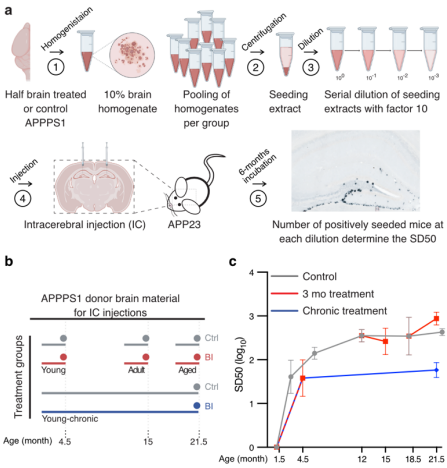

Figure 7 Brain Aβ seeding activity in APPPS1 mice after short-term or chronic BACE1 inhibition. **a**) Brain extracts from all mice within a group were pooled, serially diluted, and intracerebrally (IC) injected into the hippocampus of 2- to 3-month-old female APP23 host mice. APP23 host mice were analysed for Aβ deposition using immunohistochemistry (CN6 and Congo Red double-staining) 6 months later. (**b**) Treatment groups for which SD_{50} was determined ('young', 'adult', 'aged' and 'young-chronic'). (**c**) SD_{50} (defined as the log 10 of the brain extract dilution at which 50% of the host mice showed induced Aβ deposition) was computed for each BI treatment group and complemented with the trajectories of SD_{50} from Ye *et al.*, 2017. BI treatments in amyloid-laden 'adult' and 'aged' mice did not consistently affect the seeding activity. When BI treatment was initiated before appreciable Aβ deposition was present (i.e., at 1.5 months of age) SD_{50} almost reached control levels after 3-month acute BI treatment. After chronic treatment, SD_{50} was about 1 log (10-fold dilution) below the control (i.e. saturated seeding activity). Since the chronic treatment is, in a way, an extension of the acute treatment, the line is drawn from the 3-month acute treatment to the end of the chronic treatment, suggesting that SD_{50} remains at this level when Aβ generation is continuously blocked. Created with Affinity Designer version 1.10.4.

Almost no change in SD_{50} has been observed in short-term BACE1 inhibitor treated APPPS1 mice compared to untreated APPPS1 mice (Fig. 7c). Based on these data, one might speculate that once formed Aβ seeds in APPPS1 mice possess great stability over a long time and/or they escape common protein clearance mechanisms. Indeed, Aβ seeding-active species, although not further characterized, were shown to be stable *in vivo* in mice lacking APP and thus Aβ, for up to 6 months while retaining their biological activity, as shown by a subsequent seeding assay in APP23 host mice (Ye *et al.*, 2015). The detailed characterization of such Aβ seeding-active species remains to be carried out. The strongest reduction of SD_{50}

compared to untreated APPPS1 mice was detected in the 'young-chronic' group. In this treatment group, the SD_{50} was approximately 10-fold lower (one log scale), compared to the untreated APPPS1 mice (Fig. 7c). Due to the indirect estimation of seeding-active units in brain extracts, the underlying effect(s) of BACE1 inhibition on Aβ SD_{50} remain(s) elusive. The assumption that the leading aggregation pathway in the presence of Aβ fibrils is the fibril-catalysed secondary nucleation (Cohen *et al.*, 2013), provides a potential explanation for the observed reduction of SD_{50} in the 'young-chronic' treatment group. As described, the cortical Aβ load in 'young-chronic' was reduced by 69.2%, thereby putatively providing less Aβ fibril surface area necessary for secondary nucleation. The disease-related Aβ modification resulting in pyroglutamate Aβ (pE-Aβ) was detected in brain material of aged APP23 mice (Uhlmann *et al.*, 2020) and AD patients (Saido *et al.*, 1995; Portelius *et al.*, 2010). This modification was associated with advanced aggregation kinetics compared to unmodified Aβ (He and Barrow, 1999). Further, pE-Aβ positive plaques were hypothesized to be more resistant to degradation due to advanced stability (Wirths *et al.*, 2010). Therefore, age-related modifications in APPPS1 mice might influence the sensitivity of seeding-active Aβ species to treatment interventions. However, further characterization of such species in 'young' and 'chronic-young' inhibitor-treated mice is needed to fully understand the formation of seeding competent Aβ species, age-related modifications and clearance *in vivo*.

3.1.3 Increase of neurofilament light in cerebrospinal fluid despite a reduction of brain amyloid-β

Previous data highlighted the connection between Aβ and CSF NfL in APPPS1 mice (Bacioglu et al. 2016). In accordance with these data, an Aβ reduction as a response to NB-360 treatment in APPPS1 mice resulted in a decrease of CSF NfL compared to age-matched untreated mice at every disease stage tested, however, failed to halt further increase compared to baseline levels (Fig. 8a, b).

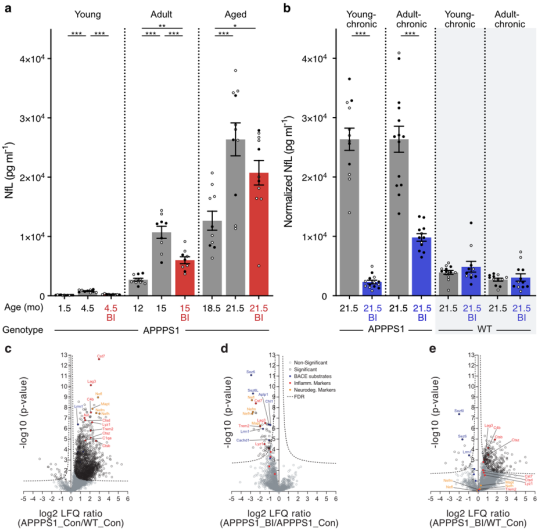

Figure 8 NfL in CSF after short-term and chronic BACE1 inhibition. (**a**) CSF NfL was measured at baseline and after short-term BACE1 inhibitor (BI) treatment in 'young', 'adult', and 'aged' mice (note that insufficient CSF amount and/or measurement errors for APPPS1 occurred in 'adult control', n=1; 'aged control', n=3; 'aged BI', n=5; 'young-chronic' control, n=1; 'young-chronic' BI, n=1; and for WT 'young-chronic' control, n=2). BI treatment in the 'young' group prevented an NfL increase, while in the 'adult' and 'aged' groups, NfL still increased compared to baseline levels, albeit less than in the control groups (one-way ANOVA: 'young', $F_{(2,\ 27)}$= 80.58; 'adult', $F_{(2,\ 25)}$= 36.51; 'aged', $F_{(2,\ 29)}$= 9.254, all P<0.001; post hoc Tukey's multiple comparisons, *P<0.05, **P<0.01, ***P<0.001). (**b**) CSF NfL in the 'young-chronic' and 'adult-chronic' groups were normalized to the 21.5-month-old control mice of the 3-month treatment group shown in (a). Two-tailed unpaired *t*-tests revealed significantly lower CSF NfL levels in the BI-treated APPPS1 mice ('young chronic': $t_{(24)}$=13.64; 'adult-chronic': $t_{(24)}$=6.754, both ***P<0.001). The same chronic treatment was also undertaken in WT mice, but BI treatment did not affect CSF NfL. Similar NfL levels in chronically treated APPPS1 mice and WT mice at 21.5 months indicate that the NfL increase in APPPS1 could be completely blocked by the chronic BI treatment. All data are represented as group means ± s.e.m. Open circles are data obtained from male and filled circles from female mice. (**c-d**) CSF proteomic analysis after chronic treatment was measured for the 'young-chronic` groups, BI- and control-treated APPPS1 and WT. For this, 8 animals from each group were randomly selected. **(c)** Volcano plots comparing the CSF proteome of control-treated APPPS1 versus control-treated WT mice (n=8 versus n=8). Selected proteins are labelled with their UniProt gene names. Note the general increase in the abundance of many neurodegenerative markers (orange) such as Nefl, Nefm, Nefh, and Mapt (Tau) and inflammation-related proteins (red) such as Trem2, Lag3, Ctsz, and Lyz1 in APPPS1 mice compared to WT mice. **(d)** Volcano plots comparing the CSF proteome of 1.5 to 21.5-months-BI-treated versus control-treated APPPS1 mice (n=8 versus n=8) demonstrate that chronic BI treatment largely prevents the changes shown in (c). **(e)** 'Young-chronic' BI-treated APPPS1 mice versus control-treated WT control mice (n=8 versus n=8). The significant reduction of the well-known BACE1 substrates (blue) such as Sez6 and Sez6l validates the successful BACE1 inhibition until old age. For all Volcano plots, the –log10 of the *p*-value of each protein is plotted against its log2 fold difference for each group comparison. The hyperbolic curves indicate the thresholds of the permutation-based FDR correction for multiple hypotheses (p=0.05; s_0=0.1). Proteins above the FDR curves (black circles) are significantly changed. Created with Affinity Designer version 1.10.4.

Comparing the 'young', 'adult' and 'aged' treatment groups, revealed a decreased effect size of BACE1 inhibition on lowering CSF NfL levels, compared to age-matched controls, the later the treatment was initiated. Interestingly, although in the BACE1 inhibitor treated 'adult' group the brain Aβ was reduced below baseline, the CSF NfL levels more than doubled (2.2-times more) within the 3-month treatment period. A similar trend has been observed for the 'aged' treatment group, although less pronounced (1.6-times more). Interestingly, at this disease stage, Aβ seeding activity already reached its plateau (Fig. 5) and was not lowered as a response to BACE1 inhibition (Fig. 7c), highlighting a putative relationship between CSF NfL levels and saturated Aβ seeding activity. It should be noted, that in the 'young' group treated with BACE1 inhibitor 2.1-times higher CSF NfL levels were detected compared to baseline (Fig 8a). However, these NfL values are similar to those obtained for 3-month-old WT mice (239 pg ml^{-1} ± 27.2 (n= 6)) and therefore might not reflect a disease-associated CSF NfL increase. Furthermore, WT APPPS1 littermates were treated chronically with NB-360 or control pellets and no difference in the CSF NfL levels at old age was detected, indicating no direct effect of BACE1 inhibition on NfL levels (Fig. 8b).

In AD, CSF Tau and not NfL was strongly associated with Aβ pathology, indicating CSF NfL reflects neurodegeneration independently of Aβ (Mattsson *et al.*, 2016). Our data indicate that early BACE1 inhibition in the 'young-chronic' group completely diminished Aβ-associated NfL increase, resulting in NfL levels comparable to age-matched WT littermates (Fig. 8b). Furthermore, proteomic analyses of CSF from aged APPPS1 detected an upregulation of proteins involved in neurodegenerative processes and inflammatory pathways such as the neurofilament subunits and Trem2, respectively, compared to WT (Fig. 8c). Chronic BACE1 inhibition beginning at 1.5 months however prevented largely the protein upregulation compared to untreated APPPS1 mice and, apart from known BACE1 cleavage substrates such as Sez6, revealed a proteomic signature similar to age-matched WT mice (Fig. 8d, e). These data indicate that Aβ-dependent degenerative process(es) might take place at the early disease stage which, once in progress, could drive neurodegeneration in an Aβ-independent manner at advanced disease stages in APPPS1 mice.

3.1.4 Brain amyloid-β load is mirrored by microglial activation

Secondary pathologies in AD, such as microglial activation and tau have been considered to bridge Aβ pathology and neurodegeneration (Ising *et al.*, 2019; Pascoal *et al.*, 2021; Pereira *et al.*, 2021). In AD patients, a positive correlation of a CSF marker for microglial activation, soluble Trem2 (sTrem2), and CSF NfL indicated the involvement of microglia in degenerative processes in AD (Park *et al.*, 2021). However, another study proposed a protective role for

inflammation in prodromal AD, based on an inverse correlation of microglial activation and plasma NfL concentration at this early disease stage (Parbo *et al.*, 2020). In APPPS1 mice, Aβ reduction as a response to NB-360 treatment was immune-histologically and biochemically estimated and revealed that microglial activation mirrored the level of brain Aβ (Fig. 9a, b, e, f).

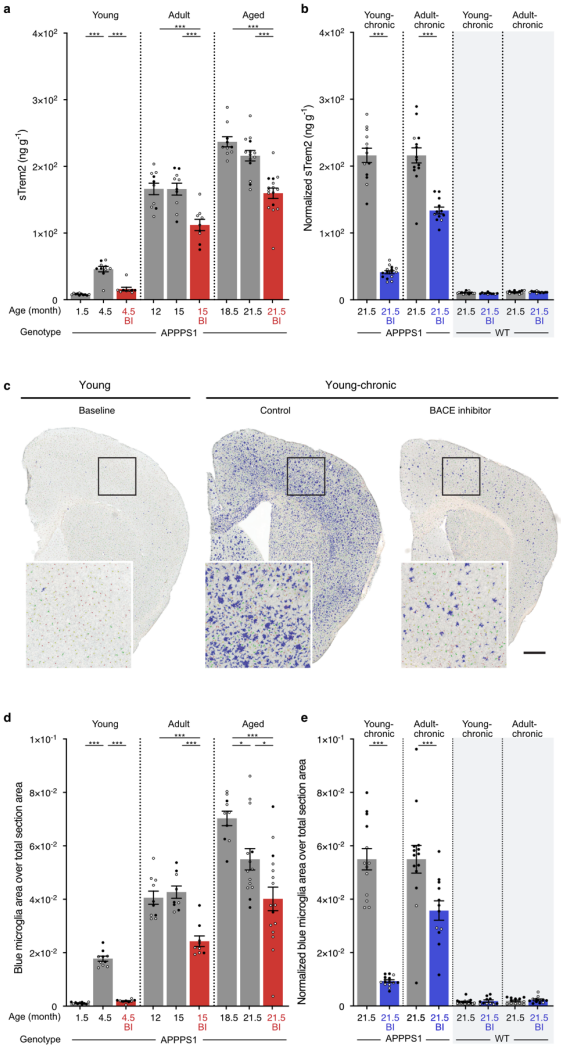

Figure 9 Soluble Trem2 and activated microglia after short-term and chronic BACE1 inhibition. (a-b) Soluble Trem2 and (c-e) microglial activation in brains of APPPS1 and WT mice. (**a**) BACE1 inhibitor (BI) treatment for 3 months caused a significant decrease in soluble Trem2 (sTrem2) compared to the respective age-matched control group, and sTrem2 was below baseline in the 'adult' and 'aged' groups (one-way ANOVA: 'young', $F_{(2, 27)}$= 54.04; 'adult', $F_{(2, 26)}$= 12.25; 'aged', $F_{(2, 37)}$= 25.54, all P<0.001; post hoc Tukey's multiple comparisons, ***P<0.001). (**b**) Brain sTrem2 in the 'young-chronic' and 'adult-chronic' groups were normalized to the 21.5-month-old control mice of the 3-month treatment group shown in (a). Two-tailed unpaired *t*-tests revealed significantly lower brain Aβ levels in the BI-treated

mice ('young chronic': $t_{(26)}$=17.15; 'adult-chronic': $t_{(24)}$=6.229, both ***P<0.001). BI treatment of WT mice had no effect on brain sTrem2. (**c**) Iba1-immunostained microglia in the cortex of APPPS1 and WT mice were categorized and coloured based on size: Red: area <50 µm^2 (resting); yellow: area 50 to ≤ 80 µm^2 (resting-intermediate); green: area 80 to ≤120 µm^2 (activated); blue: area ≥120 µm^2 (activated, plaque-associated). Representative sections from a 1.5-month-old APPPS1 mouse ('young' baseline), two 21.5-month-old APPPS1 mice of the 'young-chronic' group, one control-treated and one BI-treated. Scale bar insert, 100 µm. (**d**) Quantitative analysis revealed a significant decrease of the activated (blue) microglia over the total section area in BI-treated mice compared to controls, and additionally below baseline in the 'adult' and 'aged' groups (one way ANOVA: 'young', $F_{(2, 26)}$= 279.9; 'adult', $F_{(2, 25)}$= 18.81; 'aged', $F_{(2, 37)}$= 12.85, all P<0.001; post hoc Tukey's multiple comparisons, *P<0.05, **P<0.01, ***P<0.001). Note that one 'young baseline' and one 'adult control' mouse were excluded because of a processing error. (**e**) Activated (blue) microglia in the 'young-chronic' and 'adult-chronic' groups were normalized to the 21.5-month-old control mice of the 3-month treatment group shown in (d). Two-tailed unpaired t-tests revealed significantly lower brain Aβ levels in the BI-treated mice ('young-chronic' and 'adult-chronic' $t_{(26)}$=12.11; P<0.001 and $t_{(24)}$=2.948; P=0.0070, respectively). BI treatment of WT mice had no effect on microglial activation. Note the similarities of the results of sTrem2 and activated microglia to the results for total brain Aβ immunostaining (Fig. 6). All data are represented as group means ± s.e.m. Open circles are data obtained from male and filled circles from female mice. Created with Affinity Designer version 1.10.4.

Similar to brain Aβ, microglial activation was lowered at all disease-stages compared to age-matched untreated APPPS1 mice (Fig. 9). In amyloid-laden brains, sTrem (Fig. 9a, b) and the cortical area covered by microglia (Fig. 9c-e) were as response to Aβ reduced below baseline. WT littermates treated chronically with NB-360 or control pellets revealed no difference in brain sTrem levels (Fig. 9b) and blue microglia area per section area (Fig. 9e), indicating no direct effect of BACE1 inhibition on microglial activation. These results are in line with previously published data for APPPS1 mice (Radde *et al.*, 2006) and a longitudinal study in AD patients (Fan *et al.*, 2015), indicating a correlation between Aβ deposition and microglial activation. In summary, BACE1 inhibitor treated APPPS1 mice at advanced disease-stage ('adult' and 'aged') revealed, with regards to the respective baseline, an increase in CSF NfL which was accompanied by reduced microglial activation and brain Aβ load. Our data suggest a direct relationship between microglial activation and Aβ load, however, no direct relationship between neurodegeneration and microglial activation could be proven with the applied measures in these mice.

3.1.5 Conclusion

As already mentioned, an age-dependent increase of NfL, although mechanistically not fully understood, has been reported in healthy individuals (Idland *et al.*, 2017). To correctly estimate AD-associated neurodegeneration in elderly individuals by the use of NfL measures, it is inevitable to fully understand the underlying molecular processes of Aβ-dependent, Aβ-independent and age-related NfL increase. The proof of biomarker causalities along the AD continuum is missing in humans since such biomarker studies rely, due to limited intervention

possibilities, mainly on observed correlations. In the past decades, the AD research community has reached a consensus that treatment intervention, if available, should be applied as earliest as possible to prevent disease progression (McDade and Bateman, 2017; Polanco *et al.*, 2017). Thus, before the clinical disease onset and ahead of irreversible neurodegeneration.

Our study indicates biomarker dependencies change in the course of the disease progression. Thus, Aβ-targeting treatment would need to be initiated before neurodegeneration becomes independent of Aβ pathology, which might refer to an even earlier timepoint than currently suggested. This consequently leads to the great challenge of finding and evaluating biomarkers specific for this early disease stage and defining a timeframe for a successful treatment intervention targeting Aβ.

3.2 Initial amyloid-β seed formation as a putative treatment target

The time point of the initial Aβ seed formation in humans is currently unknown and highly sensitive measures to detect such an event *in vivo* at a molecular size range are not available. Additionally, the Aβ seed formation is mechanistically not defined and due to its transient nature, investigation of its biochemical and structural features is limited. These obstacles make the early Aβ seed formation as a target for therapeutic intervention in AD challenging to evaluate. We aimed to detect and characterize pre-amyloid Aβ seeds before plaque formation and to validate their suitability as a target for passive immunotherapy in APP23 transgenic mice. The increase of brain Aβ in the well-characterized APP23 mouse model follows a sigmoidal curve (Fig. 10) as it was seen for APPPS1 mice (Fig. 5) and described for humans (Clifford *et al.*, 2013).

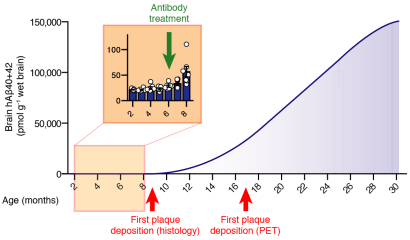

Figure 10 Targeting Aβ seeds in APP23 mice at the pre-amyloid stage. The human Aβ concentration ($hAβ_{x-40}$ and $hAβ_{x-42}$ combined) at 10–30 months of age in male APP23 mice is shown as a function of age as a polynomial (4th degree) curve, which was calculated based on previous publications (Maia *et al.*, 2013, 2015; Ye *et al.*, 2017). In addition to these data, $hAβ_{x-40}$ and $hAβ_{x-42}$ were measured in 2–8-month-old male APP23 mice (n = 7, 6, 7, 7, 7, 6 and 7 for 2, 3, 4, 5, 6, 7 and 8-month-old mice, respectively) on the Simoa™ platform. The first notable increase in human Aβ was observed at 7–8 months of age, which is at least 1 month earlier than Aβ plaque deposition becomes apparent histologically in male APP23 mice (Eisele *et al.*, 2010; Langer *et al.*, 2011; Ye *et al.*, 2017). Adapted from Uhlmann *et al.*, 2020 and created with Affinity Designer version 1.10.4.

Due to the relatively late plaque onset in APP23, this mouse line exhibits a longer lag phase compared to APPPS1 mice (Sturchler-Pierrat *et al.*, 1997; Radde *et al.*, 2006). The first Aβ plaques in male APP23 mice become apparent by histological staining at around 8-9 months (Sturchler-Pierrat *et al.*, 1997). However, a slight increase in $Aβ_{42}$ and $Aβ_{40}$ was biochemically detectable between 7 and 8 months of age (Fig. 10), putatively reflecting the formation of Aβ seeds. Based on these data, we used male APP23 mice at the age of 6 months as a model to evaluate the therapeutic targeting of Aβ seed formation.

3.2.1 Therapeutic antibodies with distinct epitope recognition on amyloid-β for passive immunotherapy

Since the detailed characterization of a therapeutic target is crucial for the design of an antibody, many preclinical and clinical studies tested antibodies that specifically target either soluble Aβ species or conformational epitopes such as oligomeric Aβ and amyloid fibrils (Sevigny *et al.*, 2016; Yang *et al.*, 2019; Salloway *et al.*, 2021). To cover a broad range of possible pre-amyloid seed conformations, a set of therapeutic Aβ-targeting antibodies with distinct epitope recognition was tested for their ability to target, engage and clear early Aβ-seeds *in vivo* in pre-amyloid APP23 mice as illustrated in Figure 11.

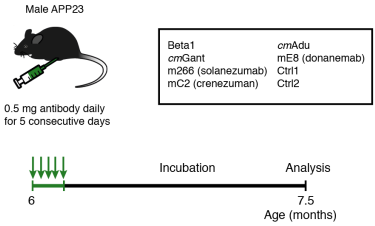

Figure 11 Schematic overview of passive immunization in pre-depositing APP23 mice. Six-month-old male APP23 mice received on 5 consecutive days intraperitoneally 0.5 mg of one of the six antibodies directed against Aβ (n=8 Beta1, n=7 cmGant, n=8 m266, n=8 mC2, n=8 cmAdu, n=8 mE8) or corresponding control (Ctrl) antibodies (n=13 Ctrl1, n=8 Ctrl2) or PBS (n= 11). Note that one cmGant-injected animal died. mE8 immunization and additional controls were performed in a separate experiment, explaining the higher number of mice receiving control antibodies and PBS. Mice were sacrificed and analysed at 7.5 months of age. Adapted from Uhlmann *et al.*, 2020 and created with Affinity Designer version 1.10.4.

The chimeric murine versions (cm) of aducanumab (cmAdu), gantenerumab (cmGant), the murine parent version of crenezumab (mC2), solanezumab (m266) and donanemab (mE8) were used for early Aβ seed targeting in pre-amyloid APP23 mice (Fig. 11). Additionally, two control antibodies, control 1 (Ctrl1) and control 2 (Ctrl2) targeting wheat auxin and an unknown epitope (Sevigny *et al.*, 2016), respectively, were used. Furthermore, the Aβ-targeting antibody Beta1, which was able to immune-deplete Aβ seeding-active assemblies from brain extracts (Meyer-Luehmann *et al.*, 2006) was included. The Aβ load 1.5-month post passive immunotherapy of pre-depositing APP23 was determined by a highly sensitive immunoassay after Triton-X 100 and subsequent formic acid extraction (Fig. 12a).

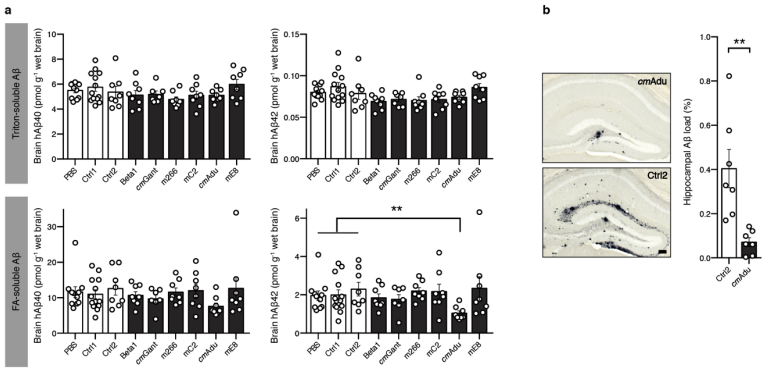

Figure 12 Effect of Aβ load and seeding activity after passive immunotherapy of APP23 mice at pre—amyloid stage. (**a**) Brain homogenates were prepared by a 2-step extraction with Triton X-100 and subsequently formic acid. Human $Aβ_{x-40}$ and $Aβ_{x-42}$ concentrations were measured by MSD immunoassays. For this analysis, mice receiving PBS, Ctrl1 and Ctrl2 were pooled. A Kruskal–Wallis test was performed and indicated no group differences for the Triton X-100-extracted hAβ ($Aβ_{x-40}$, $H_{(6)}$= 8.865, P= 0.1813; $hAβ_{x-42}$, $H_{(6)}$= 14.84, P= 0.0215; no significant group differences between Ctrls and any other group with post hoc Dunn's multiple comparisons test). Measurements of hAβ in the formic acid-soluble fraction revealed group differences for $hAβ_{x-42}$ ($H_{(6)}$= 14.73; P=0.0225, post hoc Dunn's multiple comparisons test between cmAdu-injected mice and controls, P= 0.006). **(b)** The brain homogenates from cmAdu- and Ctrl2-treated 7.5-month-old mice were pooled within a treatment group and inoculated into the hippocampus of 3-month-old male APP23 hosts mice (n= 7 for both cmAdu and Ctrl2). Inoculated mice were sacrificed after an 8-month incubation period. The brain homogenate of cmAdu-treated mice induced markedly less Aβ deposition compared to Ctrl2-treated mice (two-tailed unpaired t-test; $t_{(12)}$= 3.726; P= 0.003). All data are represented as group means ± s.e.m.; $^{**}P< 0.01$. Scale bar 100 µm. Adapted from Uhlmann *et al.*, 2020 and created with Affinity Designer version 1.10.4.

Compared to the mice receiving either a control antibody (Ctrl1 or Ctrl2) or PBS, no Aβ-targeting antibody tested reduced soluble brain Aβ levels measured after Triton-X 100 extraction, however, passive immunization with cmAdu significantly reduced formic acid-soluble $Aβ_{42}$ in pre-amyloid mice (Fig. 12a). Formic acid extraction is a common method used to monomerize insoluble Aβ and a correlation of insoluble $Aβ_{42}$ with amyloid plaque load in AD brains has been observed (Funato *et al.*, 1998).

The antibody solanezumab and its murine version m266 are directed against the central domain of Aβ (DeMattos *et al.*, 2001), showed binding to soluble, monomeric Aβ (Yamada *et al.*, 2009) and failed to alter the Aβ oligomeric level in an APP transgenic mouse model (Mably *et al.*, 2015). The epitope recognized by solanezumab becomes unavailable due to Aβ oligomerization as indicated by crystallography of the solanezumab Fab fragment bound to the mid-region of Aβ (Crespi *et al.*, 2015). This is in line with the observation that peripheral

administration of m266 was not followed by antibody decoration of Aβ plaques in the brain (DeMattos *et al.*, 2001). However, m266 reversed memory impairment in an APP transgenic mouse line (Dodart *et al.*, 2002). Due to the published binding specificity of m266 for soluble Aβ, it was somewhat surprising that no Aβ reduction in the Triton-X 100 extraction was achieved in pre-amyloid APP23 (Fig. 12a). Reasons for this remain speculative. For instance, a 1.5-month incubation time between antibody administration and analysis might have been too long to detect an effect on Aβ. If the antibody engaged with its target (soluble Aβ) shortly after its application and was cleared, an effect of soluble Aβ could have been masked by APP overexpression in this mouse model. An investigation of this possibility would require a shorter timeframe between passive immunization and brain Aβ analyses.

The antibody crenezumab targets a broad range of Aβ from monomeric to fibrillar Aβ (Adolfsson *et al.*, 2012). Its murine version mC2 also failed to reduce Aβ in pre-amyloid APP23 mice (Fig. 12a). Despite their affinities to distinct Aβ assemblies, solanezumab and crenezumab share high sequence homology (Crespi *et al.*, 2015). In APP transgenic animals, crenezumab on a human IgG4 subclass decreased the Aβ plaque size (Adolfsson *et al.*, 2012). The antibody subclass IgG4 was considered to lower the risk of Fc receptor-mediated overactivation of microglia and thereby providing a more effective and safer treatment compared to the human IgG1 subclass (Adolfsson *et al.*, 2012). The murine version of crenezumab (mC2) on a mouse IgG2a backbone successfully targeted Aβ plaques when injected into APP transgenic mice (Fuller *et al.*, 2015). However, mC2 failed to clear Aβ plaques and did not cause detectable inflammatory changes (Fuller *et al.*, 2015). Furthermore, analyses 7 days post intracerebral injection of mC2 into APP transgenic mice did not alter Aβ levels in brain homogenates (Fuller *et al.*, 2015). These data are in line with our observed results and further indicate, that a shortened incubation time would have most likely gained the same output.

Gantenerumab is an antibody that recognizes the N-terminus and central regions of Aβ leading to an epitope specificity towards higher Aβ assemblies including oligomers and fibrils (Bohrmann *et al.*, 2012). Since an absence of such Aβ assemblies in pre-amyloid APP23 mice can be assumed, the observed unaltered Aβ levels in Triton-x-100 and formic acid fraction measured in brain homogenates of passively immunized mice were not surprising (Fig. 12a). Further, gantenerumab was shown to recruit microglia to small Aβ plaques and to promote phagocytosis, leading to a reduction in amyloid pathology in transgenic mice (Bohrmann *et al.*, 2012). Compared to mC2, the murine version of gantenerumab (cmGant) showed increased microglial activation *in vivo* (Fuller *et al.*, 2015).

To design an antibody that exclusively targets Aβ plaques, a truncated and pyroglutamated Aβ peptide ($Aβ_{p3-42}$), which was detected in Aβ plaques in humans (Saido *et al.*, 1995), has been used as an antibody target epitope (DeMattos *et al.*, 2012). The resulting antibody, mE8, reduced Aβ plaques in an APP transgenic mouse model and induced clearance in a phagocytosis assay (DeMattos *et al.*, 2012). In AD patients, the humanized mE8 antibody (donanemab) reduced brain Aβ deposition below the PET baseline (Lowe *et al.*, 2021). The target engagement with exclusively Aβ plaques was considered to be advantageous for plaque reduction (DeMattos *et al.*, 2012). Recently, pE-Aβ forms were reported in AD patients' CSF and may serve as a potential biomarker for disease progression (Domingo *et al.*, 2021). However, mE8 failed to reduce brain Aβ upon passive immunization of pre-amyloid APP23 (Fig. 12a), most likely due to the absence of Aβ plaques at this stage.

The antibodies m266 and mC2 were generated in mice (Seubert *et al.*, 1992; Adolfsson *et al.*, 2012) and subsequently humanized for applications in clinics, whereas gantenerumab was developed by phage display technology (Bohrmann *et al.*, 2012). For the discovery of the antibody aducanumab, the so-called 'Reverse Translational Medicine™' (Neurimmune AG, Switzerland) platform was applied. With this approach, blood lymphocyte libraries collected from healthy, cognitively normal, aged individuals were screened for promising Aβ-targeting antibodies, which might have protected the respective individuum against Aβ accumulation (Arndt *et al.*, 2018). Aducanumab recognizes a linear epitope on Aβ from amino acids 3 to 7 and has a 10,000-fold higher specificity for aggregated compared to monomeric Aβ (Sevigny *et al.*, 2016). The epitope binding by aducanumab is considered to be rather driven by avidity than affinity (Arndt *et al.*, 2018). How this is mechanistically governed is not fully understood, but the fast off rate of aducanumab and the immobilization of Aβ C-terminus in aggregates are hypothesized to contribute (Arndt *et al.*, 2018). Characterization of the antibody structures and kinetics indicate distinct binding features of aducanumab compared to solanezumab and gantenerumab (Arndt *et al.*, 2018; Linse *et al.*, 2020). In a transgenic mouse model with cerebral Aβ pathology as well as in AD patients, aducanumab selectively targeted and reduced soluble and insoluble Aβ in a dose- and time-dependent manner (Sevigny *et al.*, 2016). Interestingly, in pre-amyloid APP23 mice cmAdu reduced formic acid soluble Aβ42 (Fig. 12a) and due to the antibody's specificity to Aβ aggregates (DeMattos *et al.*, 2012; Arndt *et al.*, 2018), our data indicate the presence of oligomeric, insoluble Aβ species at this early disease in APP23 mice. Furthermore, an *in vivo* seeding assay using brain homogenates from cmAdu-treated mice revealed reduced Aβ seeding activity (Fig. 12b). One might speculate, that the reduction of Aβ in the formic acid fraction reflects the reduction of pre-amyloid seeds in APP23 mice, indicating that the early Aβ seed formation can be targeted therapeutically.

3.2.2 Characterization of amyloid-β assemblies from late and early disease stages

A detailed biochemically characterization of early Aβ nucleation assemblies is due to their transient nature methodologically challenging. To investigate the Aβ species targeted by antibodies directed against different epitopes, we established and performed antibody recognition profiling of Aβ assemblies (ARPA) as illustrated in Figure 13.

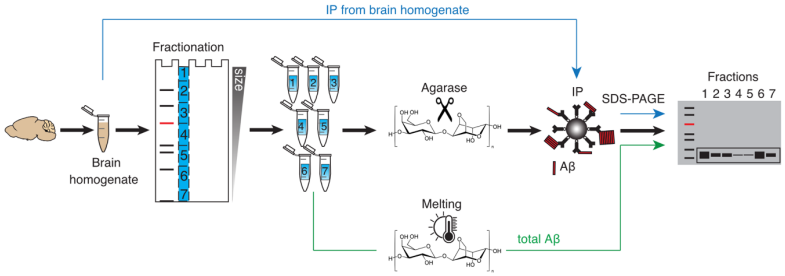

Figure 13 Schematic representation of the antibody recognition profiling of Aβ assemblies (ARPA). Brain homogenate (65 µg total protein) is either used for direct immunoprecipitation (blue line) or semi-native fractionation by size using agarose gel electrophoresis (black arrow). Agarose fractions containing Aβ assemblies within a distinct size range are either liquified by enzymatic digestion (black arrows) or melted in denaturing sample buffer and subjected to western blot analysis for an estimation of total Aβ (green line). Liberated Aβ assemblies within liquefied agarose fractions are available for further analyses such as immunoprecipitation using capture antibodies with distinct Aβ-binding characteristics. The amount of Aβ pulled-down from a fraction by an antibody is normalized to the total amount of Aβ within a fraction, providing am antibody recognition profile. Adapted from Uhlmann *et al.*, 2020 and created with Affinity Designer version 1.10.4.

In the first step of ARPA, proteins in brain homogenate are separated semi-natively by size with the means of agarose gel electrophoresis. Fractionation of the agarose gel in defined pieces facilitates a characterization and further analyses of Aβ assemblies in a determined size range. For this, Aβ assemblies are liberated from the gel matrix by enzymatic digestion of agarose. Using semi-native isolated Aβ assemblies enables the evaluation of binding affinities of anti-Aβ antibodies to Aβ in a specific agarose fraction using IP and western blot analysis (Fig. 13). Furthermore, this assay provides the opportunity to determine the biological activity, such as the *in vivo* seeding activity of Aβ assemblies. For a quantitative purpose, agarose fractions can be melted in denaturing sample buffer and applied to SDS-PAGE and western blot analysis (Fig. 13).

In order to investigate the antibody recognition profiles of anti-Aβ antibodies (used for passive immunization) on amyloid-laden brain homogenates, material from 26-month-old male APP23 mice was used to perform ARPA (Fig. 14).

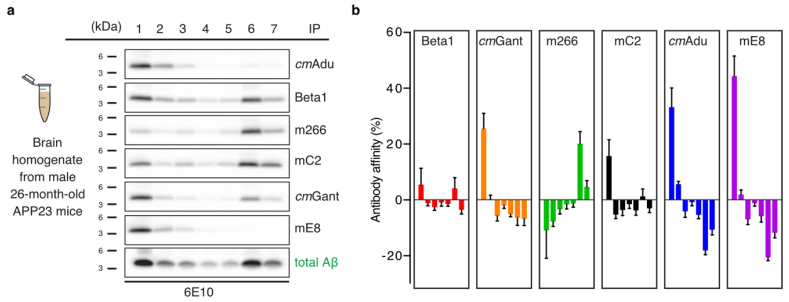

Figure 14 Antibody recognition profiling of Aβ assemblies (ARPA) using amyloid-laden brain material. ARPA using 10% brain homogenate pooled from 26-month-old APP23 mice (n= 3) revealed distinct recognition profiles for the tested antibodies. (**a**) Western Blot analysis (with 6E10 as detection antibody) of ARPA revealed cmAdu and mE8 almost exclusively pulled-down Aβ from high molecular weight fractions (F1 to F3). Similarly, cmGant preferentially binds high molecular weight Aβ (F1 and F2) but also Aβ within low molecular weight fractions (F6 and F7). Contrary to this, m266 and mC2 recognize Aβ mainly in low molecular weight fractions (F6 and F7) and only partially in the other fractions. Beta1 reveals no specificity towards a certain fraction and reveals a pattern similar to melted fractions, reflecting total Aβ. (**b**) Results from western blot analysis (a) were quantified and normalized to total Aβ within a fraction, illustrating the antibody affinity for Aβ within a specific agarose fraction. Adapted from Uhlmann *et al.*, 2020 and created with Affinity Designer version 1.10.4.

High molecular weight Aβ assemblies are running in the upper fractions such as 1 (F1) and 2 (F2), whereas low molecular weight species are restricted to fractions 5 (F5) to 7 (F7) (Uhlmann *et al.*, 2020). The Aβ distribution of amyloid-laden brain material on an agarose gel (total Aβ) reveals the strongest Aβ signals in F1 and F6, followed by F2 and F7 and less pronounced signals in F3 to F5 (Fig. 14a). This pattern indicates a great spectrum of Aβ assemblies with distinct molecular sizes and points towards the capability of ARPA to facilitate the screening of anti-Aβ antibodies with various epitope recognition for their binding affinities.

Screening for the epitope recognition profiles of cmAdu, Beta1, m266, mC2, cmGant and mE8 (Fig. 14a) and normalizing the signal intensities of each fraction to total Aβ, provided a barcode for their binding affinities (Fig. 14b). Our results align well with the binding affinities found in the literature (see section 3.2.1). Positive values in the antibody binding affinity barcode are interpreted as preferential binding of the tested antibody to Aβ assemblies in this fraction,

whereas negative values indicate a weaker affinity. The antibodies cmAdu and mE8, recognized almost exclusively high molecular weight Aβ assemblies (Fig. 14), accordingly to the reported preference for Aβ plaques and aggregates (DeMattos *et al.*, 2012; Sevigny *et al.*, 2016). Similar, cmGant pulled down preferentially high molecular weight Aβ, however also revealed some binding to low molecular weight Aβ in F6 and F7 (Fig. 14). In comparison, m266 and mC2 mainly recognized low molecular weight assemblies with the strongest Aβ signal in F6 (Fig. 14). Despite the clear binding preference to Aβ assemblies in F6, m266 and mC2 also recognized Aβ in all other fractions (Fig. 14).

In order to further interpret the recognition profiles of the tested antibodies, we aimed to determine the Aβ seeding activity within the distinct agarose fractions. Therefore, we performed the well-established endpoint titration assay to estimate SD_{50} according to Ye *et al.*, 2017. ARPA was performed with sAD brain material and revealed a similar pattern as observed for amyloid-laden mouse brain homogenate (Fig. 15a). Agarose fractions harbouring Aβ assemblies from sAD patients were serially diluted and intracerebrally injected into APP23 host mice (Fig 15b). Eight months post-injection, the number of positively seeded mice of each dilution was used to calculate the SD_{50} of each agarose fraction (Fig. 15c-e).

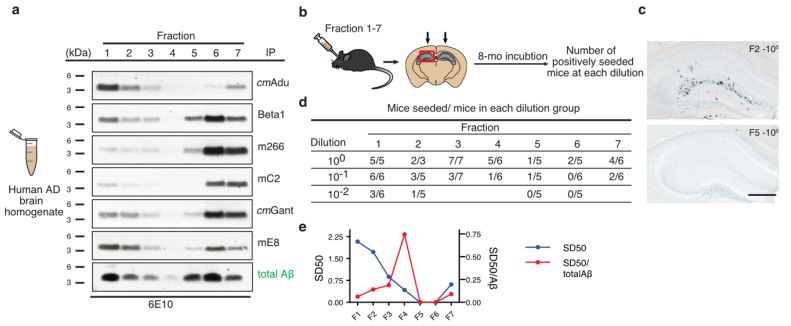

Figure 15 Antibody recognition profiling of Aβ assemblies (ARPA) with human AD brain material and estimation of the seeding activity. (**a**) Brain homogenates (10%) of 3 AD subjects (Braak stage VI) were pooled and subjected to ARPA testing various Aβ-targeting antibodies. Western blot analysis (decorated with 6E10) revealed similar results as seen for ARPA using amyloid-laden brain samples from APP23 mice. (**b**) ARPA fractions containing AD brain material and their dilutions were injected into the hippocampus of pre-depositing 2- to 3-month-old male APP23 host mice. The Aβ induction in the hippocampus was analyzed by immunohistochemical staining 8 months post-injection. (**c**) Results of immunohistochemical staining for F2 and F5 (both undiluted injected) are shown. A high seeding activity for F2 and no seeding for F5 was recognized. Scale bar, 500 µm. (**d**) The results are shown as the number of mice with induced Aβ deposition versus the number of mice inoculated within a group tested. All groups had initially 6-7 mice, of which 4 mice inoculated with undiluted F2 died. (**e**) The SD_{50} (blue

line) and specific seeding activity (red line, SD_{50}/total Aβ) were calculated for each fraction. Adapted from Uhlmann *et al.*, 2020 and created with Affinity Designer version 1.10.4.

The highest SD_{50} was calculated for F1 followed by a decreasing SD_{50} in F2, F3, F7 and F4. No SD_{50} values were calculated for the F5 and F6 due to the low number of positively seeded host mice (Fig. 15d). These results indicate a correlation between high molecular weight Aβ assemblies and high SD_{50} values. However, calculating the specific seeding activity (SD_{50}/total Aβ) revealed great Aβ-inducing potential in F4 (Fig 15e). This high specific seeding activity in F4 is most likely due to the low Aβ concentration in this fraction, nevertheless, it highlights the non-linear relationship between Aβ load and biological seeding activity. Whether this high specific seeding activity in F4 is solely based on Aβ remains to be investigated, since ARPA fractions not only contain Aβ but a great variety of proteins present in brain homogenates. Further characterization of the non-Aβ content in these fractions, for instance with the mean of mass spectrometry, would be necessary to fully understand these seeding results.

We aimed to biochemically characterize the Aβ assembly recognized by the *in vivo* tested anti-Aβ antibodies at the pre-amyloid disease phase. Based on the epitope recognition profile of cmAdu obtained with amyloid-laden brain material of AD subjects (Fig. 15a) and APP23 mice (Fig. 14a), one would expect that ARPA using brain material of pre-amyloid APP23 mice would reveal a faint signal for Aβ in high molecular weight fractions. However, due to the assumed absence of high molecular weight species at the pre-amyloid stage, the seeding results from cmAdu treated mice (Fig. 12b) and due to the high specific seeding activity in F4 (Fig. 15e), one might speculate that cmAdu would recognize Aβ in a fraction containing smaller Aβ assemblies, such as F4. To test this, ARPA using brain homogenate from 6-month-old APP23 mice was performed (Fig. 16a).

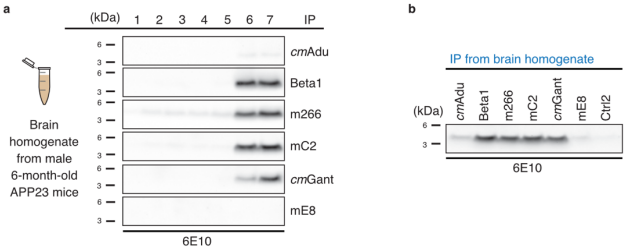

Figure 16 Antibody recognition profiling of Aβ assemblies (ARPA) using brain material from pre-depositing APP23 mice. (**a**) ARPA using 10% brain homogenate pooled from 6-month-old APP23 mice

showed Aβ was pulled down from the low molecular weight fractions (F6 and F7) only. Western blot analyses (with 6E10 as detection antibody) of ARPA revealed Aβ in F6 and F7 was pulled down by Beta1, m266, mC2 and to a lesser extent by cmGant. No Aβ in any fraction was recognized by cmAdu and mE8. (**b**) Immunoprecipitation with cmAdu as capture antibody from unfractionated, pooled brain homogenate (the same as in (a)) indicates a faint Aβ signal. Adapted from Uhlmann *et al.*, 2020 and created with Affinity Designer version 1.10.4.

ARPA with cmAdu did not reveal Aβ signals in any fraction. This was partially unexpected as cmAdu passive immunization had a measurable effect on $Aβ_{42}$ levels in the formic acid soluble fraction as well as on the seeding activity in APP23 host mice (Fig. 12), which indicates antibody target engagement at this pre-amyloid disease phase. A possible reason for this negative result might be the absence of the cmAdu target assembly in brain homogenates. Biochemical isolation of early Aβ assemblies might have led to Aβ monomerization, which in turn would not be a preferential target for cmAdu. In line with this hypothesis, ARPA with Beta1, m266, mC2 and cmGant resulted solely in detection of Aβ in low molecular weight assemblies. Also, the concentration of the Aβ pre-amyloid seed targeted by cmAdu might have been below the detection limit of ARPA, limiting further investigations. In order to test for this, direct IP on unfractionated brain material from 6-month-old APP23 mice was performed and despite a missing signal in ARPA, IP with cmAdu as capture antibody revealed a faint Aβ signal (Fig. 16b). Despite aducanumab's great affinity for Aβ aggregates (Sevigny *et al.*, 2016) the linear epitope recognized by this antibody is also present on Aβ monomers and most likely soluble Aβ assemblies (Arndt *et al.*, 2018). Therefore, the signal observed by IP cannot be attributed with certainty to the Aβ species recognized and reduced by cmAdu *in vivo.* In symptomatic AD brain homogenates, but solely in a fraction of patients with preclinical AD, pE-Aβ was detected, indicating this Aβ modification is related to a later stage of the disease (Rijal Upadhaya *et al.*, 2014). In different mouse models for AD-like pathology, Aβ deposition proceeded with the deposition of pE-Aβ (Frost *et al.*, 2013). In agreement with these data, no Aβ signal was observed by ARPA nor by direct IP using mE8 as the capture antibody (Fig. 16).

3.2.3 Amyloid-β targeting antibodies with distinct epitope recognition possess differences in kinetics

ARPA is a useful technique to determine epitope characteristics recognized by anti-Aβ antibodies *in vitro*, however, it does not provide information about the impact of antibody binding on Aβ aggregation kinetics. Indeed, a comparative analysis of therapeutic Aβ-targeting antibodies identified distinct effects on Aβ aggregation kinetics by cmAdu, m266 and cmGant (Linse *et al.*, 2020). In an *in vitro* aggregation assay, cmAdu effectively reduced the formation of oligomeric Aβ and had an impact on secondary, rather than primary, nucleation (Linse *et*

al., 2020). These data are coherent with the low affinity of cmAdu to Aβ monomers (Arndt *et al.*, 2018). The antibody cmGant targeted the elongation of fibrils, leading to reduced fibril growths, whereas m266 selectively inhibited the primary nucleation event (Linse *et al.*, 2020), consistent with its high affinity to monomeric Aβ (Yamada *et al.*, 2009). Additionally, m266 failed to inhibit Aβ fibril growths (Linse *et al.*, 2020). Based on aggregation kinetics from the literature and a strong signal in the low molecular weight fractions in ARPA using pre-depositing brain material (Fig. 16a), one would expect m266 to be a suitable antibody for the prevention of the early Aβ aggregation event *in vivo*. Contrary to this, m266 failed to have a measurable effect on Aβ, whereas cmAdu succeeded in the reduction of formic acid-soluble $Aβ_{42}$ in pre-depositing APP23 mice (Fig. 12a). To investigate whether the treatment effects *in vivo* of three antibodies with distinct ARPA profiles might have been governed by the specific pharmacokinetic features rather than purely by binding affinities, antibody titre measurements in APP23 mice and WT littermates were performed. For this, Beta1, m266 and cmAdu were intraperitoneally injected into 6-month-old APP23 or WT mice and antibody plasma levels were determined 1-, 7- and 21-days post application (Fig 17a).

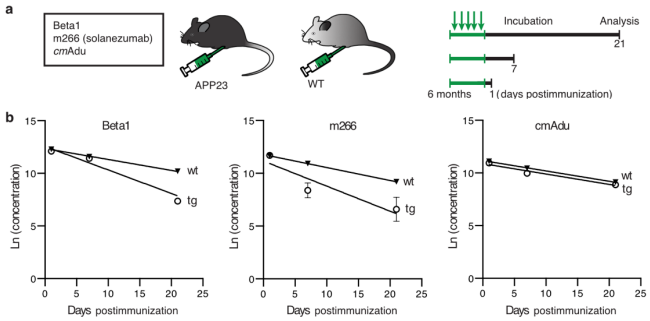

Figure 17 Antibody titre measurements of administered Aβ-targeting antibodies at the pre-amyloid stage. (**a**) Schematic representation of the experimental design. As before, 0.5 mg therapeutic antibodies were delivered intraperitoneally on 5 consecutive days to 6-month-old male transgenic APP23 mice and 6-month-old male WT mice. Either Beta1, m266 or cmAdu (n= 5 per group per antibody) were injected and mice were analysed 1-, 7- or 21-day post-injection. (**b**) The plasma logarithmic changes (ln) in antibody concentration over time (days) in APP23 and WT mice are shown. For Beta1 and m266, a faster decline in antibody concentration was reported in APP23 compared to WT, while for cmAdu, no difference between transgenic and non-transgenic mice was apparent. Adapted from Uhlmann *et al.*, 2020 and created with Affinity Designer version 1.10.4.

The plasma antibody levels of m266 and Beta1 declined faster in APP23 mice compared to WT, whereas the decline of cmAdu was indistinguishable between APP23 and WT (Fig. 17b).

Based on these results, Beta1 and m266 might have recognized soluble Aβ in the brain and/or in the blood, as it has been reported for m266 (DeMattos *et al.*, 2001), and therefore could have been cleared faster compared to cmAdu. An antibody titre measurement in the brain of antibody-treated mice was not feasible as the concentrations of the antibodies were below the detection limit. From a single intraperitoneal injection of polyclonal human IgGs in mice, 10-times more than what was used in our experiments, only ~0.009% and 0.0017% of the administered antibody reached the cortex and hippocampus, respectively (St-Amour *et al.*, 2013). Therefore, a comparison between the quantity of initially applied antibodies versus the amount reaching the brain is missing and it remains speculative whether Aβ reduction by cmAdu in pre-amyloid APP23 was due to a greater antibody availability in the brain or by its distinct binding affinities.

3.2.4 Early targeting of pre-amyloid seeds alleviates secondary pathologies

In order to investigate how an early passive immunization would affect Aβ deposition and downstream pathogenic changes such as microglial activation and neurodegeneration at a later disease stage, APP23 mice immunized at the pre-amyloid stage were analysed 6 months post-injection. Brain Aβ load was estimated after Triton-X 100 and subsequent formic acid extraction by highly sensitive Aβ immunoassays (Fig. 18a). Furthermore, immunohistochemistry was used to determine the cortical Aβ load, Aβ plaque number and size (Fig. 18b) and fluorescence staining with luminescent conjugated oligothiophenes (LCOs) to determine differences in the molecular conformation of Aβ plaques (Fig. 18c).

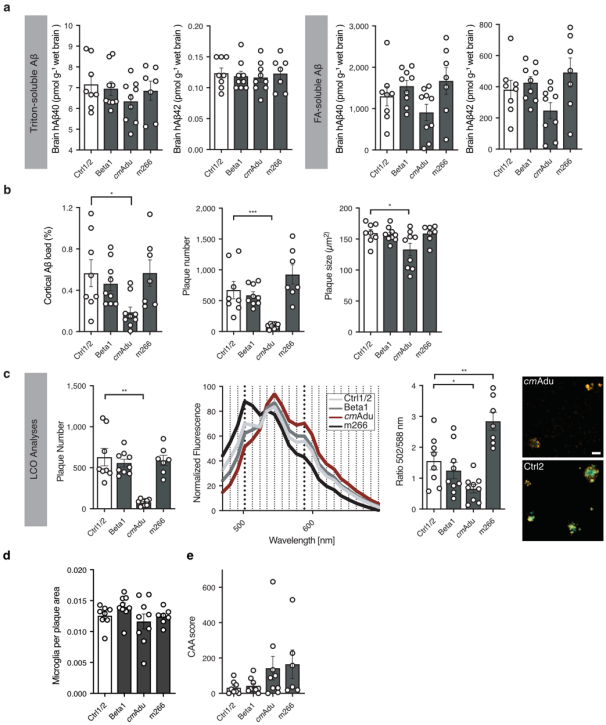

Figure 18 Long-lasting effects on Aβ by passive immunotherapy at pre-amyloid stage. As before, 6-month-old male APP23 mice (n= 10 per group) received on 5 consecutive days 0.5 mg of either Beta1, m266, cmAdu or corresponding control (Ctrl) antibodies (Ctrl1, Ctrl2) intraperitoneally. Mice were sacrificed 6 months post-injection and analysed biochemically as well as immune-histologically. (**a**) Brain homogenates were prepared by a 2-step extraction with Triton X-100 and subsequently formic acid. Human $A\beta_{x\text{-}40}$ and $A\beta_{x\text{-}42}$ concentrations were measured by MSD immunoassays. A Kruskal–Wallis test was performed and indicated no group differences for the Triton X-100-extracted hAβ ($A\beta_{x\text{-}40}$, $H_{(3)}$= 1.718, P= 0.6329; $hA\beta_{x\text{-}42}$, $H_{(3)}$= 0.4967, P= 0.9196). Also, measurements of hAβ in the formic acid-soluble fraction revealed no statistically significant differences (one-way ANOVA: $hA\beta_{x\text{-}40}$, $F_{(3,29)}$= 2.360, P= 0.0920; $hA\beta_{x\text{-}42}$, $F_{(3,29)}$= 3.0170, P= 0.0459; a subsequent post hoc Dunnett's multiple comparisons test did not indicate a difference between the combined Ctrl1/2 and any treatment group). Although, $hA\beta_{x\text{-}42}$ in cmAdu-treated mice was reduced compared to Ctrl-treated mice. (**b**) CN6 and Congo Red double-stained brain sections were used to quantify cortical Aβ load by stereology and revealed that cmAdu-treated mice had significantly less Aβ deposition compared to mice receiving Ctrl-antibodies (one-way ANOVA: $F_{(3,29)}$= 3.613; P= 0.0248; post hoc Dunnett's multiple comparisons test: P= 0.0223). Furthermore, cmAdu-treated mice showed a great reduction in plaque number (one-way ANOVA: $F_{(3,29)}$= 12.35; P< 0.0001; post hoc Dunnett's multiple comparisons test: P= 0.0007). However, the plaque size was only slightly reduced in mice receiving cmAdu (one-way ANOVA: $F_{(3,29)}$= 3.6320; P= 0.0247; post hoc Dunnett's multiple comparisons test: P= 0.0268). (**c**) Brain sections of antibody-treated mice were stained with the combination of two (qFTAA and hFTAA) LCOs and analysed for conformational differences in Aβ plaques. In line with the total plaque number in (b), the number of LCO-positive cortical plaques was lower in cmAdu-treated mice versus controls (Kruskal–Wallis test: $H_{(3)}$= 19,11; P= 0.0003;

Dunn's multiple comparisons test P= 0.0013). The mean fluorescence emission pattern of plaque cores is shown in the middle. The ratio of the fluorescence emission at 502/588 nm was quantified (one-way ANOVA: $F_{(3,29)}$= 13.10; P< 0.0001; post hoc Dunnett's multiple comparisons test Ctrl2 versus cmAdu: P= 0.037; Ctrl versus m266: P= 0.004) and indicated a red-shift in plaques for cmAdu versus Ctrl2. Representative qFTAA and hFTAA stained plaques of cmAdu- and Ctrl2-treated mice are shown (Scale bar, 25 µm). (**d**) Microglia around congophilic plaques were quantified in brain sections double-stained with PU.1 antibody and Congo Red and revealed no difference in microglia per plaques area (one-way ANOVA: $F_{(3,29)}$= 1.524, P= 0.2291). (**e**) No statistically significant difference in the amount of CAA was found among the treatment groups, although 2 mice treated with cmAdu and 3 treated with m266 had slightly increased CAA counts. Adapted from Uhlmann *et al.*, 2020 and created with Affinity Designer version 1.10.4.

In line with the prior experiments, passive immunization with m266 and Beta1 (compared to controls) failed to reduce Aβ measured biochemically and immune-histologically (Fig. 18a, b). Although, biochemical quantification revealed no significant reduction in Aβ with any Aβ-targeting antibody tested, a reduction in $Aβ_{40}$ and $Aβ_{42}$ levels in the formic acid-soluble fraction was achieved in cmAdu-treated mice (Fig. 18a). These data indicate, the reduction of formic acid soluble Aβ at pre-amyloid phase has a long-lasting effect. Histological analysis of the brain of cmAdu-treated mice also revealed a significant lowering of cortical Aβ load and plaque numbers, although the plaque sizes were largely unaffected (Fig. 18b). This is in agreement with the proposed kinetic fingerprint for cmAdu, which suggests cmAdu targets rather secondary nucleation events than Aβ fibril growth (Linse *et al.*, 2020).

Furthermore, an investigation of Aβ plaque conformations using LCO dyes indicates an altered molecular plaque structure compared to control animals in cmAdu- and m266-treated mice towards more diffuse and dense plaques, respectively (Fig. 18c). This might indicate that, the Aβ reduction by cmAdu potentially delayed Aβ plaque formation and thereby also plaque maturation to more dense plaques, as it has been indicated for APPPS1 mice (Nyström *et al.*, 2013). Another possibility is the specific targeting and clearance of Aβ conformational variants associated with dense-cored plaques by cmAdu, which in turn might have impacted plaque morphology. This hypothesis also provides an explanation for the more dense plaque structures seen in m266-treated mice (Fig. 18c). By targeting mainly soluble Aβ (Yamada *et al.*, 2009), m266 considerably reduced diffuse plaque components but failed to prevent plaque formation and maturation, leading to increasingly dense plaque structures.

Microglia were shown to engulf and thereby compact Aβ plaques (Huang *et al.*, 2021) which reduced Aβ-associated Tau pathology and dystrophic neurites (Condello *et al.*, 2015; Wang *et al.*, 2016). Therefore, different microglial responses upon passive immunization with cmAdu and m266 might have affected plaque morphology. To test for this, immune-histological analysis of microglia was performed and no change in microglia numbers per plaque was observed among Aβ-targeting antibodies compared to controls (Fig. 18d). These data indicate

that the observed plaque morphologies were not based on microglial engagement. Furthermore, no significant differences in amyloid-associated Tau pathology or CSF NfL levels were observed among treatment groups (Uhlmann *et al.*, 2020), indicating no detectable differences between diffuse and dense Aβ plaques on downstream pathology in these mice.

Amyloid-related imaging abnormalities (ARIA), referring to a variety of imaging features including vasogenic oedema and micro-haemorrhage, are detected generally in AD patients as well as those receiving treatment with Aβ-targeting antibodies (Sperling *et al.*, 2011). CAA is considered to be involved in the pathophysiological role of ARIA, but the functional relation between both is currently undefined (Greenberg *et al.*, 2020). Brain sections from mice receiving passive immunization were screened for CAA 6 months post-injection and no significant difference in CAA score was detected in mice receiving Aβ targeting antibodies compared to control (Fig. 18e). However, our data reveal a slight increase in CAA score when mice were treated with cmAdu and m266. Line of evidence suggests that clearance of Aβ via vascular might lead to deposition in vessels resulting in an increased CAA burden (Greenberg *et al.*, 2020) which could explain our observed results. Furthermore, the CAA frequency and severity were shown to increase with age in APP23 mice, which might reduce arterial wall integrity and eventually lead to parenchymal haemorrhage (Winkler *et al.*, 2001). Clearance of Aβ by perivascular drainage might overstrain vascular integrity, leading to parenchymal haemorrhage visible as ARIA (Sevigny *et al.*, 2016). Nevertheless, no CAA-associated haemorrhage was detected in any treatment group tested.

3.2.5 Conclusion

Our data from preclinical studies indicate, that a therapeutic intervention that aims to target Aβ to prevent pathological changes, is most promising when initiated before pathogenic processes are set into motion. The Aβ nucleation process, taking place in the lag phase of the aggregation cascade, is presumably the earliest pathological change in Aβ. The lack of suitable detection methods and poor characterization of these early assemblies so far haltered their therapeutic targeting. Our data suggest the existence of pre-amyloid seeds in APP23 mice at least 2 months before plaque deposition becomes histologically detectable. Furthermore, therapeutic targeting of such early pre-amyloid seeds reduced Aβ seeding activity and Aβ deposition which was accompanied by beneficial long-lasting effects on downstream pathological changes. We thereby expand the current recognized therapeutic window for Aβ targeting to the presumably, primary nucleation event of Aβ aggregation.

A major challenge in targeting the initial seed formation in humans is the identification of the proper time point for treatment intervention. Current biomarkers for Aβ indicate plaque deposition (Cohen *et al.*, 2019), which might reflect a disease stage where primary prevention is no longer efficient. To test the potential of therapeutic antibodies targeting pre-amyloid seeds as preventive intervention, the recruitment of fAD patients at a time before biomarker changes become detectable would be most promising.

4 Final remarks and speculations

The relation between Aβ aggregation, Tau pathology, neuroinflammation and neuronal loss has been extensively studied (see Long and Holtzman, 2019 for review) but the molecular mechanism connecting these pathologies along the AD continuum is ill-defined. Due to many clinical studies, which successfully reduced Aβ in AD patients but failed to slow cognitive decline (Panza *et al.*, 2019), the causative role of Aβ in this cascade has been questioned (Thambisetty *et al.*, 2021).

The present thesis successfully recapitulated the uncoupling of Aβ load and neurodegeneration, as observed in AD patients, in a translational mouse model of cerebral amyloidosis at late disease stages. Biomarker trajectories in APPPS1 mice indicate that CSF NfL, a marker for neurodegeneration, begins to rise when Aβ depositions reached half-maximal levels and Aβ seeding activity already reached its plateau. Thus, a putative link between neurodegeneration and saturation of Aβ seeding activity has been hypothesised. In line with these observations, we showed that an efficient targeting of pre-amyloid Aβ seeds at an early disease stage was accompanied by a reduced Aβ seeding activity and long-term beneficial effects on secondary pathologies.

Both studies highlight a beneficial response to a therapeutic reduction of Aβ seeding activity at early disease stages but less so at later stages. A clear explanation for these observations is missing but the observed trajectories of Aβ deposition and delayed NfL increase is reminiscent of the proposed distinct pathogenic phases of a prion infection (Sandberg *et al.*, 2011).

4.1 A hypothetical two-phase model for distinct trajectories of amyloid-β and neurodegeneration

The prion field has provided a model to explain the molecular relationship between prion infectivity and toxicity (Sandberg *et al.*, 2011). Some aspects of this model might be applicable to unravel Aβ-independent neurodegeneration at late AD stages. Characteristic of prion diseases is the accumulation of the highly infectious disease-associated isoform PrP^{Sc} in the brain of an affected organism (Prusiner, 1998b). In humans, prion infection is followed by a prolonged incubation time which can span several years before entering a rapidly progressive clinical phase (Collinge *et al.*, 2006). In laboratory models, the incubation time correlates inversely with the PrP^{C} expression level, thus high expression leads to faster progression into the phenotypic, clinical phase (Büeler *et al.*, 1994). Interestingly, the overall accumulation of

PrP^{Sc} did not necessarily lead to clinical disease onset (Büeler *et al.*, 1994). Almost 20 years later, a model which accommodates these findings was formulated, where prion propagation ('infectivity') and toxicity occur in two distinct phases (Sandberg *et al.*, 2011). Phase one describes the exponential increase in prion infectivity, terminating in a plateau. Subsequently, a second phase is initiated which ultimately leads to clinical disease onset. It has been hypothesised that the transmission from phase one to two leads to a pathway switch that initiates the production of toxic PrP species (PrP^{L}) (Sandberg *et al.*, 2014). In support of this, prion infectivity and neurotoxicity were uncoupled in an experimental setup, indicating the involvement of two distinct PrP entities (Benilova *et al.*, 2020). Although PrP^{L} awaits further characterization, it has been suggested as soon as PrP^{L} exceeds a not definite threshold, phenotypic disease onset occurs (Collinge and Clarke, 2007; Sandberg *et al.*, 2011).

A partial adaption of the prion model for infectivity and toxicity offers a putative interpretation of the observed uncoupling of brain Aβ burden and CSF NfL levels in our APP mouse model at late disease stages. In this hypothetical two-phase model, *in vivo* Aβ seeding activity would be the equivalent of prion infectivity and CFS NfL a readout for toxicity. As soon as the infectivity, thus the Aβ seeding activity reaches its plateau or exceeds a certain 'critical threshold', a molecular switch could lead to the production of 'toxic Aβ species' and/or the initiation of a yet unrecognized pathway, resulting in an increase of NfL liberation into the CSF and presumably neurodegeneration (Fig. 19).

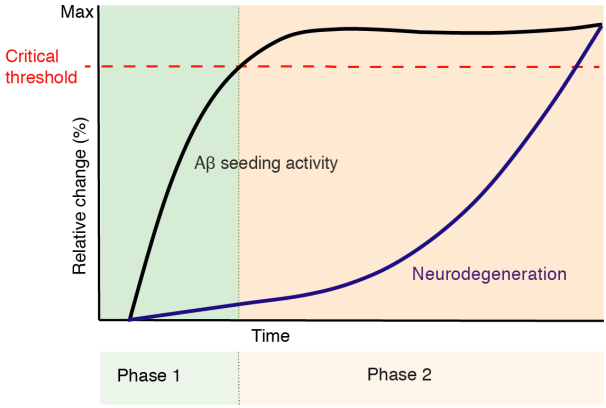

Figure 19 Presentation of a hypothetical two-phase model for Aβ-dependency of neurodegeneration. In phase one (green), Aβ seeding activity increases but has not yet reached its plateau and/or a certain threshold (red dotted line). The critical threshold would not be defined by a specific measure and might depend on individual factors which are not necessarily directly associated with Aβ. Entering phase two (orange) would be accompanied by a molecular switch leading to the build-up of a toxic Aβ species and/or the initiation of an undefined pathway, both driving disease-associated neurodegeneration, largely independent of total brain Aβ. Based on this hypothetical two-phase model, solely a reduction of total Aβ and Aβ seeding activity in the first phase could prevent disease-associated neurodegeneration. Created with Affinity Designer version 1.10.4.

4.1.1 Putative drivers of neurodegeneration

In the present thesis, the driver(s) and the molecular pathway(s) underlying CFS NfL increase along with disease progression remain unidentified and therefore, the discussion will be limited to only some putative contributing factors in neurodegenerative processes.

4.1.1.1 Oligomeric protein species

As described earlier, Aβ oligomeric species have been considered a major toxic entity in the Aβ aggregation process. Aβ oligomers from postmortem AD patients were shown to be neurotoxic (Gong *et al.*, 2003; Shankar *et al.*, 2008; Hong *et al.*, 2018). Such Aβ oligomers isolated from late disease stages could arise from secondary nucleation events involving mature Aβ fibrils, considering secondary nucleation was postulated to be the dominant aggregation pathway above a certain Aβ fibril concentration (Cohen *et al.*, 2013). The build-

up of such late stage, toxic Aβ oligomers, might explain delayed neurodegeneration observed in AD patients and our mouse model. However, Aβ oligomers (albeit not necessarily the same oligomeric species) also have been considered as early aggregation entities with neurotoxic features in the absence of Aβ fibrils (Müller-Schiffmann *et al.*, 2016; Cataldi *et al.*, 2021).

Furthermore, Tau oligomers were shown to colocalize with Aβ oligomers at synaptic terminals (Fein *et al.*, 2008; Bilousova *et al.*, 2016). The soluble toxic forms of both, Aβ and tau, were suspected to play a critical role in neurodegeneration (Spires-Jones and Hyman, 2014), whereby Aβ oligomers were considered to act upstream of Tau pathology (Roberson *et al.*, 2007; Bilousova *et al.*, 2016). Recently, data indicate that oligomeric Aβ was superseded by oligomeric Tau at synapses, indicating Tau oligomers might become the dominant toxic species at late disease stage (Marcatti *et al.*, 2022). Therefore, Tau induced toxicity downstream of Aβ pathology could explain the Aβ-independent increase of CSF NfL at late disease stage. However, the mouse model studied in the present thesis lacks frank Tau pathology such as NFT (Sturchler-Pierrat *et al.*, 1997; Radde *et al.*, 2006), although an increase in soluble phosphorylated Tau species is observed (Kaeser *et al.*, 2022).

4.1.1.2 Posttranslational modifications

Posttranslational modifications (PTMs) of proteins, including Tau and Aβ, can have a tremendous effect on their stability, structure and function, depending on the type of modification as well as the position (Russell *et al.*, 2014). The phosphorylation of Aβ at position 8 was shown to lead to the formation of pathogenic fibrillar assemblies (Rezaei-Ghaleh *et al.*, 2016), whereas at position 26, oligomeric assembly was favoured, which was accompanied by an increase in neurotoxicity (Kumar *et al.*, 2016). While phosphorylated Aβ was detected in human AD brains, its clinical relevance remains to be investigated (Kumar *et al.*, 2011, 2016; Rijal Upadhaya *et al.*, 2014). Interestingly, Aβ phosphorylation at position 8 was mainly detected in brain specimens of symptomatic AD cases (Rijal Upadhaya *et al.*, 2014). Another PTM of Aβ is the N-terminal truncation and pyroglutamination at position 3 of Aβ (pE-$Aβ_{3-x}$), which was recognized as an abundant isoform in AD brains (Saido *et al.*, 1995) and possessed higher stability compared to unmodified Aβ (He and Barrow, 1999). Interestingly, pE-$Aβ_{3-42}$ together with $Aβ_{42}$ was shown to form small oligomers with enhanced and tau-dependent cytotoxicity in neuronal cell culture (Nussbaum *et al.*, 2012). PTMs specific for late disease stages could drive neurodegenerative processes independent of total Aβ deposition.

4.1.1.3 Senescence

Cellular senescence is defined as a permanent arrest of the cell cycle (Hayflick, 1965) and was proposed as a contributor to the ageing phenotype (López-Otín *et al.*, 2013). Senescence has been associated with AD, whereby its role as a cause or consequence in disease pathogenesis is not clear (Saez-Atienzar and Masliah, 2020). In case of a non-lethal, chronic and/or severe insult, cells can undergo senescence, a permanent, non-proliferating stage (Hayflick, 1965; Song *et al.*, 2005; Spallarossa *et al.*, 2009). There are different stages of cellular senescence with specific characteristics. At an early stage, cells exit the cell cycle which is accompanied by an altered gene expression profile (Salminen *et al.*, 2012) resulting in a senescence-associated secretory phenotype (SASP) (Coppé *et al.*, 2008). This SASP is a hallmark of full-senescent cells and is characterized by cell secretion of pro-inflammatory molecules (Coppé *et al.*, 2008; Salminen *et al.*, 2012). Components of the SASP can provoke pathological changes in the surrounding tissue and impaired clearance of chronic senescent cells has been associated with neurodegeneration (Van Deursen, 2014).

The senescent inducing factor was shown to be heterogeneous (Sharpless and Sherr, 2015; Hernandez-Segura *et al.*, 2017). Experimental data indicate that protein aggregation of Aβ and Tau are tightly associated with cellular senescence. For instance, in an amyloid plaque bearing mouse model, senescent oligodendrocyte progenitor cells were observed to accumulate around Aβ plaques (Zhang *et al.*, 2019) and in a mouse model for tau-dependent neurodegeneration, senescent astrocytes and microglia were present (Bussian *et al.*, 2018). Furthermore, NFT-bearing neurons isolated from postmortem AD patients revealed transcriptional profiles corresponding to senescence (Musi *et al.*, 2018). Therapeutic removal of senescent cells reduced neuroinflammation without affecting Aβ plaque load (Zhang *et al.*, 2019), had beneficial effects on gliosis and Tau pathology (Bussian *et al.*, 2018) and reduced neuronal loss (Musi *et al.*, 2018). Impaired immune surveillance was shown to contribute to the accumulation of senescent cells in ageing (Ovadya *et al.*, 2018). The accumulation of senescent cells also referred to as primary senescence, is hypothesized to impair cell homeostasis, leaving the tissue more vulnerable to disease and other insults which in turn might induce a second wave of senescence (Childs *et al.*, 2015). Whether Aβ oligomers, fibrils, posttranslational-modified Aβ and/or a non-Aβ entity such as Tau act as an initiator for chronic senescence in the course of AD remains to be investigated. Although neuronal cell death is a well-established hallmark of neurodegenerative diseases, the mode of cell death underlying neurodegeneration remains undefined (Moujalled *et al.*, 2021).

4.1.2 Chances and limitations of the hypothetical two-phase model

The hypothetical two-phase model is in line with the broadly accepted assumption that Aβ targeting approaches are most promising at an early disease stage (Golde *et al.*, 2018). However, this hypothetical two-phase model appears short to mechanistically fully explain the observed uncoupling of Aβ deposition and CSF NfL along disease progression. Nevertheless, the concept of an individual critical threshold, offers an explanation for the high variability in clinical disease onset (Reitz *et al.*, 2020; Ayodele *et al.*, 2021) and the discrepancy in age at onset in siblings with the same inheritance of AD (Gómez-Tortosa *et al.*, 2007). Risk factors such as air pollution (Shi *et al.*, 2021a) and lifestyle (Deckers *et al.*, 2020) which have been indirectly associated with AD, might determine a patients' individual critical threshold for phase transmission. It should be noted, that the general concept of a specific threshold in neurodegenerative disease has been introduced by various threshold theories for AD and PD (Satz, 1993). A theoretical construct similar to the hypothetical two-phase model was postulated and characterised by brain 'resistance' and 'resilience' (Arenaza-Urquijo and Vemuri, 2018). 'Resistance' defines the brains' ability to prevent pathology and 'resilience' the capacity to cope with pathology. Both would depend on contributing factors such as lifestyles, education and/or metabolic processes (Arenaza-Urquijo and Vemuri, 2018). This concept of brain resistance and resilience matches the idea of an individual capacity (critical threshold) to withstand disease onset.

A detailed mechanistic evaluation of such theoretical models appears important for further studies. Determination of Aβ seeding activity in humans is methodically challenging since there is no indication of Aβ seeding activity in human body fluids such as blood (Edgren *et al.*, 2016) and CSF (Fritschi *et al.*, 2014). Data indicate that Aβ plaque load by PET is not a measure for disease progression and Aβ CSF biomarker and Aβ PET in fact might reflect different pathological processes (Chhatwal *et al.*, 2022). Therefore, to directly measure the Aβ seeding activity, *in vitro* fibrilization assays such as the Fibrillization of Recombinant Aβ Nucleation Kinetic (FRANK) assay (Nagarathinam *et al.*, 2013; Groh *et al.*, 2017) or *in vivo* end-point titration assay (Ye *et al.*, 2017), using Aβ harbouring brain material would be required. These methodical limitations impede longitudinal studies of Aβ seeding activity and correlations with the clinical presentation in AD patients. However, such longitudinal AD biomarker trajectories with regard to Aβ seeding activity would be inevitable to test the hypothetical two-phase model in humans. Patients carrying a causative mutation for AD without biomarker changes according to the A/T/N schema (Jack *et al.*, 2016) would be the most suitable participants for such as clinical study.

Naturally, the speculations in the present thesis await further investigations. Until then, the present thesis points towards a promising treatment opportunity where early reduction of Aβ below a certain threshold putatively enables the diminishment of secondary pathologies which once triggered most likely are not reversible.

5 References

'2020 Alzheimer's disease facts and figures' (2020) *Alzheimer's Dement*. John Wiley & Sons, Ltd. doi:10.1002/ALZ.12068.

'ADAM metallopeptidase domain containing' (no date) *accessed 27 April 2022, www.genenames.org/data/genegroup/#!/group/47*.

Adolfsson, O., Pihlgren, M., Toni, N., Varisco, Y., Buccarello, A.L., *et al.* (2012) 'An effector-reduced anti-β-amyloid (Aβ) antibody with unique Aβ binding properties promotes neuroprotection and glial engulfment of Aβ', *J. Neurosci.*, 32(28), pp. 9677–9689. doi:10.1523/JNEUROSCI.4742-11.2012.

Alonso, A.C., Zaidi, T., Grundke-Iqbal, I. and Iqbal, K. (1994) 'Role of abnormally phosphorylated tau in the breakdown of microtubules in Alzheimer disease.', *Proc. Natl. Acad. Sci. U. S. A.*, 91(12), p. 5562. doi:10.1073/PNAS.91.12.5562.

Alonso, A.C., Zaidi, T., Novak, M., Grundke-Iqbal, I. and Iqbal, K. (2001) 'Hyperphosphorylation induces self-assembly of τ into tangles of paired helical filaments/straight filaments', *Proc. Natl. Acad. Sci.*, 98(12), pp. 6923–6928. doi:10.1073/PNAS.121119298.

Alonso, A.C., Grundke-Iqbal, I. and Iqbal, K. (1996) 'Alzheimer's disease hyperphosphorylated tau sequesters normal tau into tangles of filaments and disassembles microtubules', *Nat. Med. 1996 27*, 2(7), pp. 783–787. doi:10.1038/nm0796-783.

Alonzo, N.C., Hyman, B.T., Rebeck, G.W. and Greenberg, S.M. (1998) 'Progression of Cerebral Amyloid Angiopathy: Accumulation of Amyloid-β40 in Affected Vessels', *J. Neuropathol. Exp. Neurol.*, 57(4), pp. 353–359. doi:10.1097/00005072-199804000-00008.

Alzheimer, A. (1907) 'Über eine eigenartige Erkrankung der Hirnrinde', *Allg. Zeitschrift fur Psychiatr. und Psych. Medizin.*, (64), pp. 146–148.

Amaral, A.C., Perez-Nievas, B.G., Siao Tick Chong, M., Gonzalez-Martinez, A., Argente-Escrig, H., *et al.* (2021) 'Isoform-selective decrease of glycogen synthase kinase-3-beta (GSK-3β) reduces synaptic tau phosphorylation, transcellular spreading, and aggregation', *iScience*, 24(2), p. 102058. doi:10.1016/J.ISCI.2021.102058.

Ancolio, K., Dumanchin, C., Barelli, H., Warter, J.M., Brice, A., *et al.* (1999) 'Unusual phenotypic alteration of β amyloid precursor protein (βAPP) maturation by a new Val-715 → Met βAPP-770 mutation responsible for probable early-onset Alzheimer's disease', *Proc. Natl. Acad. Sci. U. S. A.*, 96(7), p. 4119. doi:10.1073/PNAS.96.7.4119.

Arenaza-Urquijo, E.M. and Vemuri, P. (2018) 'Resistance vs resilience to Alzheimer disease: Clarifying terminology for preclinical studies', *Neurology*, 90(15), p. 695. doi:10.1212/WNL.0000000000005303.

Arispe, N., Pollard, H. and Rojas, E. (1994) 'The ability of amyloid beta-protein [A beta P (1-40)] to form Ca2+ channels provides a mechanism for neuronal death in Alzheimer's disease', *Ann. N. Y. Acad. Sci.*, 747, pp. 256–266. doi:10.1111/J.1749-6632.1994.TB44414.X.

Arndt, J.W., Qian, F., Smith, B.A., Quan, C., Kilambi, K.P., *et al.* (2018) 'Structural and kinetic basis for the selectivity of aducanumab for aggregated forms of amyloid-β', *Sci. Rep.*, 8(1), pp. 1–16. doi:10.1038/s41598-018-24501-0.

Arriagada, P. V, Growdon, J.H., Hedley-Whyte, E.T. and Hyman, B.T. (1992) 'Neurofibrillary tangles but not senile plaques parallel duration and severity of Alzheimer's disease.', *Neurology*, 42(3 Pt 1), pp. 631–9.

Ashton, N.J., Pascoal, T.A., Karikari, T.K., Benedet, A.L., Lantero-Rodriguez, J., *et al.* (2021) 'Plasma p-tau231: a new biomarker for incipient Alzheimer's disease pathology', *Acta Neuropathol. 2021 1415*, 141(5), pp. 709–724. doi:10.1007/S00401-021-02275-6.

Atri, A. (2019) 'The Alzheimer's Disease Clinical Spectrum: Diagnosis and Management', *Med. Clin. North Am.*, 103(2), pp. 263–293. doi:10.1016/J.MCNA.2018.10.009.

Ayodele, T., Rogaeva, E., Kurup, J.T., Beecham, G. and Reitz, C. (2021) 'Early-Onset Alzheimer's Disease: What Is Missing in Research?', *Curr. Neurol. Neurosci. Reports 2021 212*, 21(2), pp. 1–10. doi:10.1007/S11910-020-01090-Y.

Bacioglu, M., Maia, L.F., Preische, O., Schelle, J., Apel, A., *et al.* (2016) 'Neurofilament Light Chain in Blood and CSF as Marker of Disease Progression in Mouse Models and in Neurodegenerative Diseases', *Neuron*, 91(1), pp. 56–66. doi:10.1016/j.neuron.2016.05.018.

Bagriantsev, S.N., Kushnirov, V. V. and Liebman, S.W. (2006) 'Analysis of Amyloid Aggregates Using Agarose Gel Electrophoresis', *Methods Enzymol.* Academic Press, pp. 33–48. doi:10.1016/S0076-6879(06)12003-0.

Bao, F., Wicklund, L., Lacor, P.N., Klein, W.L., Nordberg, A., *et al.* (2012) 'Different β-amyloid oligomer assemblies in Alzheimer brains correlate with age of disease onset and impaired cholinergic activity', *Neurobiol. Aging*, 33(4), pp. 825.e1-825.e13. doi:10.1016/J.NEUROBIOLAGING.2011.05.003.

Barthélemy, N.R., Li, Y., Joseph-Mathurin, N., Gordon, B.A., Hassenstab, J., *et al.* (2020a) 'A soluble phosphorylated tau signature links tau, amyloid and the evolution of stages of dominantly inherited Alzheimer's disease', *Nat. Med.*, 26(3), p. 398. doi:10.1038/S41591-020-0781-Z.

Barthélemy, N.R., Horie, K., Sato, C. and Bateman, R.J. (2020b) 'Blood plasma phosphorylated-tau isoforms track CNS change in Alzheimer's disease', *J. Exp. Med.*, 217(11). doi:10.1084/JEM.20200861.

Barthélemy, N.R., Bateman, R.J., Hirtz, C., Marin, P., Becher, F., *et al.* (2020c) 'Cerebrospinal fluid phospho-tau T217 outperforms T181 as a biomarker for the differential diagnosis of Alzheimer's disease and PET amyloid-positive patient identification', *Alzheimers. Res. Ther.*, 12(1). doi:10.1186/S13195-020-00596-4.

Bature, F., Guinn, B.A., Pang, D. and Pappas, Y. (2017) 'Signs and symptoms preceding the diagnosis of Alzheimer's disease: A systematic scoping review of literature from 1937 to 2016', *BMJ Open*. BMJ Publishing Group. doi:10.1136/bmjopen-2016-015746.

Benilova, I., Reilly, M., Terry, C., Wenborn, A., Schmidt, C., *et al.* (2020) 'Highly infectious prions are not directly neurotoxic', *Proc. Natl. Acad. Sci.*, p. 202007406. doi:10.1073/pnas.2007406117.

Benilova, I., Karran, E. and De Strooper, B. (2012) 'The toxic Aβ oligomer and Alzheimer's disease: an emperor in need of clothes', *Nat. Neurosci. 2012 153*, 15(3), pp. 349–357. doi:10.1038/nn.3028.

Bennett, R.E., DeVos, S.L., Dujardin, S., Corjuc, B., Gor, R., *et al.* (2017) 'Enhanced Tau Aggregation in the Presence of Amyloid β', *Am. J. Pathol.*, 187(7), pp. 1601–1612. doi:10.1016/J.AJPATH.2017.03.011.

Bilousova, T., Miller, C.A., Poon, W.W., Vinters, H. V., Corrada, M., *et al.* (2016) 'Synaptic Amyloid-β Oligomers Precede p-Tau and Differentiate High Pathology Control Cases', *Am. J. Pathol.*, 186(1), p. 185. doi:10.1016/J.AJPATH.2015.09.018.

Bode, D., Freeley, M., Nield, J., Palma, M. and JH, V. (2019) 'Amyloid-β oligomers have a profound detergent-like effect on lipid membrane bilayers, imaged by atomic force and electron microscopy', *J. Biol. Chem.*, 294(19), pp. 7566–7572. doi:10.1074/JBC.AC118.007195.

Bohrmann, B., Baumann, K., Benz, J., Gerber, F., Huber, W., *et al.* (2012) 'Gantenerumab: A novel human anti-Aβ antibody demonstrates sustained cerebral amyloid-β binding and elicits cell-mediated removal of human amyloid-β', *J. Alzheimer's Dis.*, 28(1), pp. 49–69. doi:10.3233/JAD-2011-110977.

Bolduc, D.M., Montagna, D.R., Gu, Y., Selkoe, D.J. and Wolfe, M.S. (2016a) 'Nicastrin functions to sterically hinder γ-secretase–substrate interactions driven by substrate transmembrane domain', *Proc. Natl. Acad. Sci. U. S. A.*, 113(5), p. E509. doi:10.1073/PNAS.1512952113.

Bolduc, D.M., Montagna, D.R., Seghers, M.C., Wolfe, M.S. and Selkoe, D.J. (2016b) 'The amyloid-beta forming tripeptide cleavage mechanism of γ-secretase', *Elife*, 5(AUGUST). doi:10.7554/ELIFE.17578.

Boon, B.D.C., Bulk, M., Jonker, A.J., Morrema, T.H.J., van den Berg, E., *et al.* (2020) 'The coarse-grained plaque: a divergent Aβ plaque-type in early-onset Alzheimer's disease', *Acta Neuropathol. 2020 1406*, 140(6), pp. 811–830. doi:10.1007/S00401-020-02198-8.

Borchelt, D.R., Thinakaran, G., Eckman, C.B., Lee, M.K., Davenport, F., *et al.* (1996) 'Familial Alzheimer's Disease–Linked Presenilin 1 Variants Elevate Aβ1–42/1–40 Ratio In Vitro and In Vivo', *Neuron*, 17(5), pp. 1005–1013. doi:10.1016/S0896-6273(00)80230-5.

Braak, H., Braak, E., Grundke-Iqbal, I. and Iqbal, K. (1986) 'Occurrence of neuropil threads in the senile human brain and in Alzheimer's disease: a third location of paired helical filaments outside of neurofibrillary tangles and neuritic plaques', *Neurosci. Lett.*, 65(3), pp. 351–355. doi:10.1016/0304-3940(86)90288-0.

Brokaw, D.L., Piras, I.S., Mastroeni, D., Weisenberger, D.J., Nolz, J., *et al.* (2020) 'Cell death and survival pathways in Alzheimer's disease: an integrative hypothesis testing approach utilizing -omic data sets', *Neurobiol. Aging*, 95, pp. 15–25. doi:10.1016/J.NEUROBIOLAGING.2020.06.022.

Brureau, A., Blanchard-Bregeon, V., Pech, C., Hamon, S., Chaillou, P., *et al.* (2017) 'NF-L in cerebrospinal fluid and serum is a biomarker of neuronal damage in an inducible mouse model of neurodegeneration', *Neurobiol. Dis.*, 104, pp. 73–84. doi:10.1016/J.NBD.2017.04.007.

Bucci, M., Chiotis, K. and Nordberg, A. (2021) 'Alzheimer's disease profiled by fluid and imaging markers: tau PET best predicts cognitive decline', *Mol. Psychiatry 2021*, pp. 1–11. doi:10.1038/s41380-021-01263-2.

Büeler, H., Raeber, A., Sailer, A., Fischer, M., Aguzzi, A., *et al.* (1994) 'High Prion and PrPSc Levels but Delayed Onset of Disease in Scrapie-Inoculated Mice Heterozygous for a Disrupted PrP Gene', *Mol. Med. 1994 11*, 1(1), pp. 19–30. doi:10.1007/BF03403528.

Bullich, S., Roé-Vellvé, N., Marquié, M., Landau, S.M., Barthel, H., *et al.* (2021) 'Early detection of amyloid load using 18F-florbetaben PET', *Alzheimer's Res. Ther.*, 13(1), pp. 1–15. doi:10.1186/S13195-021-00807-6/FIGURES/7.

Busche, M.A. and Hyman, B.T. (2020) ‘Synergy between amyloid-β and tau in Alzheimer’s disease’, *Nat. Neurosci.* Nature Research, pp. 1183–1193. doi:10.1038/s41593-020-0687-6.

Buss, R.R., Sun, W. and Oppenheim, R.W. (2006) ‘Adaptive Roles of Programmed Cell Death During Nervous System Development’, *Annu. Rev. Neurosci.*, 29, pp. 1–35. doi:10.1146/ANNUREV.NEURO.29.051605.112800.

Bussian, T.J., Aziz, A., Meyer, C.F., Swenson, B.L., van Deursen, J.M., *et al.* (2018) ‘Clearance of senescent glial cells prevents tau-dependent pathology and cognitive decline’, *Nature*, 562(7728), pp. 578–582. doi:10.1038/s41586-018-0543-y.

Capell, A., Meyn, L., Fluhrer, R., Teplow, D.B., Walter, J., *et al.* (2002) ‘Apical Sorting of β-Secretase Limits Amyloid β-Peptide Production *’, *J. Biol. Chem.*, 277(7), pp. 5637–5643. doi:10.1074/JBC.M109119200.

Carmona, S., Hardy, J. and Guerreiro, R. (2018) ‘The genetic landscape of Alzheimer disease’, *Handb. Clin. Neurol.*, 148, pp. 395–408. doi:10.1016/B978-0-444-64076-5.00026-0.

Cataldi, R., Chia, S., Pisani, K., Ruggeri, F.S., Xu, C.K., *et al.* (2021) ‘A dopamine metabolite stabilizes neurotoxic amyloid-β oligomers’, *Commun. Biol. 2021 41*, 4(1), pp. 1–10. doi:10.1038/s42003-020-01490-3.

Chatani, E. and Yamamoto, N. (2018) ‘Recent progress on understanding the mechanisms of amyloid nucleation’, *Biophys. Rev.*, 10(2), pp. 527–534. doi:10.1007/S12551-017-0353-8.

Chen, G.F., Xu, T.H., Yan, Y., Zhou, Y.R., Jiang, Y., *et al.* (2017) ‘Amyloid beta: Structure, biology and structure-based therapeutic development’, *Acta Pharmacol. Sin.* Nature Publishing Group, pp. 1205–1235. doi:10.1038/aps.2017.28.

Chen, Y.-R. and Glabe, C.G. (2006) ‘Distinct Early Folding and Aggregation Properties of Alzheimer Amyloid-β Peptides Aβ40 and Aβ42: Stable Trimer or Tetramer Formation by Aβ42*’, *J. Biol. Chem.*, 281(34), pp. 24414–24422. doi:10.1074/JBC.M602363200.

Chhatwal, J.P., Schultz, S.A., McDade, E., Schultz, A.P., Liu, L., *et al.* (2022) ‘Variant-dependent heterogeneity in amyloid β burden in autosomal dominant Alzheimer’s disease: cross-sectional and longitudinal analyses of an observational study’, *Lancet. Neurol.*, 21(2), pp. 140–152. doi:10.1016/S1474-4422(21)00375-6.

Childs, B.G., Durik, M., Baker, D.J. and Van Deursen, J.M. (2015) ‘Cellular senescence in aging and age-related disease: from mechanisms to therapy’, *Nat. Med. 2015 2112*, 21(12), pp. 1424–1435. doi:10.1038/nm.4000.

Choi, S.H., Kim, Y.H., Hebisch, M., Sliwinski, C., Lee, S., *et al.* (2014) ‘A three-dimensional human neural cell culture model of Alzheimer’s disease’, *Nature*, 515(7526), pp. 274–278. doi:10.1038/nature13800.

Choy, R.W.-Y., Cheng, Z. and Schekman, R. (2012) ‘Amyloid precursor protein (APP) traffics from the cell surface via endosomes for amyloid β (Aβ) production in the trans-Golgi network’, *Proc. Natl. Acad. Sci.*, 109(30), pp. E2077–E2082. doi:10.1073/PNAS.1208635109.

Cirrito, J.R., Kang, J.-E., Lee, J., Stewart, F.R., Verges, D.K., *et al.* (2008) ‘Endocytosis Is Required for Synaptic Activity-Dependent Release of Amyloid-β In Vivo’, *Neuron*, 58(1), pp. 42–51. doi:10.1016/J.NEURON.2008.02.003.

Ciryam, P., Tartaglia, G.G., Morimoto, R.I., Dobson, C.M. and Vendruscolo, M. (2013) ‘Widespread Aggregation and Neurodegenerative Diseases Are Associated with Supersaturated Proteins’, *Cell Rep.*, 5(3), pp. 781–790.

doi:10.1016/J.CELREP.2013.09.043/ATTACHMENT/DC20366B-E20A-48C8-87B5-D26376EC6D06/MMC2.XLSX.

Ciryam, P., Kundra, R., Morimoto, R.I., Dobson, C.M. and Vendruscolo, M. (2015) 'Supersaturation is a major driving force for protein aggregation in neurodegenerative diseases', *Trends Pharmacol. Sci.*, 36(2), p. 72. doi:10.1016/J.TIPS.2014.12.004.

Citron, M., Oltersdorf, T., Haass, C., McConlogue, L., Hung, A.Y., *et al.* (1992) 'Mutation of the β-amyloid precursor protein in familial Alzheimer's disease increases β-protein production', *Nat. 1992 3606405*, 360(6405), pp. 672–674. doi:10.1038/360672a0.

Ciudad, S., Puig, E., Botzanowski, T., Meigooni, M., Arango, A., *et al.* (2020) 'Aβ(1-42) tetramer and octamer structures reveal edge conductivity pores as a mechanism for membrane damage', *Nat. Commun.*, 11(1). doi:10.1038/S41467-020-16566-1.

Clark, C., Lewczuk, P., Kornhuber, J., Richiardi, J., Maréchal, B., *et al.* (2021) 'Plasma neurofilament light and phosphorylated tau 181 as biomarkers of Alzheimer's disease pathology and clinical disease progression', *Alzheimers. Res. Ther.*, 13(1). doi:10.1186/S13195-021-00805-8.

Clark, C.M., Schneider, J.A., Bedell, B.J., Beach, T.G., Bilker, W.B., *et al.* (2011) 'Use of florbetapir-PET for imaging beta-amyloid pathology', *JAMA*, 305(3), pp. 275–283. doi:10.1001/JAMA.2010.2008.

Clifford, Jack, Wiste, H.J., Lesnick, T.G., Weigand, S.D., *et al.* (2013) 'Brain β-amyloid load approaches a plateau', *Neurology*, 80(10), p. 890. doi:10.1212/WNL.0B013E3182840BBE.

Cohen, A.D., Landau, S.M., Snitz, B.E., Klunk, W.E., Blennow, K., *et al.* (2019) 'Fluid and PET biomarkers for amyloid pathology in Alzheimer's disease', *Mol. Cell. Neurosci.*, 97, pp. 3–17. doi:10.1016/J.MCN.2018.12.004.

Cohen, S.I.A., Linse, S., Luheshi, L.M., Hellstrand, E., White, D.A., *et al.* (2013) 'Proliferation of amyloid-β42 aggregates occurs through a secondary nucleation mechanism', *Proc. Natl. Acad. Sci. U. S. A.*, 110(24), p. 9758. doi:10.1073/PNAS.1218402110.

Collaborators GBD 2019 Dementia Forecasting (2022) 'Estimation of the global prevalence of dementia in 2019 and forecasted prevalence in 2050: an analysis for the Global Burden of Disease Study 2019', *Lancet Public Heal.* [Preprint]. doi:10.1016/S2468-2667(21)00249-8.

Collinge, J., Whitfield, J., McKintosh, E., Beck, J., Mead, S., *et al.* (2006) 'Kuru in the 21st century--an acquired human prion disease with very long incubation periods', *Lancet (London, England)*, 367(9528), pp. 2068–2074. doi:10.1016/S0140-6736(06)68930-7.

Collinge, J. and Clarke, A.R. (2007) 'A general model of prion strains and their pathogenicity', *Science (80-.).*, 318(5852), pp. 930–936. doi:10.1126/SCIENCE.1138718/SUPPL_FILE/COLLINGE.SOM.PDF.

Condello, C., Yuan, P., Schain, A. and Grutzendler, J. (2015) 'Microglia constitute a barrier that prevents neurotoxic protofibrillar Aβ42 hotspots around plaques', *Nat. Commun. 2015 61*, 6(1), pp. 1–14. doi:10.1038/ncomms7176.

Coppé, J.P., Patil, C.K., Rodier, F., Sun, Y., Muñoz, D.P., *et al.* (2008) 'Senescence-associated secretory phenotypes reveal cell-nonautonomous functions of oncogenic RAS and the p53 tumor suppressor', *PLoS Biol.*, 6(12). doi:10.1371/JOURNAL.PBIO.0060301.

Crespi, G.A.N., Hermans, S.J., Parker, M.W. and Miles, L.A. (2015) 'Molecular basis for mid-region amyloid-β capture by leading Alzheimer's disease immunotherapies', *Sci. Rep.*, 5.

doi:10.1038/SREP09649.

Cullen, N.C., Leuzy, A., Janelidze, S., Palmqvist, S., Svenningsson, A.L., *et al.* (2021) 'Plasma biomarkers of Alzheimer's disease improve prediction of cognitive decline in cognitively unimpaired elderly populations', *Nat. Commun. 2021 121*, 12(1), pp. 1–9. doi:10.1038/s41467-021-23746-0.

Dani, M., Wood, M., Mizoguchi, R., Fan, Z., Walker, Z., *et al.* (2018) 'Microglial activation correlates in vivo with both tau and amyloid in Alzheimer's disease', *Brain*, 141(9), pp. 2740–2754. doi:10.1093/BRAIN/AWY188.

Darling, A.L. and Shorter, J. (2020) 'Atomic Structures of Amyloid-β Oligomers Illuminate a Neurotoxic Mechanism', *Trends Neurosci.*, 43(10), p. 740. doi:10.1016/J.TINS.2020.07.006.

Das, A., Kim, S.H., Arifuzzaman, S., Yoon, T., Chai, J.C., *et al.* (2016) 'Transcriptome sequencing reveals that LPS-triggered transcriptional responses in established microglia BV2 cell lines are poorly representative of primary microglia', *J. Neuroinflammation 2016 131*, 13(1), pp. 1–18. doi:10.1186/S12974-016-0644-1.

Dear, A., Michaels, T., Meisl, G., Klenerman, D., Wu, S., *et al.* (2020) 'Kinetic diversity of amyloid oligomers', *Proc. Natl. Acad. Sci. U. S. A.*, 117(22). doi:10.1073/PNAS.1922267117.

Deckers, K., Barbera, M., Köhler, S., Ngandu, T., van Boxtel, M., *et al.* (2020) 'Long-term dementia risk prediction by the LIBRA score: A 30-year follow-up of the CAIDE study', *Int. J. Geriatr. Psychiatry*, 35(2), pp. 195–203. doi:10.1002/GPS.5235.

Delmotte, K., Schaeverbeke, J., Poesen, K. and Vandenberghe, R. (2021) 'Prognostic value of amyloid/tau/neurodegeneration (ATN) classification based on diagnostic cerebrospinal fluid samples for Alzheimer's disease', *Alzheimer's Res. Ther.*, 13(1), pp. 1–13. doi:10.1186/S13195-021-00817-4/TABLES/3.

Deltombe, M., Fillee, C., Vincent Van Pesch, ·, Van Pesch, V. and Be, V.V. (2022) 'Clinical usefulness of the CSF β-amyloid Aβ1-42/Aβ1-40 ratio for Alzheimer's disease diagnosis: a retrospective study in a Belgian academic hospital', *Acta Neurol. Belgica 2021*, 1, pp. 1–3. doi:10.1007/S13760-021-01846-4.

DeMattos, R.B., Bales, K.R., Cummins, D.J., Dodart, J.C., Paul, S.M., *et al.* (2001) 'Peripheral anti-Aβ antibody alters CNS and plasma Aβ clearance and decreases brain Aβ burden in a mouse model of Alzheimer's disease', *Proc. Natl. Acad. Sci. U. S. A.*, 98(15), pp. 8850–8855. doi:10.1073/pnas.151261398.

DeMattos, R.B., Lu, J., Tang, Y., Racke, M.M., DeLong, C.A., *et al.* (2012) 'A plaque-specific antibody clears existing β-amyloid plaques in Alzheimer's disease mice', *Neuron*, 76(5), pp. 908–920. doi:10.1016/j.neuron.2012.10.029.

'Dementia in Europe Yearbook 2019 - Estimating the prevalence of dementia in Europe' (2019) *accessed 27 April 2022, www.alzheimer-europe.org/reports-publication/dementia-europe-yearbook-2019-estimating-prevalence-dementia-europe*.

Deng, Y., Wang, Z., Wang, R., Zhang, X., Zhang, S., *et al.* (2013) 'Amyloid-β protein (Aβ) Glu11 is the major β-secretase site of β-site amyloid-β precursor protein-cleaving enzyme 1(BACE1), and shifting the cleavage site to Aβ Asp1 contributes to Alzheimer pathogenesis', *Eur. J. Neurosci.*, 37(12), pp. 1962–1969. doi:10.1111/EJN.12235.

Despres, C., Byrne, C., Qi, H., Cantrelle, F.-X., Huvent, I., *et al.* (2017) 'Identification of the Tau phosphorylation pattern that drives its aggregation', *Proc. Natl. Acad. Sci.*, 114(34), pp. 9080–9085. doi:10.1073/PNAS.1708448114.

Van Deursen, J.M. (2014) 'The role of senescent cells in ageing', *Nature*, 509(7501), pp. 439–446. doi:10.1038/nature13193.

Dhiman, K., Gupta, V.B., Villemagne, V.L., Eratne, D., Graham, P.L., *et al.* (2020) 'Cerebrospinal fluid neurofilament light concentration predicts brain atrophy and cognition in Alzheimer's disease', *Alzheimer's Dement. Diagnosis, Assess. Dis. Monit.*, 12(1), p. e12005. doi:10.1002/DAD2.12005.

Dickson, D.W. (1997) 'The Pathogenesis of Senile Plaques', *J. Neuropathol. Exp. Neurol.*, 56(4), pp. 321–339. doi:10.1097/00005072-199704000-00001.

Dickson, T.C. and Vickers, J.C. (2001) 'The morphological phenotype of β-amyloid plaques and associated neuritic changes in Alzheimer's disease', *Neuroscience*, 105(1), pp. 99–107. doi:10.1016/S0306-4522(01)00169-5.

Dodart, J.C., Bales, K.R., Gannon, K.S., Greene, S.J., DeMattos, R.B., *et al.* (2002) 'Immunization reverses memory deficits without reducing brain Aβ burden in Alzheimer's disease model', *Nat. Neurosci.*, 5(5), pp. 452–457. doi:10.1038/nn842.

Domingo, G., Benussi, L., Saraceno, C., Bertuzzi, M., Nicsanu, R., *et al.* (2021) 'N-Terminally Truncated and Pyroglutamate-Modified Aβ Forms Are Measurable in Human Cerebrospinal Fluid and Are Potential Markers of Disease Progression in Alzheimer's Disease', *Front. Neurosci.*, 15. doi:10.3389/FNINS.2021.708119.

Drummond, E. and Wisniewski, T. (2017) 'Alzheimer's disease: experimental models and reality', *Acta Neuropathol.*, 133(2), pp. 155–175. doi:10.1007/S00401-016-1662-X.

Duff, K., Eckman, C., Zehr, C., Yu, X., Prada, C.-M., *et al.* (1996) 'Increased amyloid-β42(43) in brains of mice expressing mutant presenilin 1', *Nature*, 383(6602), pp. 710–713. doi:10.1038/383710a0.

Ebenau, J.L., Timmers, T., Wesselman, L.M.P., Verberk, I.M.W., Verfaillie, S.C.J., *et al.* (2020) 'ATN classification and clinical progression in subjective cognitive decline', *Neurology*, 95(1), pp. e46–e58. doi:10.1212/WNL.0000000000009724.

Edgren, G., Hjalgrim, H., Rostgaard, K., Lambert, P., Wikman, A., *et al.* (2016) 'Transmission of Neurodegenerative Disorders Through Blood Transfusion: A Cohort Study', *Ann. Intern. Med.*, 165(5), pp. 316–324. doi:10.7326/M15-2421.

Eisele, Y.S., Obermüller, U., Heilbronner, G., Baumann, F., Kaeser, S.A., *et al.* (2010) 'Peripherally applied Abeta-containing inoculates induce cerebral beta-amyloidosis.', *Science (80-.).*, 330(6006), pp. 980–2. doi:10.1126/science.1194516.

Eisenberg, D. and Jucker, M. (2012) 'The amyloid state of proteins in human diseases.', *Cell*, 148(6), pp. 1188–203. doi:10.1016/j.cell.2012.02.022.

Eninger, T., Müller, S.A., Bacioglu, M., Schweighauser, M., Lambert, M., *et al.* (2022) 'Signatures of glial activity can be detected in the CSF proteome', *Proc. Natl. Acad. Sci.*, 119(24). doi:10.1073/PNAS.2119804119.

Fan, Z., Okello, A., Brooks, D. and Edison, P. (2015) 'Longitudinal influence of microglial activation and amyloid on neuronal function in Alzheimer's disease', *Brain*, 138(Pt 12), pp. 3685–3698. doi:10.1093/BRAIN/AWV288.

Fan, Z., Brooks, D.J., Okello, A. and Edison, P. (2017) 'An early and late peak in microglial activation in Alzheimer's disease trajectory', *Brain*, 140(3), p. 792. doi:10.1093/BRAIN/AWW349.

Di Fede, G., Catania, M., Morbin, M., Rossi, G., Suardi, S., *et al.* (2009) 'A Recessive Mutation in the APP Gene with Dominant-Negative Effect on Amyloidogenesis', *Science*, 323(5920), p. 1473. doi:10.1126/SCIENCE.1168979.

Fein, J.A., Sokolow, S., Miller, C.A., Vinters, H. V., Yang, F., *et al.* (2008) 'Co-Localization of Amyloid Beta and Tau Pathology in Alzheimer's Disease Synaptosomes', *Am. J. Pathol.*, 172(6), pp. 1683–1692. doi:10.2353/AJPATH.2008.070829.

Fillit, H., Ding, W., Buee, L., Kalman, J., Altstiel, L., *et al.* (1991) 'Elevated circulating tumor necrosis factor levels in Alzheimer's disease', *Neurosci. Lett.*, 129(2), pp. 318–320. doi:10.1016/0304-3940(91)90490-K.

Fleisher, A.S., Chen, K., Liu, X., Roontiva, A., Thiyyagura, P., *et al.* (2011) 'Using Positron Emission Tomography and Florbetapir F 18 to Image Cortical Amyloid in Patients With Mild Cognitive Impairment or Dementia Due to Alzheimer Disease', *Arch. Neurol.*, 68(11), pp. 1404–1411. doi:10.1001/ARCHNEUROL.2011.150.

Franceschi, C., Bonafè, M., Valensin, S., Olivieri, F., De Luca, M., *et al.* (2000) 'Inflamm-aging: An Evolutionary Perspective on Immunosenescence', *Ann. N. Y. Acad. Sci.*, 908(1), pp. 244–254. doi:10.1111/J.1749-6632.2000.TB06651.X.

Franceschi, C., Garagnani, P., Parini, P., Giuliani, C. and Santoro, A. (2018) 'Inflammaging: a new immune–metabolic viewpoint for age-related diseases', *Nat. Rev. Endocrinol. 2018 1410*, 14(10), pp. 576–590. doi:10.1038/s41574-018-0059-4.

Fritschi, S., Langer, F., Kaeser, S., Maia, L., Portelius, E., *et al.* (2014) 'Highly potent soluble amyloid-β seeds in human Alzheimer brain but not cerebrospinal fluid', *Brain*, 137(Pt 11), pp. 2909–2915. doi:10.1093/BRAIN/AWU255.

Frost, J.L., Le, K.X., Cynis, H., Ekpo, E., Kleinschmidt, M., *et al.* (2013) 'Pyroglutamate-3 Amyloid-β Deposition in the Brains of Humans, Non-Human Primates, Canines, and Alzheimer Disease–Like Transgenic Mouse Models', *Am. J. Pathol.*, 183(2), pp. 369–381. doi:10.1016/J.AJPATH.2013.05.005.

Fuller, J.P., Stavenhagen, J.B., Christensen, S., Kartberg, F., Glennie, M.J., *et al.* (2015) 'Comparing the efficacy and neuroinflammatory potential of three anti-Abeta antibodies', *Acta Neuropathol.*, 130(5), pp. 699–711. doi:10.1007/s00401-015-1484-2.

Funato, H., Yoshimura, M., Kusui, K., Tamaoka, A., Ishikawa, K., *et al.* (1998) 'Quantitation of amyloid beta-protein (A beta) in the cortex during aging and in Alzheimer's disease.', *Am. J. Pathol.*, 152(6), p. 1633.

Gan, L., Cookson, M.R., Petrucelli, L. and La Spada, A.R. (2018) 'Converging pathways in neurodegeneration, from genetics to mechanisms', *Nat. Neurosci.*, 21(10), pp. 1300–1309. doi:10.1038/s41593-018-0237-7.

Garcia-Osta, A. and Alberini, C. (2009) 'Amyloid beta mediates memory formation', *Learn. Mem.*, 16(4), pp. 267–272. doi:10.1101/LM.1310209.

Garcia, G.A., Cohen, S.I.A., Dobson, C.M. and Knowles, T.P.J. (2014) 'Nucleation-conversion-polymerization reactions of biological macromolecules with prenucleation clusters', *Phys. Rev. E*, 89(3), p. 032712. doi:10.1103/PhysRevE.89.032712.

St. George-Hyslop, P.H., Tanzi, R.E., Polinsky, R.J., Haines, J.L., Nee, L., *et al.* (1987) 'The genetic defect causing familial Alzheimer's disease maps on chromosome 21', *Science (80-.).*, 235(4791), pp. 885–890. doi:10.1126/SCIENCE.2880399.

Gerrits, E., Brouwer, N., Kooistra, S.M., Woodbury, M.E., Vermeiren, Y., *et al.* (2021) 'Distinct amyloid-β and tau-associated microglia profiles in Alzheimer's disease', *Acta Neuropathol. 2021 1415*, 141(5), pp. 681–696. doi:10.1007/S00401-021-02263-W.

Ghosh, P., Vaidya, A., Kumar, A. and Rangachari, V. (2016) 'Determination of critical nucleation number for a single nucleation amyloid-β aggregation model', *Math. Biosci.*, 273, p. 70. doi:10.1016/J.MBS.2015.12.004.

Glabe, C.G. (2008) 'Structural Classification of Toxic Amyloid Oligomers *', *J. Biol. Chem.*, 283(44), pp. 29639–29643. doi:10.1074/JBC.R800016200.

Goate, A., Chartier-Harlin, M.C., Mullan, M., Brown, J., Crawford, F., *et al.* (1991) 'Segregation of a missense mutation in the amyloid precursor protein gene with familial Alzheimer's disease', *Nature*, 349(6311), pp. 704–706. doi:10.1038/349704A0.

Goedert, M., Wischik, C., Crowther, R., Walker, J. and Klug, A. (1988) 'Cloning and sequencing of the cDNA encoding a core protein of the paired helical filament of Alzheimer disease: identification as the microtubule-associated protein tau', *Proc. Natl. Acad. Sci. U. S. A.*, 85(11), pp. 4051–4055. doi:10.1073/PNAS.85.11.4051.

Goedert, M., Spillantini, M.G., Potier, M.C., Ulrich, J. and Crowther, R.A. (1989a) 'Cloning and sequencing of the cDNA encoding an isoform of microtubule-associated protein tau containing four tandem repeats: differential expression of tau protein mRNAs in human brain.', *EMBO J.*, 8(2), p. 393. doi:10.1002/J.1460-2075.1989.TB03390.X.

Goedert, M., Spillantini, M.G., Jakes, R., Rutherford, D. and Crowther, R.A. (1989b) 'Multiple isoforms of human microtubule-associated protein tau: sequences and localization in neurofibrillary tangles of Alzheimer's disease', *Neuron*, 3(4), pp. 519–526. doi:10.1016/0896-6273(89)90210-9.

Golde, T., DeKosky, S. and Galasko, D. (2018) 'Alzheimer's disease: The right drug, the right time', *Science*, 362(6420), pp. 1250–1251. doi:10.1126/SCIENCE.AAU0437.

Goldgaber, D., Lerman, M.I., McBride, O.W., Saffiotti, U. and Gajdusek, D.C. (1987) 'Characterization and Chromosomal Localization of a cDNA Encoding Brain Amyloid of Alzheimer's Disease', *Science (80-.).*, 235(4791), pp. 877–880. doi:10.1126/SCIENCE.3810169.

Gómez-Tortosa, E., Barquero, M.S., Barón, M., Sainz, M.J., Manzano, S., *et al.* (2007) 'Variability of Age at Onset in Siblings With Familial Alzheimer Disease', *Arch. Neurol.*, 64(12), pp. 1743–1748. doi:10.1001/ARCHNEUR.64.12.1743.

Gong, Y., Chang, L., Viola, K.L., Lacor, P.N., Lambert, M.P., *et al.* (2003) 'Alzheimer's disease-affected brain: Presence of oligomeric Aβ ligands (ADDLs) suggests a molecular basis for reversible memory loss', *Proc. Natl. Acad. Sci. U. S. A.*, 100(18), pp. 10417–10422. doi:10.1073/PNAS.1834302100.

Götz, A., Mylonas, N., Högel, P., Silber, M., Heinel, H., *et al.* (2019) 'Modulating Hinge Flexibility in the APP Transmembrane Domain Alters γ-Secretase Cleavage', *Biophys. J.*, 116(11), p. 2103. doi:10.1016/J.BPJ.2019.04.030.

Götz, J., Chen, F., Van Dorpe, J. and Nitsch, R.M. (2001) 'Formation of neurofibrillary tangles in P301L tau transgenic mice induced by Aβ42 fibrils', *Science (80-.).*, 293(5534), pp. 1491–1495. doi:10.1126/SCIENCE.1062097.

Graham, N.S.N., Zimmerman, K.A., Moro, F., Heslegrave, A., Maillard, S.A., *et al.* (2021) 'Axonal marker neurofilament light predicts long-term outcomes and progressive

neurodegeneration after traumatic brain injury', *Sci. Transl. Med.*, 13(613), p. 9922. doi:10.1126/SCITRANSLMED.ABG9922.

Grasso, G. and Danani, A. (2020) 'Molecular simulations of amyloid beta assemblies', *Adv. Phys.*, 5(1), p. 1770627. doi:10.1080/23746149.2020.1770627.

Greenberg, S.M., Bacskai, B.J., Hernandez-Guillamon, M., Pruzin, J., Sperling, R., *et al.* (2020) 'Cerebral amyloid angiopathy and Alzheimer disease — one peptide, two pathways', *Nat. Rev. Neurol.*, 16(1), p. 30. doi:10.1038/S41582-019-0281-2.

Griffith, J.S. (1967) 'Self-replication and scrapie', *Nature*, 215(5105), pp. 1043–1044. doi:10.1038/2151043A0.

Grigolato, F. and Arosio, P. (2021) 'The role of surfaces on amyloid formation', *Biophys. Chem.*, 270, p. 106533. doi:10.1016/J.BPC.2020.106533.

Grimm, M.O.W., Grimm, H.S., Pätzold, A.J., Zinser, E.G., Halonen, R., *et al.* (2005) 'Regulation of cholesterol and sphingomyelin metabolism by amyloid-β and presenilin', *Nat. Cell Biol. 2005 711*, 7(11), pp. 1118–1123. doi:10.1038/ncb1313.

Grober, E., Hall, C.B., Lipton, R.B., Zonderman, A.B., Resnick, S.M., *et al.* (2008) 'Memory impairment, executive dysfunction, and intellectual decline in preclinical Alzheimer's disease', *J. Int. Neuropsychol. Soc.*, 14(2), pp. 266–278. doi:10.1017/S1355617708080302.

Groh, N., Bühler, A., Huang, C., Li, K.W., van Nierop, P., *et al.* (2017) 'Age-dependent protein aggregation initiates amyloid-β aggregation', *Front. Aging Neurosci.*, 9(MAY). doi:10.3389/fnagi.2017.00138.

Grundke-Iqbal, I., Iqbal, K., Quinlan, M., Tung, Y.-C., Zaidi, M.S., *et al.* (1986) 'Microtubule-associated protein tau. A component of Alzheimer paired helical filaments.', *J. Biol. Chem.*, 261(13), pp. 6084–6089. doi:10.1016/S0021-9258(17)38495-8.

Guerreiro, R., Wojtas, A., Bras, J., Carrasquillo, M., Rogaeva, E., *et al.* (2013) 'TREM2 Variants in Alzheimer's Disease', *N. Engl. J. Med.*, 368(2), p. 117. doi:10.1056/NEJMOA1211851.

Haass, C. and Selkoe, D.J. (1993) 'Cellular processing of β-amyloid precursor protein and the genesis of amyloid β-peptide', *Cell*, 75(6), pp. 1039–1042. doi:10.1016/0092-8674(93)90312-E.

Habchi, J., Chia, S., Galvagnion, C., Michaels, T.C.T., Bellaiche, M.M.J., *et al.* (2018) 'Cholesterol catalyses Aβ42 aggregation through a heterogeneous nucleation pathway in the presence of lipid membranes', *Nat. Chem. 2018 106*, 10(6), pp. 673–683. doi:10.1038/s41557-018-0031-x.

Hampel, H., Hardy, J., Blennow, K., Chen, C., Perry, G., *et al.* (2021) 'The Amyloid-β Pathway in Alzheimer's Disease', *Mol. Psychiatry 2021*, pp. 1–23. doi:10.1038/s41380-021-01249-0.

Hanseeuw, B.J., Betensky, R.A., Jacobs, H.I.L., Schultz, A.P., Sepulcre, J., *et al.* (2019) 'Association of Amyloid and Tau With Cognition in Preclinical Alzheimer Disease: A Longitudinal Study', *JAMA Neurol.*, 76(8), pp. 915–924. doi:10.1001/JAMANEUROL.2019.1424.

Hansson, O. (2021) 'Biomarkers for neurodegenerative diseases', *Nat. Med.*, 27(6), pp. 954–963. doi:10.1038/s41591-021-01382-x.

Haraguchi, T., Fisher, S., Olofsson, S., Endo, T., Groth, D., *et al.* (1989) 'Asparagine-linked glycosylation of the scrapie and cellular prion proteins', *Arch. Biochem. Biophys.*, 274(1), pp. 1–13. doi:10.1016/0003-9861(89)90409-8.

Hardy, J. and Allsop, D. (1991) 'Amyloid deposition as the central event in the aetiology of Alzheimer's disease', *Trends Pharmacol. Sci.* Elsevier Current Trends, pp. 383–388. doi:10.1016/0165-6147(91)90609-V.

Harper, J.D. and Lansbury, P.T. (1997) 'MODELS OF AMYLOID SEEDING IN ALZHEIMER'S DISEASE AND SCRAPIE:Mechanistic Truths and Physiological Consequences of the Time-Dependent Solubility of Amyloid Proteins', *Annu. Rev. Biochem.*, 66(1), pp. 385–407. doi:10.1146/annurev.biochem.66.1.385.

Hashimoto, T., Fujii, D., Naka, Y., Kashiwagi-Hakozaki, M., Matsuo, Y., *et al.* (2020) 'Collagenous Alzheimer amyloid plaque component impacts on the compaction of amyloid-β plaques', *Acta Neuropathol. Commun. 2020 81*, 8(1), pp. 1–18. doi:10.1186/S40478-020-01075-5.

Hayflick, L. (1965) 'The limited in vitro lifetime of human diploid cell strains', *Exp. Cell Res.*, 37(3), pp. 614–636. doi:10.1016/0014-4827(65)90211-9.

He, L., Morley, J.E., Aggarwal, G., Nguyen, A.D., Vellas, B., *et al.* (2021) 'Plasma neurofilament light chain is associated with cognitive decline in non-dementia older adults', *Sci. Reports 2021 111*, 11(1), pp. 1–9. doi:10.1038/s41598-021-91038-0.

He, W. and Barrow, C.J. (1999) 'The Aβ 3-Pyroglutamyl and 11-Pyroglutamyl Peptides Found in Senile Plaque Have Greater β-Sheet Forming and Aggregation Propensities in Vitro than Full-Length Aβ', *Biochemistry*, 38(33), pp. 10871–10877. doi:10.1021/BI990563R.

He, Z., Guo, J.L., McBride, J.D., Narasimhan, S., Kim, H., *et al.* (2017) 'Amyloid-β plaques enhance Alzheimer's brain tau-seeded pathologies by facilitating neuritic plaque tau aggregation', *Nat. Med.* [Preprint]. doi:10.1038/nm.4443.

Heneka, M.T., Kummer, M.P., Stutz, A., Delekate, A., Schwartz, S., *et al.* (2012) 'NLRP3 is activated in Alzheimer's disease and contributes to pathology in APP/PS1 mice', *Nature*, 493(7434), pp. 674–678. doi:10.1038/nature11729.

Hernandez-Segura, A., de Jong, T. V., Melov, S., Guryev, V., Campisi, J., *et al.* (2017) 'Unmasking Transcriptional Heterogeneity in Senescent Cells', *Curr. Biol.*, 27(17), pp. 2652-2660.e4. doi:10.1016/J.CUB.2017.07.033.

Hickman, D.L., Johnson, J., Vemulapalli, T.H., Crisler, J.R. and Shepherd, R. (2017) 'Commonly Used Animal Models', *Princ. Anim. Res. Grad. Undergrad. Students*, p. 117. doi:10.1016/B978-0-12-802151-4.00007-4.

Hickman, S.E. and Khoury, J. El (2014) 'TREM2 and the neuroimmunology of Alzheimer's disease', *Biochem. Pharmacol.*, 88(4), p. 495. doi:10.1016/J.BCP.2013.11.021.

Hippius, H. and Neundörfer, G. (2003) 'The discovery of Alzheimer's disease', *Dialogues Clin. Neurosci.*, 5(1), pp. 101–108. doi:10.31887/dcns.2003.5.1/hhippius.

Hong, W., Wang, Z., Liu, W., O'Malley, T.T., Jin, M., *et al.* (2018) 'Diffusible, highly bioactive oligomers represent a critical minority of soluble Aβ in Alzheimer's disease braain', *Acta Neuropathol.*, pp. 1–22. doi:10.1007/s00401-018-1846-7.

Hope, J., Reekie, L.J.D., Hunter, N., Multhaup, G., Beyreuther, K., *et al.* (1988) 'Fibrils from brains of cows with new cattle disease contain scrapie-associated protein', *Nature*,

336(6197), pp. 390–392. doi:10.1038/336390a0.

Hu, X., Crick, S.L., Bu, G., Frieden, C., Pappu, R. V., *et al.* (2009) 'Amyloid seeds formed by cellular uptake, concentration, and aggregation of the amyloid-beta peptide', *Proc. Natl. Acad. Sci.*, 106(48), pp. 20324–20329. doi:10.1073/PNAS.0911281106.

Huang, Y., Happonen, K.E., Burrola, P.G., O'Connor, C., Hah, N., *et al.* (2021) 'Microglia use TAM receptors to detect and engulf amyloid β plaques', *Nat. Immunol. 2021 225*, 22(5), pp. 586–594. doi:10.1038/s41590-021-00913-5.

Hutton, M., Lendon, C.L., Rizzu, P., Baker, M., Froelich, S., *et al.* (1998) 'Association of missense and 5′-splice-site mutations in tau with the inherited dementia FTDP-17', *Nature*, 393(6686), pp. 702–705. doi:10.1038/31508.

Idland, A.V., Sala-Llonch, R., Borza, T., Watne, L.O., Wyller, T.B., *et al.* (2017) 'CSF neurofilament light levels predict hippocampal atrophy in cognitively healthy older adults', *Neurobiol. Aging*, 49, pp. 138–144. doi:10.1016/J.NEUROBIOLAGING.2016.09.012.

Ikeda, S., Allsop, D. and Glenner, G. (1989) 'Morphology and distribution of plaque and related deposits in the brains of Alzheimer's disease and control cases. An immunohistochemical study using amyloid beta-protein antibody.', *Lab. Invest.*, 60(1), pp. 113–122.

Ingelsson, M., Fukumoto, H., Newell, K.L., Growdon, J.H., Hedley–Whyte, E.T., *et al.* (2004) 'Early Aβ accumulation and progressive synaptic loss, gliosis, and tangle formation in AD brain', *Neurology*, 62(6), pp. 925–931. doi:10.1212/01.WNL.0000115115.98960.37.

Ishiguro, K., Ohno, H., Arai, H., Yamaguchi, H., Urakami, K., *et al.* (1999) 'Phosphorylated tau in human cerebrospinal fluid is a diagnostic marker for Alzheimer's disease', *Neurosci. Lett.*, 270(2), pp. 91–94. doi:10.1016/S0304-3940(99)00476-0.

Ising, C., Venegas, C., Zhang, S., Scheiblich, H., Schmidt, S. V., *et al.* (2019) 'NLRP3 inflammasome activation drives tau pathology', *Nature*, 575(7784), pp. 669–673. doi:10.1038/s41586-019-1769-z.

Jack, C.R., Knopman, D.S., Jagust, W.J., Petersen, R.C., Weiner, M.W., *et al.* (2013) 'Tracking pathophysiological processes in Alzheimer's disease: an updated hypothetical model of dynamic biomarkers', *Lancet Neurol.*, 12(2), pp. 207–216. doi:10.1016/S1474-4422(12)70291-0.

Jack, C.R., Bennett, D.A., Blennow, K., Carrillo, M.C., Feldman, H.H., *et al.* (2016) 'A/T/N: An unbiased descriptive classification scheme for Alzheimer disease biomarkers', *Neurology*. Lippincott Williams and Wilkins, pp. 539–547. doi:10.1212/WNL.0000000000002923.

Jack, C.R., Bennett, D.A., Blennow, K., Carrillo, M.C., Dunn, B., *et al.* (2018) 'NIA-AA Research Framework: Toward a biological definition of Alzheimer's disease', *Alzheimer's Dement.*, 14(4), pp. 535–562. doi:10.1016/j.jalz.2018.02.018.

Jackson, R.J., Rudinskiy, N., Herrmann, A.G., Croft, S., Kim, J.M., *et al.* (2016) 'Human tau increases amyloid β plaque size but not amyloid β-mediated synapse loss in a novel mouse model of Alzheimer's disease', *Eur. J. Neurosci.*, 44(12), pp. 3056–3066. doi:10.1111/EJN.13442.

Janelidze, S., Zetterberg, H., Mattsson, N., Palmqvist, S., Vanderstichele, H., *et al.* (2016) 'CSF Aβ42/Aβ40 and Aβ42/Aβ38 ratios: better diagnostic markers of Alzheimer disease', *Ann. Clin. Transl. Neurol.*, 3(3), pp. 154–165. doi:10.1002/ACN3.274.

Janelidze, S., Stomrud, E., Smith, R., Palmqvist, S., Mattsson, N., *et al.* (2020a) 'Cerebrospinal fluid p-tau217 performs better than p-tau181 as a biomarker of Alzheimer's disease', *Nat. Commun. 2020 111*, 11(1), pp. 1–12. doi:10.1038/s41467-020-15436-0.

Janelidze, S., Mattsson, N., Palmqvist, S., Smith, R., Beach, T.G., *et al.* (2020b) 'Plasma P-tau181 in Alzheimer's disease: relationship to other biomarkers, differential diagnosis, neuropathology and longitudinal progression to Alzheimer's dementia', *Nat. Med. 2020 263*, 26(3), pp. 379–386. doi:10.1038/s41591-020-0755-1.

Jansen, W.J., Ossenkoppele, R., Knol, D.L., Tijms, B.M., Scheltens, P., *et al.* (2015) 'Prevalence of Cerebral Amyloid Pathology in Persons Without Dementia: A Meta-analysis', *JAMA*, 313(19), p. 1924. doi:10.1001/JAMA.2015.4668.

Jarrett, J.T. and Lansbury, P.T. (1993) 'Seeding "one-dimensional crystallization" of amyloid: A pathogenic mechanism in Alzheimer's disease and scrapie?', *Cell*, pp. 1055–1058. doi:10.1016/0092-8674(93)90635-4.

Jin, M., Cao, L. and Dai, Y. (2019) 'Role of Neurofilament Light Chain as a Potential Biomarker for Alzheimer's Disease: A Correlative Meta-Analysis', *Front. Aging Neurosci.*, 0, p. 254. doi:10.3389/FNAGI.2019.00254.

De Jonghe, C., Esselens, C., Kumar-Singh, S., Craessaerts, K., Serneels, S., *et al.* (2001) 'Pathogenic APP mutations near the gamma-secretase cleavage site differentially affect Abeta secretion and APP C-terminal fragment stability', *Hum. Mol. Genet.*, 10(16), pp. 1665–1671. doi:10.1093/HMG/10.16.1665.

Jonsson, T., Atwal, J.K., Steinberg, S., Snaedal, J., Jonsson, P. V., *et al.* (2012) 'A mutation in APP protects against Alzheimer's disease and age-related cognitive decline', *Nature*, 488(7409), pp. 96–99. doi:10.1038/nature11283.

Jonsson, T., Stefansson, H., Steinberg, S., Jonsdottir, I., Jonsson, P. V., *et al.* (2013) 'Variant of TREM2 Associated with the Risk of Alzheimer's Disease', *N. Engl. J. Med.*, 368(2), p. 107. doi:10.1056/NEJMOA1211103.

Joshi, P., Turola, E., Ruiz, A., Bergami, A., Libera, D.D., *et al.* (2013) 'Microglia convert aggregated amyloid-β into neurotoxic forms through the shedding of microvesicles', *Cell Death Differ. 2014 214*, 21(4), pp. 582–593. doi:10.1038/cdd.2013.180.

Kaeser, S.A., Lehallier, B., Thinggaard, M., Häsler, L.M., Apel, A., *et al.* (2021) 'A neuronal blood marker is associated with mortality in old age', *Nat. Aging*, 1(2), pp. 218–225. doi:10.1038/s43587-021-00028-4.

Kaeser, S.A., Häsler, L.M., Lambert, M., Bergmann, C., Bottelbergs, A., *et al.* (2022) 'CSF p-tau increase in response to Aβ-type and Danish-type cerebral amyloidosis and in the absence of neurofibrillary tangles', *Acta Neuropathol.*, 143(2), pp. 287–290. doi:10.1007/S00401-021-02400-5.

Kanata, E., Golanska, E., Villar-Piqué, A., Karsanidou, A., Dafou, D., *et al.* (2019) 'Cerebrospinal fluid neurofilament light in suspected sporadic Creutzfeldt-Jakob disease', *J. Clin. Neurosci.*, 60, pp. 124–127. doi:10.1016/J.JOCN.2018.09.031.

Kane, M.D., Lipinski, W.J., Callahan, M.J., Bian, F., Durham, R.A., *et al.* (2000) 'Evidence for Seeding of Beta-Amyloid by Intracerebral Infusion of Alzheimer Brain Extracts in Beta-Amyloid Precursor Protein- Transgenic Mice'.

Kang, J., Lemaire, H.-G., Unterbeck, A., Salbaum, J.M., Masters, C.L., *et al.* (1987) 'The precursor of Alzheimer's disease amyloid A4 protein resembles a cell-surface receptor',

Nature, 325(6106), pp. 733–736. doi:10.1038/325733a0.

Katzmarski, N., Ziegler-Waldkirch, S., Scheffler, N., Witt, C., Abou-Ajram, C., *et al.* (2020) 'Aβ oligomers trigger and accelerate Aβ seeding', *Brain Pathol.*, 30(1), p. 36. doi:10.1111/BPA.12734.

Keren-Shaul, H., Spinrad, A., Weiner, A., Matcovitch-Natan, O., Dvir-Szternfeld, R., *et al.* (2017) 'A Unique Microglia Type Associated with Restricting Development of Alzheimer's Disease', *Cell*, 169(7), pp. 1276-1290.e17. doi:10.1016/J.CELL.2017.05.018.

Kimberly, W.T., LaVoie, M.J., Ostaszewski, B.L., Ye, W., Wolfe, M.S., *et al.* (2003) 'γ-Secretase is a membrane protein complex comprised of presenilin, nicastrin, aph-1, and pen-2', *Proc. Natl. Acad. Sci.*, 100(11), pp. 6382–6387. doi:10.1073/PNAS.1037392100.

Kinney, J.W., Bemiller, S.M., Murtishaw, A.S., Leisgang, A.M., Salazar, A.M., *et al.* (2018) 'Inflammation as a central mechanism in Alzheimer's disease', *Alzheimer's Dement. Transl. Res. Clin. Interv.*, 4, pp. 575–590. doi:10.1016/J.TRCI.2018.06.014.

Klesney-Tait, J., Turnbull, I.R. and Colonna, M. (2006) 'The TREM receptor family and signal integration', *Nat. Immunol. 2006 712*, 7(12), pp. 1266–1273. doi:10.1038/ni1411.

Klunk, W.E., Engler, H., Nordberg, A., Wang, Y., Blomqvist, G., *et al.* (2004) 'Imaging brain amyloid in Alzheimer's disease with Pittsburgh Compound-B', *Ann. Neurol.*, 55(3), pp. 306–319. doi:10.1002/ANA.20009.

Kuhn, P.-H., Wang, H., Dislich, B., Colombo, A., Zeitschel, U., *et al.* (2010) 'ADAM10 is the physiologically relevant, constitutive α-secretase of the amyloid precursor protein in primary neurons', *EMBO J.*, 29(17), pp. 3020–3032. doi:10.1038/EMBOJ.2010.167.

Kumar, S., Rezaei-Ghaleh, N., Terwel, D., Thal, D.R., Richard, M., *et al.* (2011) 'Extracellular phosphorylation of the amyloid β-peptide promotes formation of toxic aggregates during the pathogenesis of Alzheimer's disease', *EMBO J.*, 30(11), p. 2255. doi:10.1038/EMBOJ.2011.138.

Kumar, S., Wirths, O., Stüber, K., Wunderlich, P., Koch, P., *et al.* (2016) 'Phosphorylation of the amyloid β-peptide at Ser26 stabilizes oligomeric assembly and increases neurotoxicity', *Acta Neuropathol.*, 131(4), pp. 525–537. doi:10.1007/S00401-016-1546-0/FIGURES/4.

Kuragano, M., Yamashita, R., Chikai, Y., Kitamura, R. and Tokuraku, K. (2020) 'Three-dimensional real time imaging of amyloid β aggregation on living cells', *Sci. Reports 2020 101*, 10(1), pp. 1–12. doi:10.1038/s41598-020-66129-z.

Langer, F., Eisele, Y.S., Fritschi, S.K., Staufenbiel, M., Walker, L.C., *et al.* (2011) 'Soluble Aβ seeds are potent inducers of cerebral β-amyloid deposition.', *J. Neurosci.*, 31(41), pp. 14488–95. doi:10.1523/JNEUROSCI.3088-11.2011.

Laurent, S.A., Hoffmann, F.S., Kuhn, P.-H., Cheng, Q., Chu, Y., *et al.* (2015) 'γ-secretase directly sheds the survival receptor BCMA from plasma cells', *Nat. Commun.*, 6. doi:10.1038/NCOMMS8333.

Lee, J., Culyba, E.K., Powers, E.T. and Kelly, J.W. (2011) 'Amyloid-β forms fibrils by nucleated conformational conversion of oligomers', *Nat. Chem. Biol. 2011 79*, 7(9), pp. 602–609. doi:10.1038/nchembio.624.

Lee, J.H., Yu, W.H., Kumar, A., Lee, S., Mohan, P.S., *et al.* (2010) 'Lysosomal proteolysis and autophagy require presenilin 1 and are disrupted by Alzheimer-related PS1 mutations', *Cell*, 141(7), pp. 1146–1158. doi:10.1016/j.cell.2010.05.008.

Lee, S.H., Meilandt, W.J., Xie, L., Gandham, V.D., Ngu, H., *et al.* (2021) 'Trem2 restrains the enhancement of tau accumulation and neurodegeneration by β-amyloid pathology', *Neuron*, 109(8), pp. 1283-1301.e6. doi:10.1016/J.NEURON.2021.02.010.

Leng, F. and Edison, P. (2020) 'Neuroinflammation and microglial activation in Alzheimer disease: where do we go from here?', *Nat. Rev. Neurol. 2020 173*, 17(3), pp. 157–172. doi:10.1038/s41582-020-00435-y.

Lesné, S., Koh, M.T., Kotilinek, L., Kayed, R., Glabe, C.G., *et al.* (2006) 'A specific amyloid-β protein assembly in the brain impairs memory', *Nature*, 440(7082), pp. 352–357. doi:10.1038/nature04533.

Leuzy, A., Chiotis, K., Lemoine, L., Gillberg, P.G., Almkvist, O., *et al.* (2019) 'Tau PET imaging in neurodegenerative tauopathies—still a challenge', *Mol. Psychiatry 2019 248*, 24(8), pp. 1112–1134. doi:10.1038/s41380-018-0342-8.

LeVine, H. (1993) 'Thioflavine T interaction with synthetic Alzheimer's disease beta-amyloid peptides: detection of amyloid aggregation in solution.', *Protein Sci.*, 2(3), p. 404. doi:10.1002/PRO.5560020312.

Lian, H., Litvinchuk, A., Chiang, A.C.A., Aithmitti, N., Jankowsky, J.L., *et al.* (2016) 'Astrocyte-Microglia Cross Talk through Complement Activation Modulates Amyloid Pathology in Mouse Models of Alzheimer's Disease', *J. Neurosci.*, 36(2), pp. 577–589. doi:10.1523/JNEUROSCI.2117-15.2016.

Liddelow, S.A., Guttenplan, K.A., Clarke, L.E., Bennett, F.C., Bohlen, C.J., *et al.* (2017) 'Neurotoxic reactive astrocytes are induced by activated microglia', *Nature*, 541(7638), pp. 481–487. doi:10.1038/nature21029.

Liebsch, F., Kulic, L., Teunissen, C., Shobo, A., Ulku, I., *et al.* (2019) 'Aβ34 is a BACE1-derived degradation intermediate associated with amyloid clearance and Alzheimer's disease progression', *Nat. Commun.*, 10(1), pp. 1–15. doi:10.1038/s41467-019-10152-w.

Linse, S., Scheidt, T., Bernfur, K., Vendruscolo, M., Dobson, C.M., *et al.* (2020) 'Kinetic fingerprints differentiate the mechanisms of action of anti-Aβ antibodies', *Nat. Struct. Mol. Biol. 2020 2712*, 27(12), pp. 1125–1133. doi:10.1038/s41594-020-0505-6.

Litvinchuk, A., Wan, Y.W., Swartzlander, D.B., Chen, F., Cole, A., *et al.* (2018) 'Complement C3aR Inactivation Attenuates Tau Pathology and Reverses an Immune Network Deregulated in Tauopathy Models and Alzheimer's Disease', *Neuron*, 100(6), pp. 1337-1353.e5. doi:10.1016/J.NEURON.2018.10.031.

Liu, H., Kim, C., Haldiman, T., Sigurdson, C.J., Nyström, S., *et al.* (2021) 'Distinct conformers of amyloid beta accumulate in the neocortex of patients with rapidly progressive Alzheimer's disease', *J. Biol. Chem.*, p. 101267. doi:10.1016/J.JBC.2021.101267.

Liu, L., Ding, L., Rovere, M., Wolfe, M.S. and Selkoe, D.J. (2019) 'A cellular complex of BACE1 and γ-secretase sequentially generates Aβ from its full-length precursor', *J Cell Biol*, 218(2), pp. 644–663. doi:10.1083/JCB.201806205.

Liu, Z., Condello, C., Schain, A., Harb, R. and Grutzendler, J. (2010) 'CX3CR1 in Microglia Regulates Brain Amyloid Deposition through Selective Protofibrillar Amyloid-β Phagocytosis', *J. Neurosci.*, 30(50), pp. 17091–17101. doi:10.1523/JNEUROSCI.4403-10.2010.

Long, J.M. and Holtzman, D.M. (2019) 'Alzheimer Disease: An Update on Pathobiology and Treatment Strategies', *Cell.* Cell Press, pp. 312–339. doi:10.1016/j.cell.2019.09.001.

López-Otín, C., Blasco, M.A., Partridge, L., Serrano, M. and Kroemer, G. (2013) 'The Hallmarks of Aging', *Cell*, 153(6), pp. 1194–1217. doi:10.1016/J.CELL.2013.05.039.

Lowe, S., Duggan Evans, C., Shcherbinin, S., Cheng, Y., Willis, B., *et al.* (2021) 'Donanemab (LY3002813) Phase 1b Study in Alzheimer's Disease: Rapid and Sustained Reduction of Brain Amyloid Measured by Florbetapir F18 Imaging', *J. Prev. Alzheimer's Dis.*, 8(4), pp. 414–424. doi:10.14283/JPAD.2021.56.

Lu, P., Bai, X., Ma, D., Xie, T., Yan, C., *et al.* (2014) 'Three-dimensional structure of human γ-secretase', *Nature*, 512(7513), pp. 166–170. doi:10.1038/nature13567.

Mably, A.J., Liu, W., Donald, J.M.M., Dodart, J.-C., Bard, F., *et al.* (2015) 'Anti-Aβ antibodies incapable of reducing cerebral Aβ oligomers fail to attenuate spatial reference memory deficits in J20 mice', *Neurobiol. Dis.*, 82, p. 372. doi:10.1016/J.NBD.2015.07.008.

Maesako, M., Uemura, K., Kuzuya, A., Sasaki, K., Asada, M., *et al.* (2011) 'Presenilin Regulates Insulin Signaling via a γ-Secretase-independent Mechanism *', *J. Biol. Chem.*, 286(28), pp. 25309–25316. doi:10.1074/JBC.M111.248922.

Maia, L.F., Kaeser, S.A., Reichwald, J., Hruscha, M., Martus, P., *et al.* (2013) 'Changes in Amyloid- and Tau in the Cerebrospinal Fluid of Transgenic Mice Overexpressing Amyloid Precursor Protein', *Sci. Transl. Med.*, 5(194), p. 194re2. doi:10.1126/scitranslmed.3006446.

Maia, L.F., Kaeser, S.A., Reichwald, J., Lambert, M., Obermüller, U., *et al.* (2015) 'Increased CSF Aβ during the very early phase of cerebral Aβ deposition in mouse models', *EMBO Mol. Med.*, 7(7), pp. 895–903. doi:10.15252/emmm.201505026.

Manning, G., Whyte, D.B., Martinez, R., Hunter, T. and Sudarsanam, S. (2002) 'The protein kinase complement of the human genome', *Science (80-.).*, 298(5600), pp. 1912–1934. doi:10.1126/SCIENCE.1075762/SUPPL_FILE/MANNINGSOM.PDF.

Marcatti, M., Fracassi, A., Montalbano, M., Natarajan, · Chandramouli, Krishnan, B., *et al.* (2022) 'Aβ/tau oligomer interplay at human synapses supports shifting therapeutic targets for Alzheimer's disease', *Cell. Mol. Life Sci. 2022 794*, 79(4), pp. 1–16. doi:10.1007/S00018-022-04255-9.

Marrero-Winkens, C., Sankaran, C. and Schätzl, H.M. (2020) 'From Seeds to Fibrils and Back: Fragmentation as an Overlooked Step in the Propagation of Prions and Prion-Like Proteins', *Biomolecules*, 10(9), pp. 1–20. doi:10.3390/BIOM10091305.

Maruyama, M., Shimada, H., Suhara, T., Shinotoh, H., Ji, B., *et al.* (2013) 'Imaging of tau pathology in a tauopathy mouse model and in Alzheimer patients compared to normal controls', *Neuron*, 79(6), pp. 1094–1108. doi:10.1016/J.NEURON.2013.07.037.

Masters, C.L., Simms, G., Weinman, N.A., Multhaup, G., McDonald, B.L., *et al.* (1985) 'Amyloid plaque core protein in Alzheimer disease and Down syndrome.', *Proc. Natl. Acad. Sci. U. S. A.*, 82(12), p. 4245. doi:10.1073/PNAS.82.12.4245.

Mattsson, N., Insel, P.S., Palmqvist, S., Portelius, E., Zetterberg, H., *et al.* (2016) 'Cerebrospinal fluid tau, neurogranin, and neurofilament light in Alzheimer's disease', *EMBO Mol. Med.*, 8(10), pp. 1184–1196. doi:10.15252/EMMM.201606540.

McDade, E. and Bateman, R.J. (2017) 'Stop Alzheimer's before it starts', *Nature*, 547(7662), pp. 153–155. doi:10.1038/547153a.

Meier, S.R., Sehlin, D., Roshanbin, S., Falk, V.L., Saito, T., *et al.* (2021) '11C-PIB and 124I-antibody PET provide differing estimates of brain amyloid-beta after therapeutic intervention',

J. Nucl. Med., p. jnumed.121.262083. doi:10.2967/JNUMED.121.262083.

Meilandt, W.J., Ngu, H., Gogineni, A., Lalehzadeh, G., Lee, S.-H., *et al.* (2020) 'Trem2 Deletion Reduces Late-Stage Amyloid Plaque Accumulation, Elevates the Aβ42:Aβ40 Ratio, and Exacerbates Axonal Dystrophy and Dendritic Spine Loss in the PS2APP Alzheimer's Mouse Model', *J. Neurosci.*, 40(9), pp. 1956–1974. doi:10.1523/JNEUROSCI.1871-19.2019.

Melief, J., Sneeboer, M.A.M., Litjens, M., Ormel, P.R., Palmen, S.J.M.C., *et al.* (2016) 'Characterizing primary human microglia: A comparative study with myeloid subsets and culture models', *Glia*, 64(11), pp. 1857–1868. doi:10.1002/GLIA.23023.

Merz, P.A., Somerville, R.A., Wisniewski, H.M., Manuelidis, L. and Manuelidis, E.E. (1983) 'Scrapie-associated fibrils in Creutzfeldt–Jakob disease', *Nature*, 306(5942), pp. 474–476. doi:10.1038/306474a0.

Meyer-Luehmann, M., Coomaraswamy, J., Bolmont, T., Kaeser, S., Schaefer, C., *et al.* (2006) 'Exogenous Induction of Cerebral -Amyloidogenesis Is Governed by Agent and Host', *Science (80-.).*, 313(5794), pp. 1781–1784. doi:10.1126/science.1131864.

Michalowsky, B., Kaczynski, A. and Hoffmann, W. (2019) 'The economic and social burden of dementia diseases in Germany—A meta-analysis', *Bundesgesundheitsblatt - Gesundheitsforsch. - Gesundheitsschutz*, 62(8), pp. 981–992. doi:10.1007/S00103-019-02985-Z/FIGURES/1.

Milà-Alomà, M., Salvadó, G., Shekari, M., Grau-Rivera, O., Sala-Vila, A., *et al.* (2021) 'Comparative Analysis of Different Definitions of Amyloid-β Positivity to Detect Early Downstream Pathophysiological Alterations in Preclinical Alzheimer', *J. Prev. Alzheimer's Dis.*, 8(1), pp. 68–77. doi:10.14283/JPAD.2020.51.

Milà-Alomà, M., Salvadó, G., Gispert, J.D., Vilor-Tejedor, N., Grau-Rivera, O., *et al.* (2020) 'Amyloid beta, tau, synaptic, neurodegeneration, and glial biomarkers in the preclinical stage of the Alzheimer's continuum', *Alzheimer's Dement.*, 16(10), p. 1358. doi:10.1002/ALZ.12131.

Morley, J., Farr, S., Banks, W., Johnson, S., Yamada, K., *et al.* (2010) 'A Physiological Role for Amyloid Beta Protein: Enhancement of Learning and Memory', *J. Alzheimers. Dis.*, 19(2), pp. 441–449. doi:10.3233/JAD-2009-1230.

Moujalled, D., Strasser, A. and Liddell, J.R. (2021) 'Molecular mechanisms of cell death in neurological diseases', *Cell Death Differ. 2021 287*, 28(7), pp. 2029–2044. doi:10.1038/s41418-021-00814-y.

Mullan, M., Crawford, F., Axelman, K., Houlden, H., Lilius, L., *et al.* (1992) 'A pathogenic mutation for probable Alzheimer's disease in the APP gene at the N–terminus of β–amyloid', *Nat. Genet.*, 1(5), pp. 345–347. doi:10.1038/ng0892-345.

Müller-Schiffmann, A., Herring, A., Abdel-Hafiz, L., Chepkova, A.N., Schäble, S., *et al.* (2016) 'Amyloid-β dimers in the absence of plaque pathology impair learning and synaptic plasticity', *Brain*, 139(2), pp. 509–525. doi:10.1093/BRAIN/AWV355.

Müller, U.C., Deller, T. and Korte, M. (2017) 'Not just amyloid: Physiological functions of the amyloid precursor protein family', *Nat. Rev. Neurosci.* Nature Publishing Group, pp. 281–298. doi:10.1038/nrn.2017.29.

Musi, N., Valentine, J.M., Sickora, K.R., Baeuerle, E., Thompson, C.S., *et al.* (2018) 'Tau protein aggregation is associated with cellular senescence in the brain', *Aging Cell*, 17(6), p. e12840. doi:10.1111/ACEL.12840.

Nagarathinam, A., Höflinger, P., Bühler, A., Schäfer, C., McGovern, G., *et al.* (2013) 'Membrane-anchored Aβ accelerates amyloid formation and exacerbates amyloid-associated toxicity in mice.', *J. Neurosci.*, 33(49), pp. 19284–94. doi:10.1523/JNEUROSCI.2542-13.2013.

Nakamura, A., Kaneko, N., Villemagne, V.L., Kato, T., Doecke, J., *et al.* (2018) 'High performance plasma amyloid-β biomarkers for Alzheimer's disease', *Nature*, 554(7691), pp. 249–254. doi:10.1038/nature25456.

Nelson, P.T., Alafuzoff, I., Bigio, E.H., Bouras, C., Braak, H., *et al.* (2012) 'Correlation of Alzheimer Disease Neuropathologic Changes With Cognitive Status: A Review of the Literature', *J. Neuropathol. Exp. Neurol.*, 71(5), pp. 362–381. doi:10.1097/NEN.0B013E31825018F7.

Neumann, U., Rueeger, H., Machauer, R., Veenstra, S.J., Lueoend, R.M., *et al.* (2015) 'A novel BACE inhibitor NB-360 shows a superior pharmacological profile and robust reduction of amyloid-β and neuroinflammation in APP transgenic mice', *Mol. Neurodegener.*, 10(1), p. 44. doi:10.1186/s13024-015-0033-8.

Neumann, U., Machauer, R. and Shimshek, D.R. (2019) 'The β-secretase (BACE) inhibitor NB-360 in preclinical models: From amyloid-β reduction to downstream disease-relevant effects', *Br. J. Pharmacol.* John Wiley and Sons Inc., pp. 3435–3446. doi:10.1111/bph.14582.

Nguyen, P.T., Dorman, L.C., Pan, S., Vainchtein, I.D., Han, R.T., *et al.* (2020) 'Microglial Remodeling of the Extracellular Matrix Promotes Synapse Plasticity', *Cell*, 182(2), pp. 388-403.e15. doi:10.1016/J.CELL.2020.05.050.

Nhan, H.S., Chiang, K. and Koo, E.H. (2015) 'The multifaceted nature of amyloid precursor protein and its proteolytic fragments: friends and foes', *Acta Neuropathol.*, 129(1), p. 1. doi:10.1007/S00401-014-1347-2.

Nichols, E., Steinmetz, J.D., Vollset, S.E., Fukutaki, K., Chalek, J., *et al.* (2022) 'Estimation of the global prevalence of dementia in 2019 and forecasted prevalence in 2050: an analysis for the Global Burden of Disease Study 2019', *Lancet Public Heal.*, 7(2), pp. e105–e125. doi:10.1016/S2468-2667(21)00249-8.

Niimura, M., Isoo, N., Takasugi, N., Tsuruoka, M., Ui-Tei, K., *et al.* (2005) 'Aph-1 Contributes to the Stabilization and Trafficking of the γ-Secretase Complex through Mechanisms Involving Intermolecular and Intramolecular Interactions *', *J. Biol. Chem.*, 280(13), pp. 12967–12975. doi:10.1074/JBC.M409829200.

Nilsson, K.P.R., Åslund, A., Berg, I., Nyström, S., Konradsson, P., *et al.* (2007) 'Imaging Distinct Conformational States of Amyloid-β Fibrils in Alzheimer's Disease Using Novel Luminescent Probes', *ACS Chem. Biol.*, 2(8), pp. 553–560. doi:10.1021/cb700116u.

Nimmerjahn, A., Kirchhoff, F. and Helmchen, F. (2005) 'Neuroscience: Resting microglial cells are highly dynamic surveillants of brain parenchyma in vivo', *Science (80-.).*, 308(5726), pp. 1314–1318. doi:10.1126/SCIENCE.1110647/SUPPL_FILE/1110647S9.MOV.

Nitz, E., Smitka, M., Schallner, J., Akgün, K., Ziemssen, T., *et al.* (2021) 'Serum neurofilament light chain in pediatric spinal muscular atrophy patients and healthy children', *Ann. Clin. Transl. Neurol.*, 8(10), pp. 2013–2024. doi:10.1002/ACN3.51449.

Noble, W., Hanger, D.P., Miller, C.C.J. and Lovestone, S. (2013) 'The Importance of Tau Phosphorylation for Neurodegenerative Diseases', *Front. Neurol.*, 4. doi:10.3389/FNEUR.2013.00083.

Novo, M., Freire, S. and Al-Soufi, W. (2018) 'Critical aggregation concentration for the formation of early Amyloid-β (1–42) oligomers', *Sci. Reports 2018 81*, 8(1), pp. 1–8. doi:10.1038/s41598-018-19961-3.

Nussbaum, J.M., Schilling, S., Cynis, H., Silva, A., Swanson, E., *et al.* (2012) 'Prion-like behaviour and tau-dependent cytotoxicity of pyroglutamylated amyloid-β', *Nature*, 485(7400), pp. 651–655. doi:10.1038/nature11060.

Nyström, S., Psonka-Antonczyk, K.M., Ellingsen, P.G., Johansson, L.B.G., Reitan, N., *et al.* (2013) 'Evidence for age-dependent in vivo conformational rearrangement within Aβ amyloid deposits', *ACS Chem. Biol.*, 8(6), pp. 1128–1133. doi:10.1021/cb4000376.

O'Connor, A., Karikari, T.K., Poole, T., Ashton, N.J., Rodriguez, J.L., *et al.* (2020) 'Plasma phospho-tau181 in presymptomatic and symptomatic familial Alzheimer's disease: a longitudinal cohort study', *Mol. Psychiatry 2020*, pp. 1–10. doi:10.1038/s41380-020-0838-x.

Oddo, S., Caccamo, A., Shepherd, J.D., Murphy, M.P., Golde, T.E., *et al.* (2003) 'Triple-transgenic model of Alzheimer's Disease with plaques and tangles: Intracellular Aβ and synaptic dysfunction', *Neuron*, 39(3), pp. 409–421. doi:10.1016/S0896-6273(03)00434-3.

Olsson, B., Portelius, E., Cullen, N.C., Sandelius, Å., Zetterberg, H., *et al.* (2019) 'Association of Cerebrospinal Fluid Neurofilament Light Protein Levels With Cognition in Patients With Dementia, Motor Neuron Disease, and Movement Disorders', *JAMA Neurol.*, 76(3), pp. 318–325. doi:10.1001/JAMANEUROL.2018.3746.

Olsson, I. and Sandøe, P. (2010) '"What's wrong with my monkey?" Ethical perspectives on germline transgenesis in marmosets', *Transgenic Res.*, 19(2), pp. 181–186. doi:10.1007/S11248-009-9316-6.

Ovadya, Y., Landsberger, T., Leins, H., Vadai, E., Gal, H., *et al.* (2018) 'Impaired immune surveillance accelerates accumulation of senescent cells and aging', *Nat. Commun. 2018 91*, 9(1), pp. 1–15. doi:10.1038/s41467-018-07825-3.

Paganetti, P.A., Lis, M., Klafki, H.-W. and Staufenbiel, M. (1996) 'Amyloid precursor protein truncated at any of the y-secretase sites is not cleaved to β-amyloid', *J. Neurosci. Res.*, 46(3), pp. 283–293. doi:10.1002/(SICI)1097-4547(19961101)46:3<283::AID-JNR1>3.0.CO;2-G.

Pagano, K., Galante, D., D'Arrigo, C., Corsaro, A., Nizzari, M., *et al.* (2018) 'Effects of Prion Protein on Aβ42 and Pyroglutamate-Modified AβpE3-42 Oligomerization and Toxicity', *Mol. Neurobiol. 2018 563*, 56(3), pp. 1957–1971. doi:10.1007/S12035-018-1202-X.

Palmqvist, S., Tideman, P., Cullen, N., Zetterberg, H., Blennow, K., *et al.* (2021) 'Prediction of future Alzheimer's disease dementia using plasma phospho-tau combined with other accessible measures', *Nat. Med.*, 27(6), pp. 1034–1042. doi:10.1038/s41591-021-01348-z.

Pan, K.M., Baldwin, M., Nguyen, J., Gasset, M., Serban, A., *et al.* (1993) 'Conversion of alpha-helices into beta-sheets features in the formation of the scrapie prion proteins.', *Proc. Natl. Acad. Sci. U. S. A.*, 90(23), p. 10962. doi:10.1073/PNAS.90.23.10962.

Panza, F., Lozupone, M., Logroscino, G. and Imbimbo, B.P. (2019) 'A critical appraisal of amyloid-β-targeting therapies for Alzheimer disease', *Nat. Rev. Neurol.*, 15(2), pp. 73–88. doi:10.1038/s41582-018-0116-6.

Paolicelli, R.C., Bolasco, G., Pagani, F., Maggi, L., Scianni, M., *et al.* (2011) 'Synaptic pruning by microglia is necessary for normal brain development', *Science (80-.).*, 333(6048), pp. 1456–1458. doi:10.1126/SCIENCE.1202529.

Parbo, P., Madsen, L.S., Ismail, R., Zetterberg, H., Blennow, K., *et al.* (2020) 'Low plasma neurofilament light levels associated with raised cortical microglial activation suggest inflammation acts to protect prodromal Alzheimer's disease', *Alzheimer's Res. Ther. 2020 121*, 12(1), pp. 1–7. doi:10.1186/S13195-019-0574-0.

Parhizkar, S., Arzberger, T., Brendel, M., Kleinberger, G., Deussing, M., *et al.* (2019) 'Loss of TREM2 function increases amyloid seeding but reduces plaque-associated ApoE', *Nat. Neurosci.*, 22(2), pp. 191–204. doi:10.1038/s41593-018-0296-9.

Park, S.-H., Lee, E.-H., Kim, H.-J., Jo, S., Lee, S., *et al.* (2021) 'The relationship of soluble TREM2 to other biomarkers of sporadic Alzheimer's disease', *Sci. Reports 2021 111*, 11(1), pp. 1–10. doi:10.1038/s41598-021-92101-6.

Pascoal, T.A., Therriault, J., Mathotaarachchi, S., Kang, M.S., Shin, M., *et al.* (2020) 'Topographical distribution of Aβ predicts progression to dementia in Aβ positive mild cognitive impairment', *Alzheimer's Dement. Diagnosis, Assess. Dis. Monit.*, 12(1), p. e12037. doi:10.1002/DAD2.12037.

Pascoal, T.A., Benedet, A.L., Ashton, N.J., Kang, M.S., Therriault, J., *et al.* (2021) 'Microglial activation and tau propagate jointly across Braak stages', *Nat. Med. 2021 279*, 27(9), pp. 1592–1599. doi:10.1038/s41591-021-01456-w.

Patel, N.S., Paris, D., Mathura, V., Quadros, A.N., Crawford, F.C., *et al.* (2005) 'Inflammatory cytokine levels correlate with amyloid load in transgenic mouse models of Alzheimer's disease', *J. Neuroinflammation*, 2(1), pp. 1–10. doi:10.1186/1742-2094-2-9/FIGURES/5.

Pereira, J.B., Janelidze, S., Ossenkoppele, R., Kvartsberg, H., Brinkmalm, A., *et al.* (2021) 'Untangling the association of amyloid-β and tau with synaptic and axonal lossin Alzheimer's disease', *Brain*, 144(1), p. 310. doi:10.1093/BRAIN/AWAA395.

Pereira, J.B., Westman, E. and Hansson, O. (2017) 'Association between cerebrospinal fluid and plasma neurodegeneration biomarkers with brain atrophy in Alzheimer's disease', *Neurobiol. Aging*, 58, pp. 14–29. doi:10.1016/J.NEUROBIOLAGING.2017.06.002.

Peters, F., Salihoglu, H., Rodrigues, E., Herzog, E., Blume, T., *et al.* (2017) 'BACE1 inhibition more effectively suppresses initiation than progression of β-amyloid pathology', *Acta Neuropathol.*, pp. 401–17. doi:10.1007/s00401-017-1804-9.

Pickett, E.K., Herrmann, A.G., McQueen, J., Abt, K., Dando, O., *et al.* (2019) 'Amyloid Beta and Tau Cooperate to Cause Reversible Behavioral and Transcriptional Deficits in a Model of Alzheimer's Disease', *Cell Rep.*, 29(11), pp. 3592-3604.e5. doi:10.1016/J.CELREP.2019.11.044.

Polanco, J.C., Li, C., Bodea, L.-G., Martinez-Marmol, R., Meunier, F.A., *et al.* (2017) 'Amyloid-β and tau complexity — towards improved biomarkers and targeted therapies', *Nat. Rev. Neurol.*, 14(1), pp. 22–39. doi:10.1038/nrneurol.2017.162.

Portelius, E., Bogdanovic, N., Gustavsson, M.K., Volkmann, I., Brinkmalm, G., *et al.* (2010) 'Mass spectrometric characterization of brain amyloid beta isoform signatures in familial and sporadic Alzheimer's disease', *Acta Neuropathol.*, 120(2), pp. 185–193. doi:10.1007/s00401-010-0690-1.

Preische, O., Schultz, S.A., Apel, A., Kuhle, J., Kaeser, S.A., *et al.* (2019) 'Serum neurofilament dynamics predicts neurodegeneration and clinical progression in presymptomatic Alzheimer's disease', *Nat. Med.*, 25(2), pp. 277–283. doi:10.1038/s41591-018-0304-3.

Prescott, M.J. (2020) 'Ethical and Welfare Implications of Genetically Altered Non-Human Primates for Biomedical Research', *J. Appl. Anim. Ethics Res.*, 2(2), pp. 151–176. doi:10.1163/25889567-BJA10002.

Prince, M., Wimo, A., Guerchet, M., Gemma-Claire Ali, M., Wu, Y.-T., *et al.* (2015) *World Alzheimer Report 2015. The Global Impact of Dementia.*

Prokop, S., Shirotani, K., Edbauer, D., Haass, C. and Steiner, H. (2004) 'Requirement of PEN-2 for Stabilization of the Presenilin N-/C-terminal Fragment Heterodimer within the γ-Secretase Complex *', *J. Biol. Chem.*, 279(22), pp. 23255–23261. doi:10.1074/JBC.M401789200.

Prokop, S., Miller, K.R., Labra, S.R., Pitkin, R.M., Hoxha, K., *et al.* (2019) 'Impact of TREM2 risk variants on brain region-specific immune activation and plaque microenvironment in Alzheimer's disease patient brain samples', *Acta Neuropathol.*, 138(4), p. 613. doi:10.1007/S00401-019-02048-2.

Prusiner, S.B. (1982) 'Novel proteinaceous infectious particles cause scrapie.', *Science*, 216(4542), pp. 136–44. doi:10.1126/SCIENCE.6801762.

Prusiner, S.B. (1998a) 'Prions', *Proc. Natl. Acad. Sci.*, 95(23), pp. 13363–13383. doi:10.1073/PNAS.95.23.13363.

Prusiner, S.B. (1998b) 'The Prion Diseases', *Brain Pathol.*, 8(3), pp. 499–513. doi:10.1111/J.1750-3639.1998.TB00171.X.

Prusiner, S.B. (2012) 'A unifying role for prions in neurodegenerative diseases', *Science (80-.).*, 336(6088), pp. 1511–1513. doi:10.1126/SCIENCE.1222951.

'PSEN-1 - ALZFORUM' (no date) *accessed 27 April 2022, www.alzforum.org/mutations/psen-1*.

Puzzo, D., Privitera, L., Fa', M., Staniszewski, A., Hashimoto, G., *et al.* (2011) 'Endogenous amyloid-β is necessary for hippocampal synaptic plasticity and memory', *Ann. Neurol.*, 69(5), pp. 819–830. doi:10.1002/ANA.22313.

Qi, H., Prabakaran, S., Cantrelle, F.-X., Chambraud, B., Gunawardena, J., *et al.* (2016) 'Characterization of Neuronal Tau Protein as a Target of Extracellular Signal-regulated Kinase *', *J. Biol. Chem.*, 291(14), pp. 7742–7753. doi:10.1074/JBC.M115.700914.

Qiang, W., Yau, W.M., Lu, J.X., Collinge, J. and Tycko, R. (2017) 'Structural variation in amyloid-β fibrils from Alzheimer's disease clinical subtypes', *Nature*, 541(7636), pp. 217–221. doi:10.1038/nature20814.

Querol-Vilaseca, M., Sirisi, S., Molina-Porcel, L., Molina, B., Pegueroles, J., *et al.* (2022) 'Neuropathology of a patient with Alzheimer disease treated with low doses of verubecestat', *Neuropathol. Appl. Neurobiol.*, 48(3), pp. 12781–12787. doi:10.1111/NAN.12781.

Radde, R., Bolmont, T., Kaeser, S.A., Coomaraswamy, J., Lindau, D., *et al.* (2006) 'Abeta42-driven cerebral amyloidosis in transgenic mice reveals early and robust pathology.', *EMBO Rep.*, 7(9), pp. 940–6. doi:10.1038/sj.embor.7400784.

Radde, R., Duma, C., Goedert, M. and Jucker, M. (2008) 'The value of incomplete mouse models of Alzheimer's disease', *Eur. J. Nucl. Med. Mol. Imaging*, 35 Suppl 1(SUPPL. 1). doi:10.1007/S00259-007-0704-Y.

Ransohoff, R.M. and Cardona, A.E. (2010) 'The myeloid cells of the central nervous system

parenchyma', *Nature*, 468(7321), pp. 253–262. doi:10.1038/nature09615.

Rasmussen, J., Mahler, J., Beschorner, N., Kaeser, S.A., Häsler, L.M., *et al.* (2017) 'Amyloid polymorphisms constitute distinct clouds of conformational variants in different etiological subtypes of Alzheimer's disease.', *Proc. Natl. Acad. Sci. U. S. A.*, 114(49), pp. 13018–13023. doi:10.1073/pnas.1713215114.

Reitz, C., Rogaeva, E. and Beecham, G.W. (2020) 'Late-onset vs nonmendelian early-onset Alzheimer disease', *Neurol. Genet.*, 6(5). doi:10.1212/NXG.0000000000000512.

Rezaei-Ghaleh, N., Amininasab, M., Kumar, S., Walter, J. and Zweckstetter, M. (2016) 'Phosphorylation modifies the molecular stability of β-amyloid deposits', *Nat. Commun. 2016 71*, 7(1), pp. 1–9. doi:10.1038/ncomms11359.

Rijal Upadhaya, A., Kosterin, I., Kumar, S., von Arnim, C., Yamaguchi, H., *et al.* (2014) 'Biochemical stages of amyloid-β peptide aggregation and accumulation in the human brain and their association with symptomatic and pathologically preclinical Alzheimer's disease', *Brain*, 137(3), pp. 887–903. doi:10.1093/BRAIN/AWT362.

Rivera-Escalera, F., Pinney, J.J., Owlett, L., Ahmed, H., Thakar, J., *et al.* (2019) 'IL-1β-driven amyloid plaque clearance is associated with an expansion of transcriptionally reprogrammed microglia', *J. Neuroinflammation 2019 161*, 16(1), pp. 1–17. doi:10.1186/S12974-019-1645-7.

Roberson, E.D., Scearce-Levie, K., Palop, J.J., Yan, F., Cheng, I.H., *et al.* (2007) 'Reducing endogenous tau ameliorates amyloid β-induced deficits in an Alzheimer's disease mouse model', *Science (80-.).*, 316(5825), pp. 750–754. doi:10.1126/SCIENCE.1141736.

Röhr, D., Boon, B.D.C., Schuler, M., Kremer, K., Hoozemans, J.J.M., *et al.* (2020) 'Label-free vibrational imaging of different Aβ plaque types in Alzheimer's disease reveals sequential events in plaque development', *Acta Neuropathol. Commun. 2020 81*, 8(1), pp. 1–13. doi:10.1186/S40478-020-01091-5.

Russell, C., Koncarevic, S. and DWard, M. (2014) 'Post-translational modifications in Alzheimer's disease and the potential for new biomarkers', *J. Alzheimers. Dis.*, 41(2), pp. 345–364. doi:10.3233/JAD-132312.

Ryu, W.I., Bormann, M.K., Shen, M., Kim, D., Forester, B., *et al.* (2021) 'Brain cells derived from Alzheimer's disease patients have multiple specific innate abnormalities in energy metabolism', *Mol. Psychiatry 2021 2610*, 26(10), pp. 5702–5714. doi:10.1038/s41380-021-01068-3.

Saez-Atienzar, S. and Masliah, E. (2020) 'Cellular senescence and Alzheimer disease: the egg and the chicken scenario', *Nat. Rev. Neurosci. 2020 218*, 21(8), pp. 433–444. doi:10.1038/s41583-020-0325-z.

Saido, T.C., Iwatsubo, T., Mann, D.M.A., Shimada, H., Ihara, Y., *et al.* (1995) 'Dominant and differential deposition of distinct β-amyloid peptide species, AβN3(pE), in senile plaques', *Neuron*, 14(2), pp. 457–466. doi:10.1016/0896-6273(95)90301-1.

Sala Frigerio, C., Lau, P., Troakes, C., Deramecourt, V., Gele, P., *et al.* (2015) 'On the identification of low allele frequency mosaic mutations in the brains of Alzheimer's disease patients', *Alzheimer's Dement.*, 11(11), pp. 1265–1276. doi:10.1016/J.JALZ.2015.02.007.

Salloway, S., Farlow, M., McDade, E., Clifford, D.B., Wang, G., *et al.* (2021) 'A trial of gantenerumab or solanezumab in dominantly inherited Alzheimer's disease', *Nat. Med.*, 27(7), pp. 1187–1196. doi:10.1038/s41591-021-01369-8.

Salminen, A., Kauppinen, A. and Kaarniranta, K. (2012) 'Emerging role of NF-κB signaling in the induction of senescence-associated secretory phenotype (SASP)', *Cell. Signal.*, 24(4), pp. 835–845. doi:10.1016/J.CELLSIG.2011.12.006.

Sandberg, M.K., Al-Doujaily, H., Sharps, B., Clarke, A.R. and Collinge, J. (2011) 'Prion propagation and toxicity in vivo occur in two distinct mechanistic phases', *Nature*, 470(7335), pp. 540–542. doi:10.1038/nature09768.

Sandberg, M.K., Al-Doujaily, H., Sharps, B., De Oliveira, M.W., Schmidt, C., *et al.* (2014) 'Prion neuropathology follows the accumulation of alternate prion protein isoforms after infective titre has peaked', *Nat. Commun.*, 5(1), pp. 1–7. doi:10.1038/ncomms5347.

Sassi, C., Guerreiro, R., Gibbs, R., Ding, J., Lupton, M.K., *et al.* (2014) 'Exome sequencing identifies 2 novel presenilin 1 mutations (p.L166V and p.S230R) in British early-onset Alzheimer's disease', *Neurobiol. Aging*, 35(10), p. 2422.e13. doi:10.1016/J.NEUROBIOLAGING.2014.04.026.

Sato, K., Sasaguri, H., Kumita, W., Inoue, T., Kurotaki, Y., *et al.* (2020) 'A non-human primate model of familial Alzheimer's disease', *bioRxiv*, p. 2020.08.24.264259. doi:10.1101/2020.08.24.264259.

Sato, T., Dohmae, N., Qi, Y., Kakuda, N., Misonou, H., *et al.* (2003) 'Potential Link between Amyloid β-Protein 42 and C-terminal Fragment γ 49–99 of β-Amyloid Precursor Protein *', *J. Biol. Chem.*, 278(27), pp. 24294–24301. doi:10.1074/JBC.M211161200.

Sato, T., Diehl, T.S., Narayanan, S., Funamoto, S., Ihara, Y., *et al.* (2007) 'Active γ-secretase complexes contain only one of each component', *J. Biol. Chem.*, 282(47), pp. 33985–33993. doi:10.1074/JBC.M705248200/ATTACHMENT/572D24B8-1E36-41A1-8EBE-575236E23F1F/MMC1.PDF.

Satz, P. (1993) 'Brain Reserve Capacity on Symptom Onset After Brain Injury: A Formulation and Review of Evidence for Threshold Theory', *Neuropsychology*, 7(3), pp. 273–295. doi:10.1037/0894-4105.7.3.273.

Schauenburg, L., Liebsch, F., Eravci, M., Mayer, M.C., Weise, C., *et al.* (2018) 'APLP1 is endoproteolytically cleaved by gamma-secretase without previousectodomain shedding', *Sci. Rep.*, 8(1). doi:10.1038/S41598-018-19530-8.

Schelle, J., Häsler, L.M., Göpfert, J.C., Joos, T.O., Vanderstichele, H., *et al.* (2017) 'Prevention of tau increase in cerebrospinal fluid of APP transgenic mice suggests downstream effect of BACE1 inhibition', *Alzheimer's Dement.*, 13(6), pp. 701–709. doi:10.1016/J.JALZ.2016.09.005.

Schelle, J., Wegenast-Braun, B.M., Fritschi, S.K., Kaeser, S.A., Jährling, N., *et al.* (2019) 'Early Aβ reduction prevents progression of cerebral amyloid angiopathy', *Ann. Neurol.*, 86(4), pp. 561–571. doi:10.1002/ana.25562.

Scheltens, P., Blennow, K., Breteler, M.M.B., de Strooper, B., Frisoni, G.B., *et al.* (2016) 'Alzheimer's disease', *Lancet*, 388(10043), pp. 505–517. doi:10.1016/S0140-6736(15)01124-1.

Scheuner, D., Eckman, C., Jensen, M., Song, X., Citron, M., *et al.* (1996) 'Secreted amyloid β–protein similar to that in the senile plaques of Alzheimer's disease is increased in vivo by the presenilin 1 and 2 and APP mutations linked to familial Alzheimer's disease', *Nat. Med. 1996 28*, 2(8), pp. 864–870. doi:10.1038/nm0896-864.

Selkoe, D.J. and Hardy, J. (2016) 'The amyloid hypothesis of Alzheimer's disease at

25 years.', *EMBO Mol. Med.*, 8(6), pp. 595–608. doi:10.15252/emmm.201606210.

Serio, T.R., Cashikar, A.G., Kowal, A.S., Sawicki, G.J., Moslehi, J.J., *et al.* (2000) 'Nucleated conformational conversion and the replication of conformational information by a prion determinant', *Science*, 289(5483), pp. 1317–1321. doi:10.1126/SCIENCE.289.5483.1317.

Serrano-Pozo, A., Qian, J., Monsell, S.E., Frosch, M.P., Betensky, R.A., *et al.* (2013) 'Examination of the Clinicopathologic Continuum of Alzheimer Disease in the Autopsy Cohort of the National Alzheimer Coordinating Center', *J. Neuropathol. Exp. Neurol.*, 72(12), pp. 1182–1192. doi:10.1097/NEN.0000000000000016.

Seubert, P., Vigo-Pelfrey, C., Esch, F., Lee, M., Dovey, H., *et al.* (1992) 'Isolation and quantification of soluble Alzheimer's β-peptide from biological fluids', *Nature*, 359(6393), pp. 325–327. doi:10.1038/359325a0.

Sevigny, J., Chiao, P., Bussière, T., Weinreb, P.H., Williams, L., *et al.* (2016) 'The antibody aducanumab reduces Aβ plaques in Alzheimer's disease', *Nature*, 537(7618), pp. 50–56. doi:10.1038/nature19323.

Shah, S., Lee, S.F., Tabuchi, K., Hao, Y.H., Yu, C., *et al.* (2005) 'Nicastrin functions as a γ-secretase-substrate receptor', *Cell*, 122(3), pp. 435–447. doi:10.1016/J.CELL.2005.05.022/ATTACHMENT/31AB9089-7ADC-4416-BD2C-EE8287F54A2E/MMC1.PDF.

Shankar, G.M., Li, S., Mehta, T.H., Garcia-Munoz, A., Shepardson, N.E., *et al.* (2008) 'Amyloid-β protein dimers isolated directly from Alzheimer's brains impair synaptic plasticity and memory', *Nat. Med.*, 14(8), pp. 837–842. doi:10.1038/nm1782.

Shankar, G.M., Leissring, M.A., Adame, A., Sun, X., Spooner, E., *et al.* (2009) 'Biochemical and immunohistochemical analysis of an Alzheimer's disease mouse model reveals the presence of multiple cerebral Aβ assembly forms throughout life', *Neurobiol. Dis.*, 36(2), pp. 293–302. doi:10.1016/J.NBD.2009.07.021.

Sharpless, N.E. and Sherr, C.J. (2015) 'Forging a signature of in vivo senescence', *Nat. Rev. Cancer 2015 157*, 15(7), pp. 397–408. doi:10.1038/nrc3960.

Shi, L., Steenland, K., Li, H., Liu, P., Zhang, Y., *et al.* (2021a) 'A national cohort study (2000–2018) of long-term air pollution exposure and incident dementia in older adults in the United States', *Nat. Commun. 2021 121*, 12(1), pp. 1–9. doi:10.1038/s41467-021-27049-2.

Shi, Y., Zhang, W., Yang, Y., Murzin, A.G., Falcon, B., *et al.* (2021b) 'Structure-based classification of tauopathies', *Nature*, pp. 1–5. doi:10.1038/s41586-021-03911-7.

Shoghi-Jadid, K., Small, G.W., Agdeppa, E.D., Kepe, V., Ercoli, L.M., *et al.* (2002) 'Localization of Neurofibrillary Tangles and Beta-Amyloid Plaques in the Brains of Living Patients With Alzheimer Disease', *Am. J. Geriatr. Psychiatry*, 10(1), pp. 24–35. doi:10.1097/00019442-200201000-00004.

Sierksma, A., Lu, A., Mancuso, R., Fattorelli, N., Thrupp, N., *et al.* (2020) 'Novel Alzheimer risk genes determine the microglia response to amyloid-β but not to TAU pathology', *EMBO Mol. Med.*, 12(3). doi:10.15252/EMMM.201910606.

Sinha, S., Anderson, J.P., Barbour, R., Basi, G.S., Caccaveffo, R., *et al.* (1999) 'Purification and cloning of amyloid precursor protein β-secretase from human brain', *Nature*, 402(6761), pp. 537–540. doi:10.1038/990114.

Sisodia, S.S. (1992) 'Beta-amyloid precursor protein cleavage by a membrane-bound

protease', *Proc. Natl. Acad. Sci.*, 89(13), pp. 6075–6079. doi:10.1073/PNAS.89.13.6075.

So, M., Hall, D. and Goto, Y. (2016) 'Revisiting supersaturation as a factor determining amyloid fibrillation', *Curr. Opin. Struct. Biol.*, 36, pp. 32–39. doi:10.1016/J.SBI.2015.11.009.

Sobue, A., Komine, O., Hara, Y., Endo, F., Mizoguchi, H., *et al.* (2021) 'Microglial gene signature reveals loss of homeostatic microglia associated with neurodegeneration of Alzheimer's disease', *Acta Neuropathol. Commun. 2020 91*, 9(1), pp. 1–17. doi:10.1186/S40478-020-01099-X.

Song, R., Wu, X., Liu, H., Guo, D., Tang, L., *et al.* (2022) 'Prediction of Cognitive Progression in Individuals with Mild Cognitive Impairment Using Radiomics as an Improvement of the ATN System: A Five-Year Follow-Up Study', *Korean J. Radiol.*, 23(1), p. 89. doi:10.3348/KJR.2021.0323.

Song, Y.S., Lee, B.Y. and Hwang, E.S. (2005) 'Dinstinct ROS and biochemical profiles in cells undergoing DNA damage-induced senescence and apoptosis', *Mech. Ageing Dev.*, 126(5), pp. 580–590. doi:10.1016/J.MAD.2004.11.008.

Soto, C. and Pritzkow, S. (2018) 'Protein misfolding, aggregation, and conformational strains in neurodegenerative diseases', *Nat. Neurosci.*, 21(10), pp. 1332–1340. doi:10.1038/s41593-018-0235-9.

Souza, J.S.M., Lisboa, A.B.P., Santos, T.M., Andrade, M.V.S., Neves, V.B.S., *et al.* (2020) 'The evolution of ADAM gene family in eukaryotes', *Genomics*, 112(5), pp. 3108–3116. doi:10.1016/J.YGENO.2020.05.010.

Spallarossa, P., Altieri, P., Aloi, C., Garibaldi, S., Barisione, C., *et al.* (2009) 'Doxorubicin induces senescence or apoptosis in rat neonatal cardiomyocytes by regulating the expression levels of the telomere binding factors 1 and 2', *Am. J. Physiol. - Hear. Circ. Physiol.*, 297(6), pp. 2169–2181. doi:10.1152/AJPHEART.00068.2009/ASSET/IMAGES/LARGE/ZH40120991210009.JPEG.

Sperling, R.A., Jack, C.R., Black, S.E., Frosch, M.P., Greenberg, S.M., *et al.* (2011) 'Amyloid-related imaging abnormalities in amyloid-modifying therapeutic trials: recommendations from the Alzheimer's Association Research Roundtable Workgroup', *Alzheimer's Dement.*, 7(4), pp. 367–385. doi:10.1016/j.jalz.2011.05.2351.

Sperling, R.A., Mormino, E.C., Schultz, A.P., Betensky, R.A., Papp, K. V., *et al.* (2019) 'The impact of amyloid-beta and tau on prospective cognitive decline in older individuals', *Ann. Neurol.*, 85(2), pp. 181–193. doi:10.1002/ANA.25395.

Spillantini, M.G., Bird, T.D. and Ghetti, B. (1998) 'Frontotemporal Dementia and Parkinsonism Linked to Chromosome 17: A New Group of Tauopathies', *Brain Pathol.*, 8(2), pp. 387–402. doi:10.1111/J.1750-3639.1998.TB00162.X.

Spillantini, M.G. and Goedert, M. (2013) 'Tau pathology and neurodegeneration', *Lancet Neurol.*, 12(6), pp. 609–622. doi:10.1016/S1474-4422(13)70090-5.

Spires-Jones, T.L. and Hyman, B.T. (2014) 'The intersection of amyloid beta and tau at synapses in Alzheimer's disease', *Neuron*, 82(4), p. 756. doi:10.1016/J.NEURON.2014.05.004.

Srivastava, A.K., Pittman, J.M., Zerweck, J., Venkata, B.S., Moore, P.C., *et al.* (2019) 'β-Amyloid aggregation and heterogeneous nucleation', *Protein Sci.*, 28(9), pp. 1567–1581. doi:10.1002/PRO.3674.

St-Amour, I., Paré, I., Alata, W., Coulombe, K., Ringuette-Goulet, C., *et al.* (2013) 'Brain bioavailability of human intravenous immunoglobulin and its transport through the murine blood–brain barrier', *J. Cereb. Blood Flow Metab.*, 33(12), p. 1983. doi:10.1038/JCBFM.2013.160.

Stahl, N., Borchelt, D.R., Hsiao, K. and Prusiner, S.B. (1987) 'Scrapie prion protein contains a phosphatidylinositol glycolipid', *Cell*, 51(2), pp. 229–240. doi:10.1016/0092-8674(87)90150-4.

De Strooper, B., Saftig, P., Craessaerts, K., Vanderstichele, H., Guhde, G., *et al.* (1998) 'Deficiency of presenilin-1 inhibits the normal cleavage of amyloid precursor protein', *Nature*, 391(6665), pp. 387–390. doi:10.1038/34910.

De Strooper, B., Annaert, W., Cupers, P., Saftig, P., Craessaerts, K., *et al.* (1999) 'A presenilin-1-dependent γ-secretase-like protease mediates release of Notch intracellular domain', *Nature*, 398(6727), pp. 518–522. doi:10.1038/19083.

De Strooper, B. and Karran, E. (2016) 'The Cellular Phase of Alzheimer's Disease', *Cell*. Cell Press, pp. 603–615. doi:10.1016/j.cell.2015.12.056.

Struhl, G. and Adachi, A. (2000) 'Requirements for Presenilin-Dependent Cleavage of Notch and Other Transmembrane Proteins', *Mol. Cell*, 6(3), pp. 625–636. doi:10.1016/S1097-2765(00)00061-7.

Sturchler-Pierrat, C., Abramowski, D., Duke, M., Wiederhold, K.-H., Mistl, C., *et al.* (1997) 'Two amyloid precursor protein transgenic mouse models with Alzheimer disease-like pathology', *Neurobiology*, 94, pp. 13287–13292.

Suárez-Calvet, M., Karikari, T.K., Ashton, N.J., Rodríguez, J.L., Milà-Alomà, M., *et al.* (2020) 'Novel tau biomarkers phosphorylated at T181, T217 or T231 rise in the initial stages of the preclinical Alzheimer's continuum when only subtle changes in Aβ pathology are detected', *EMBO Mol. Med.*, 12(12), p. e12921. doi:10.15252/EMMM.202012921.

Sugarman, M., Zetterberg, H., Blennow, K., Tripodis, Y., McKee, A., *et al.* (2020) 'A longitudinal examination of plasma neurofilament light and total tau for the clinical detection and monitoring of Alzheimer's disease', *Neurobiol. Aging*, 94, pp. 60–70. doi:10.1016/J.NEUROBIOLAGING.2020.05.011.

Sun, L., Zhou, R., Yang, G. and Shi, Y. (2017) 'Analysis of 138 pathogenic mutations in presenilin-1 on the in vitro production of Aβ42 and Aβ40 peptides by γ-secretase.', *Proc. Natl. Acad. Sci. U. S. A.*, 114(4), pp. E476–E485. doi:10.1073/pnas.1618657114.

Suzuki, N., Cheung, T.T., Cai, X.D., Odaka, A., Otvos, L., *et al.* (1994a) 'An Increased Percentage of Long Amyloid β Protein Secreted by Familial Amyloid β Protein Precursor (βApp717) Mutants', *Science (80-.).*, 264(5163), pp. 1336–1340. doi:10.1126/SCIENCE.8191290.

Suzuki, N., Iwatsubo, T., Odaka, A., Ishibashi, Y., Kitada, C., *et al.* (1994b) 'High tissue content of soluble beta 1-40 is linked to cerebral amyloid angiopathy.', *Am. J. Pathol.*, 145(2), p. 452.

Takami, M., Nagashima, Y., Sano, Y., Ishihara, S., Morishima-Kawashima, M., *et al.* (2009) 'gamma-Secretase: successive tripeptide and tetrapeptide release from the transmembrane domain of beta-carboxyl terminal fragment', *J. Neurosci.*, 29(41), pp. 13042–13052. doi:10.1523/JNEUROSCI.2362-09.2009.

Takeda, K., Uda, A., Mitsubori, M., Nagashima, S., Iwasaki, H., *et al.* (2021) 'Mitochondrial

ubiquitin ligase alleviates Alzheimer's disease pathology via blocking the toxic amyloid-β oligomer generation', *Commun. Biol. 2021 41*, 4(1), pp. 1–13. doi:10.1038/s42003-021-01720-2.

Tan, J.Z.A. and Gleeson, P.A. (2019) 'The role of membrane trafficking in the processing of amyloid precursor protein and production of amyloid peptides in Alzheimer's disease', *Biochim. Biophys. Acta - Biomembr.*, 1861(4), pp. 697–712. doi:10.1016/J.BBAMEM.2018.11.013.

Tanzi, R.E., Gusella, J.F., Watkins, P.C., Bruns, G.A.P., St. George-Hyslop, P., *et al.* (1987) 'Amyloid β Protein Gene: cDNA, mRNA Distribution, and Genetic Linkage Near the Alzheimer Locus', *Science (80-.).*, 235(4791), pp. 880–884. doi:10.1126/SCIENCE.2949367.

Teunissen, C.E., Verberk, I.M.W., Thijssen, E.H., Vermunt, L., Hansson, O., *et al.* (2022) 'Blood-based biomarkers for Alzheimer's disease: towards clinical implementation', *Lancet Neurol.*, 21(1), pp. 66–77. doi:10.1016/S1474-4422(21)00361-6.

Thal, D.R., Capetillo-Zarate, E., Larionov, S., Staufenbiel, M., Zurbruegg, S., *et al.* (2009) 'Capillary cerebral amyloid angiopathy is associated with vessel occlusion and cerebral blood flow disturbances', *Neurobiol. Aging*, 30(12), pp. 1936–1948. doi:10.1016/J.NEUROBIOLAGING.2008.01.017.

Thal, D.R. (2015) 'Clearance of amyloid β-protein and its role in the spreading of Alzheimer's disease pathology', *Front. Aging Neurosci.*, 0(MAR), p. 25. doi:10.3389/FNAGI.2015.00025.

Thambisetty, M., Howard, R., Glymour, M.M. and Schneider, L.S. (2021) 'Alzheimer's drugs: Does reducing amyloid work?', *Science (80-.).*, 374(6567), pp. 544–545. doi:10.1126/SCIENCE.ABL8366.

Thebault, S., Booth, R.A. and Freedman, M.S. (2020) 'Blood Neurofilament Light Chain: The Neurologist's Troponin?', *Biomedicines*, 8(11), pp. 1–11. doi:10.3390/BIOMEDICINES8110523.

Therriault, J., Benedet, A., Pascoal, T., Lussier, F., Tissot, C., *et al.* (2021) 'Association of plasma P-tau181 with memory decline in non-demented adults', *Brain Commun.*, 3(3). doi:10.1093/BRAINCOMMS/FCAB136.

Thompson, T.B., Meisl, G., Knowles, T.P.J. and Goriely, A. (2021) 'The role of clearance mechanisms in the kinetics of pathological protein aggregation involved in neurodegenerative diseases', *J. Chem. Phys.*, 154(12), p. 125101. doi:10.1063/5.0031650.

Toh, W.H., Tan, J.Z.A., Zulkefli, K.L., Houghton, F.J. and Gleeson, P.A. (2017a) 'Amyloid precursor protein traffics from the Golgi directly to early endosomes in an Arl5b- and AP4-dependent pathway', *Traffic*, 18(3), pp. 159–175. doi:10.1111/TRA.12465.

Toh, W.H., Chia, P.Z.C., Hossain, M.I. and Gleeson, P.A. (2017b) 'GGA1 regulates signal-dependent sorting of BACE1 to recycling endosomes which moderates Aβ production.', *Mol. Biol. Cell*, 29(2), pp. 191–208. doi:10.1091/mbc.E17-05-0270.

Tomasselli, A.G., Qahwash, I., Emmons, T.L., Lu, Y., Leonem, J.W., *et al.* (2003) 'Employing a superior BACE1 cleavage sequence to probe cellular APP processing', *J. Neurochem.*, 84(5), pp. 1006–1017. doi:10.1046/J.1471-4159.2003.01597.X.

Törnquist, M., Michaels, C.T.T., Sanagavarapu, K., Yang, X., Meisl, G., *et al.* (2018) 'Secondary nucleation in amyloid formation', *Chem. Commun.*, 54(63), pp. 8667–8684. doi:10.1039/C8CC02204F.

Tycko, R. (2015) 'Amyloid Polymorphism: Structural Basis and Neurobiological Relevance', *Neuron*, 86(3), pp. 632–645. doi:10.1016/j.neuron.2015.03.017.

Uhlmann, R.E., Rother, C., Rasmussen, J., Schelle, J., Bergmann, C., *et al.* (2020) 'Acute targeting of pre-amyloid seeds in transgenic mice reduces Alzheimer-like pathology later in life', *Nat. Neurosci.*, 23(12), pp. 1580–1588. doi:10.1038/s41593-020-00737-w.

Vassar, R., Bennett, B.D., Babu-Khan, S., Kahn, S., Mendiaz, E.A., *et al.* (1999) 'β-Secretase cleavage of Alzheimer's amyloid precursor protein by the transmembrane aspartic protease BACE', *Science (80-.).*, 286(5440), pp. 735–741. doi:10.1126/science.286.5440.735.

Vassar, R., Kuhn, P.H., Haass, C., Kennedy, M.E., Rajendran, L., *et al.* (2014) 'Function, therapeutic potential and cell biology of BACE proteases: current status and future prospects', *J. Neurochem.*, 130(1), p. 4. doi:10.1111/JNC.12715.

Vergara, C., Houben, S., Suain, V., Yilmaz, Z., De Decker, R., *et al.* (2019) 'Amyloid-β pathology enhances pathological fibrillary tau seeding induced by Alzheimer PHF in vivo', *Acta Neuropathol. 2019 1373*, 137(3), pp. 397–412. doi:10.1007/S00401-018-1953-5.

Vieira, S.I., Rebelo, S., Esselmann, H., Wiltfang, J., Lah, J., *et al.* (2010) 'Retrieval of the Alzheimer's amyloid precursor protein from the endosome to the TGN is S655 phosphorylation state-dependent and retromer-mediated', *Mol. Neurodegener. 2010 51*, 5(1), pp. 1–21. doi:10.1186/1750-1326-5-40.

Walker, L.C. (2020) 'Aβ Plaques', *Free Neuropathol.*, 1. doi:10.17879/FREENEUROPATHOLOGY-2020-3025.

Walker, L.C. and Jucker, M. (2015) 'Neurodegenerative Diseases: Expanding the Prion Concept', *Annu. Rev. Neurosci.*, 38(1), pp. 87–103. doi:10.1146/annurev-neuro-071714-033828.

Walker, L.C. and Jucker, M. (2017) 'The Exceptional Vulnerability of Humans to Alzheimer's Disease', *Trends Mol. Med.*, 23(6), p. 534. doi:10.1016/J.MOLMED.2017.04.001.

Walsh, D.M., Tseng, B.P., Rydel, R.E., Podlisny, M.B. and Selkoe, D.J. (2000) 'The Oligomerization of Amyloid β-Protein Begins Intracellularly in Cells Derived from Human Brain†', *Biochemistry*, 39(35), pp. 10831–10839. doi:10.1021/BI001048S.

Wang, J.Z., Grundke-Iqbal, I. and Iqbal, K. (1996) 'Glycosylation of microtubule–associated protein tau: An abnormal posttranslational modification in Alzheimer's disease', *Nat. Med. 1996 28*, 2(8), pp. 871–875. doi:10.1038/nm0896-871.

Wang, Y., Ulland, T.K., Ulrich, J.D., Song, W., Tzaferis, J.A., *et al.* (2016) 'TREM2-mediated early microglial response limits diffusion and toxicity of amyloid plaques', *J. Exp. Med.*, 213(5), p. 667. doi:10.1084/JEM.20151948.

Wang, Y.T. and Edison, P. (2019) 'Tau Imaging in Neurodegenerative Diseases Using Positron Emission Tomography', *Curr. Neurol. Neurosci. Rep.*, 19(7). doi:10.1007/S11910-019-0962-7.

Webers, A., Heneka, M.T. and Gleeson, P.A. (2020) 'The role of innate immune responses and neuroinflammation in amyloid accumulation and progression of Alzheimer's disease', *Immunol. Cell Biol.*, 98(1), pp. 28–41. doi:10.1111/IMCB.12301.

Weidemann, A., Eggert, S., Reinhard, F., Vogel, M., Paliga, K., *et al.* (2002) 'A Novel ε-Cleavage within the Transmembrane Domain of the Alzheimer Amyloid Precursor Protein

Demonstrates Homology with Notch Processing†', *Biochemistry*, 41(8), pp. 2825–2835. doi:10.1021/BI015794O.

Weingarten, M., Lockwood, A., Hwo, S. and Kirschner, M. (1975) 'A protein factor essential for microtubule assembly', *Proc. Natl. Acad. Sci. U. S. A.*, 72(5), pp. 1858–1862. doi:10.1073/PNAS.72.5.1858.

Wilkaniec, A., Gąssowska-Dobrowolska, M., Strawski, M., Adamczyk, A. and Czapski, G.A. (2018) 'Inhibition of cyclin-dependent kinase 5 affects early neuroinflammatory signalling in murine model of amyloid beta toxicity', *J. Neuroinflammation 2018 151*, 15(1), pp. 1–18. doi:10.1186/S12974-017-1027-Y.

Wimo, A., Guerchet, M., Ali, G.C., Wu, Y.T., Prina, A.M., *et al.* (2017) 'The worldwide costs of dementia 2015 and comparisons with 2010', *Alzheimer's Dement.*, 13(1), pp. 1–7. doi:10.1016/J.JALZ.2016.07.150.

Winkler, D.T., Bondolfi, L., Herzig, M.C., Jann, L., Calhoun, M.E., *et al.* (2001) 'Spontaneous Hemorrhagic Stroke in a Mouse Model of Cerebral Amyloid Angiopathy', *J. Neurosci.*, 21(5), p. 1619. doi:10.1523/JNEUROSCI.21-05-01619.2001.

Wirths, O., Bethge, T., Marcello, A., Harmeier, A., Jawhar, S., *et al.* (2010) 'Pyroglutamate Abeta pathology in APP/PS1KI mice, sporadic and familial Alzheimer's disease cases', *J. Neural Transm.*, 117(1), pp. 85–96. doi:10.1007/S00702-009-0314-X.

De Wolf, F., Ghanbari, M., Licher, S., McRae-McKee, K., Gras, L., *et al.* (2020) 'Plasma tau, neurofilament light chain and amyloid-β levels and risk of dementia; a population-based cohort study', *Brain*, 143(4), p. 1220. doi:10.1093/BRAIN/AWAA054.

Wolfe, M.S., Xia, W., Ostaszewski, B.L., Diehl, T.S., Kimberly, W.T., *et al.* (1999) 'Two transmembrane aspartates in presenilin-1 required for presenilin endoproteolysis and γ-secretase activity', *Nat. 1999 3986727*, 398(6727), pp. 513–517. doi:10.1038/19077.

Wood, J.G., Mirra, S.S., Pollock, N.J. and Bindert, L.I. (1986) 'Neurofibrillary tangles of Alzheimer disease share antigenic determinants with the axonal microtubule-associated protein tau', *Proc. Nail. Acad. Sci. USA*, 83, pp. 4040–4043. doi:10.1073/pnas.83.11.4040.

Wu, Y.T., Beiser, A.S., Breteler, M.M.B., Fratiglioni, L., Helmer, C., *et al.* (2017) 'The changing prevalence and incidence of dementia over time — current evidence', *Nat. Rev. Neurol. 2017 136*, 13(6), pp. 327–339. doi:10.1038/nrneurol.2017.63.

Xiong, F., Ge, W. and Ma, C. (2019) 'Quantitative proteomics reveals distinct composition of amyloid plaques in Alzheimer's disease', *Alzheimer's Dement.*, 15(3), pp. 429–440. doi:10.1016/J.JALZ.2018.10.006.

Yamada, K., Yabuki, C., Seubert, P., Schenk, D., Hori, Y., *et al.* (2009) 'Aβ Immunotherapy: Intracerebral Sequestration of Aβ by an Anti-Aβ Monoclonal Antibody 266 with High Affinity to Soluble Aβ', *J. Neurosci.*, 29(36), pp. 11393–11398. doi:10.1523/JNEUROSCI.2021-09.2009.

Yang, G., Zhou, R., Zhou, Q., Guo, X., Yan, C., *et al.* (2018) 'Structural basis of Notch recognition by human γ-secretase', *Nature*, 565(7738), pp. 192–197. doi:10.1038/s41586-018-0813-8.

Yang, H.S., Onos, K.D., Choi, K., Keezer, K.J., Skelly, D.A., *et al.* (2021) 'Natural genetic variation determines microglia heterogeneity in wild-derived mouse models of Alzheimer's disease', *Cell Rep.*, 34(6). doi:10.1016/J.CELREP.2021.108739.

Yang, T., Dang, Y., Ostaszewski, B., Mengel, D., Steffen, V., *et al.* (2019) 'Target engagement in an alzheimer trial: Crenezumab lowers amyloid β oligomers in cerebrospinal fluid', *Ann. Neurol.*, 86(2), pp. 215–224. doi:10.1002/ANA.25513.

Yates, P.A., Sirisriro, R., Villemagne, V.L., Farquharson, S., Masters, C.L., *et al.* (2011) 'Cerebral microhemorrhage and brain β-amyloid in aging and Alzheimer disease', *Neurology*, 77(1), pp. 48–54. doi:10.1212/WNL.0B013E318221AD36.

Ye, L., Fritschi, S.K., Schelle, J., Obermüller, U., Degenhardt, K., *et al.* (2015) 'Persistence of Aβ seeds in APP null mouse brain', *Nat. Neurosci.*, 18(11), pp. 1559–1561. doi:10.1038/nn.4117.

Ye, L., Rasmussen, J., Kaeser, S.A., Marzesco, A.-M., Obermüller, U., *et al.* (2017) 'Aβ seeding potency peaks in the early stages of cerebral β-amyloidosis.', *EMBO Rep.*, 18(9), pp. 1536–1544. doi:10.15252/embr.201744067.

Yuan, A., Rao, M. V., Veeranna and Nixon, R.A. (2017) 'Neurofilaments and Neurofilament Proteins in Health and Disease', *Cold Spring Harb. Perspect. Biol.*, 9(4), p. a018309. doi:10.1101/CSHPERSPECT.A018309.

Yuan, P., Condello, C., Keene, C.D., Wang, Y., Bird, T.D., *et al.* (2016) 'TREM2 Haplodeficiency in Mice and Humans Impairs the Microglia Barrier Function Leading to Decreased Amyloid Compaction and Severe Axonal Dystrophy', *Neuron*, 90(4), pp. 724–739. doi:10.1016/J.NEURON.2016.05.003.

Zetterberg, H., Skillbäck, T., Mattsson, N., Trojanowski, J.Q., Portelius, E., *et al.* (2016) 'Association of Cerebrospinal Fluid Neurofilament Light Concentration With Alzheimer Disease Progression', *JAMA Neurol.*, 73(1), p. 60. doi:10.1001/JAMANEUROL.2015.3037.

Zetterberg, H. and Blennow, K. (2021) 'Moving fluid biomarkers for Alzheimer's disease from research tools to routine clinical diagnostics', *Mol. Neurodegener.*, 16(1), pp. 1–7. doi:10.1186/S13024-021-00430-X/TABLES/1.

Zhang, F., Gannon, M., Chen, Y., Yan, S., Zhang, S., *et al.* (2020) 'β-amyloid redirects norepinephrine signaling to activate the pathogenic GSK3β/tau cascade', *Sci. Transl. Med.*, 12(526). doi:10.1126/SCITRANSLMED.AAY6931.

Zhang, P., Kishimoto, Y., Grammatikakis, I., Gottimukkala, K., Cutler, R.G., *et al.* (2019) 'Senolytic therapy alleviates Aβ-associated oligodendrocyte progenitor cell senescence and cognitive deficits in an Alzheimer's disease model', *Nat. Neurosci. 2019 225*, 22(5), pp. 719–728. doi:10.1038/s41593-019-0372-9.

Zhang, Z., Hartmann, H., Minh Do, V., Abramowski, D., Sturchler-Pierrat, C., *et al.* (1998) 'Destabilization of β-catenin by mutations in presenilin-1 potentiates neuronal apoptosis', *Nature*, 395(6703), pp. 698–702. doi:10.1038/27208.

Zheng, W., Tsai, M.-Y., Chen, M. and Wolynes, P.G. (2016) 'Exploring the aggregation free energy landscape of the amyloid-β protein (1–40)', *Proc. Natl. Acad. Sci.*, 113(42), pp. 11835–11840. doi:10.1073/PNAS.1612362113.

Zhou, R., Yang, G., Guo, X., Zhou, Q., Lei, J., *et al.* (2019) 'Recognition of the amyloid precursor protein by human g-secretase', *Science (80-.).*, 363(6428). doi:10.1126/SCIENCE.AAW0930.

Zhu, X.-C., Tan, L., Wang, H.-F., Jiang, T., Cao, L., *et al.* (2015) 'Rate of early onset Alzheimer's disease: a systematic review and meta-analysis', *Ann. Transl. Med.*, 3(3), p. 38. doi:10.3978/J.ISSN.2305-5839.2015.01.19.

Zimmermann, M.R., Bera, S.C., Meisl, G., Dasadhikari, S., Ghosh, S., *et al.* (2021) 'Mechanism of Secondary Nucleation at the Single Fibril Level from Direct Observations of Aβ42 Aggregation', *J. Am. Chem. Soc.*, p. jacs.1c07228. doi:10.1021/JACS.1C07228.

6 Statement of contributions

Statement of contributions according to §9 (2):

Data and text in chapter 3.1 were adapted from a manuscript submitted for publication at the time this dissertation was written.

Experimental evidence for an uncoupling of Aβ deposition and downstream neurodegenerative sequelae

Christine Rother*, Ruth E. Uhlmann*, Stephan A. Müller, Stephan A. Kaeser, Juliane Schelle, Angelos Skodras, Ulrike Obermüller, Lisa E. Häsler, Marius Lambert, Frank Baumann, Ying Xu, Giulia Salvadori, Irena Brzak, Derya Shimshek, Ulf Neumann, Lary C. Walker, Stephanie Schulz, Jasmeer P. Chhatwal, Stefan F. Lichtenthaler, Matthias Staufenbiel, Mathias Jucker
*contributed equally

Personal contribution:
Writing and editing of the manuscript (with MJ, LCW, MS and REU). Experimental design of the study (together with REU, JS, MS and MJ). Figure design and editing (Fig. 1, 3, Ext. Fig. 2, 6 and Fig. 2, 4 Ext. Fig 3, 4 with REU). Chronic BACE1 inhibitor treatment of mice and collection of CSF, brain and blood (together with REU, Fig. 2B-C, 4B-C, Ext. Fig. 2A, 3B-C, 4B-C, E, 6B-C). Brain tissue homogenisation of chronically treated mice (together with REU, Fig. 2B-C, 4B-C, Ext. Fig. 3 B-C, Ext. Fig. 4B-C, E, 6B-C). Statistical data analysis (Fig. 2A-B, 4A-B, Ext. Fig. 3A-B, 4A-B, D-E). Design and performance of endpoint titration assay to estimate the 50% seeding dose (Fig. 3A). Intracerebral injections in mice (with the help of UO, Fig. 3B, Ext. Fig 2B). Brain collection of seeded mice (Fig. 3A). Immunohistochemistry of brain sections of seeded mice (with the help of UO) and image acquisition (Fig. 3A). Analysis and determination of the 50% seeding dose (with the help of FB, Fig. 3C, Ext. Fig. 2C). Stereological analysis of brain Aβ load (together with AS Ext. Fig. 3B, REU and GS Ext. Fig. 3A, C). Image acquisition, processing and microglia subtype analysis (together with AS, Ext. Fig 4C-E).

Others: JS and REU performed acute BACE1 inhibitor treatment of mice (Fig. 2A, 4A, Ext. Fig. 2A, 3A, 4A, D, 6A). LMH and ML performed MSD ELISA and Simoa measurements (Fig. 2, 4). DRS, UN and IB contributed the BACE1 inhibitor and Trem2 assay (Ext. Fig, 4A-B). SAM and SFL performed the proteomic work (Ext. Fig. 5). SAK (Fig. 1A) and SS (Fig. 5) performed curve-fitting.

Data and text in chapter 3.2 were adapted from Uhlmann *et al.*, 2020.

Acute targeting of pre-amyloid seeds in transgenic mice reduces Alzheimer-like pathology later in life

Ruth E. Uhlmann* and Christine Rother*, Jay Rasmussen, Juliane Schelle, Carina Bergmann, Emily M. Ullrich Gavilanes, Sarah K. Fritschi, Anika Buehler, Frank Baumann, Angelos Skodras, Rawaa Al-Shaana, Natalie Beschorner, Lan Ye, Stephan A. Kaeser, Ulrike Obermüller, Søren Christensen, Fredrik Kartberg, Jeffrey B. Stavenhagen, Jens-Ulrich Rahfeld, Holger Cynis, Fang Qian, Paul H. Weinreb, Thierry Bussiere, Lary C. Walker, Matthias Staufenbiel, Mathias Jucker *contributed equally

Personal contribution:

Writing and editing of the manuscript (with MJ, LCW, MS, REU). Figure design and editing (together with REU). Mouse brain collection for biochemical analyses (Fig. 2, 3). Optimization of antibody recognition profiling of Aβ assemblies (with the help of JR and AB). Design and performance of antibody recognition profiling of Aβ assemblies and biochemical analysis (Fig. 2A, 3 Ext. Fig. 2). Immunoblot data acquisition and analysis (Fig. 2B-C, E, 3, Ext. Fig. 2A, 3 and Fig. 2D with the help of CB). Statistical data analysis (with REU). Spectral amyloid and plaque analysis (together with NB, Fig. 5F). Immunohistochemistry (with the help of UO and REU, Fig. 6A, D). Image and data acquisition, dystrophic neurite and microglia subtype analysis (together with A.S. Fig. 6B-C, E-G). Human brain tissue preparation for biochemical analysis (Ext. Fig. 2A) and intracerebral injections (Ext. Fig. 2B). Design and performance of endpoint titration assay to estimate the seeding dose 50 (Ext. Fig. 2D). Intracerebral injections into mice (with the help of NB Ext. Fig 2D). Immunohistochemistry of seeded mice (with the help of UO and CB) and image acquisition (Ext. Fig 2C). Analysis and calculation of the seeding dose 50 (together with FB Ext. Fig 2E) and specific seeding activity (Ext. Fig. 2E).

Others: REU, JS, SKF, LY, UO, MS and MJ designed and performed passive immunization (Fig. 1B). REU, EMU, AB and MS performed pharmacokinetics ELISA (Fig. 4, Ext. Fig. 4). UO performed seeding experiments (Fig. 1D). RA performed MSD ELISA measurements (Fig. 1C 5C). SC, FK, JBS, J-UR, HC, FQ, PHW, and TB contributed antibodies and provided experimental input (Fig. 1B).

7 Abbreviations

Aβ	Amyloid-β
AD	Alzheimer's disease
ADAM	A disintegrin and metalloprotease
AIDC	Intracellular domain of amyloid precursor protein
APH-1	Anterior pharynx-defective 1
APP	Amyloid precursor protein
ARIA	Amyloid-related imaging abnormalities
ARPA	Antibody recognition profiling of Aβ assemblies
BACE1	Beta-site amyloid precursor protein cleaving enzyme 1
CAA	Cerebral amyloid angiopathy
CJD	Creutzfeldt-Jakob disease
CSF	Cerebrospinal fluid
CTFα	Carboxyl-terminal fragment α
CTFβ	Carboxyl-terminal fragment β
DAM	Disease-associate microglia
EOAD	Early-onset Alzheimer's disease
fAD	Familial Alzheimer's disease
GSK3	Glycogen synthase kinase 3
IgG	Immunoglobulin G
IP	Immunoprecipitation
LOAD	Late-onset Alzheimer's disease
NfH	Neurofilament heavy
NfL	Neurofilament light
NfM	Neurofilament middle
NFT	Neurofibrillary tangles
NP	Neuritic plaques
NT	Neuropil threads
PEN2	Presenilin enhancer 2
PET	Positron emission tomography
PHF	Paired helical filaments
PiB	Pittsburgh compound B
PrP^{C}	Cellular prion protein
PrP^{L}	Toxic prion protein
PrP^{Sc}	Disease-associated prion protein
PS1	Presenilin-1

PS2	Presenilin-2
PTM	Posttranslational modification
sAD	Sporadic Alzheimer's disease
sAPPα	Soluble amyloid precursor protein α
sAPPβ	Soluble amyloid precursor protein β
SD_{50}	Seeding dose 50
sTrem2	Soluble triggering receptor expressed on myeloid cells 2
TGN	Trans-Golgi network
Trem2	Triggering receptor expressed on myeloid cells 2
WT	Transgene-negative mice